Optimal form-finding algorithms
for the control of structural shapes

Ph.D. Thesis
Paolo BASSO

Advisor:
Prof. Andrea E. Del Grosso
Department of Civil, Environmental and Architectural Engineering
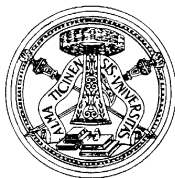*University of Genoa, Italy*

Revisor:
Prof. Lucia Faravelli
Department of Structural Mechanics
University of Pavia, Italy

Pavia, June 2012

To my family

Dottorato di Ricerca in Ingegneria Civile
Graduate School in Civil Engineering

Optimal form-finding algorithms
for the control of structural shapes

Ph.D. Thesis
Paolo BASSO

Abstract

Structures cannot be built arbitrarily but should consider performance requirements, economy of materials, needs of the building physics, ethic and aesthetic principles. To this aim, due to the infinity of the design space, it is always difficult to determine optimal criteria and optimal solutions and becomes even more problematic when the structural morphology itself is highly unconstrained.

This research is then focused on the main issues, but also the potential, derived from the adaptation of the structural morphology to the freeform and variable geometries of contemporary and innovative applications in many fields of engineering and architecture. Freedom and variability (i.e. change of configuration) are conditions which affect the form from the static and kinematic point of view respectively and are usually treated separately.

On the basis of the recent advances in structural optimization and form-finding, a holistic approach to deal with the structural form is instead proposed and specifically targeted to the design of both static and kinematic spatial framed systems, such as grid-shells, reciprocal frames, etc. or systems representable in such a way (e.g. folded shells). The algorithms developed around this concept are applied to different case studies.

Preface

Acknowledgments

The author wishes to express his sincere gratitude for both the opportunity and guidance received in the completion of this Thesis. In specific, to Professor Fabio Casciati as coordinator for envisioning, creating, and supporting a non-traditional arrangement that allowed me to complete all university program requirements balanced with other professional commitments and ambitions. To Professor Andrea Del Grosso, the research advisor of my Ph.D. thesis, who provided the topic, challenge, and countless hours of feedback through revisions and concept assistance. Thanks to Professor Del Grosso, I have had the opportunity to meet many of the leaders in the field and the authors of the books, codes, articles, and papers I've studied. Without his support, this thesis would not have been possible and travel opportunities to conferences and professional schools would have been missed. His kindness, professional expertise, and generosity will always be remembered. To Professor Lucia Faravelli who gave me the opportunity to develop and express my skills as teaching assistant in her courses during these three years and for her feedback and patience in revising this thesis. To Professor Simon Guest and Professor Billie Spencer for hosting me at their Departments and supervising me in my research work abroad. The author also gratefully acknowledges the support of the European Project IRIS[1].

I wish to thank also my friends Alberto Pugnale, Alberto Lago and Martijn Veltkamp for sharing their passion, their ideas, their work and even their homes. I am grateful to all my friends and colleagues at the Department of Structural Mechanics and particularly Clemente, Alessandro, ZhiCong, Emanuela and Veronica. Lastly, the never missed support of my all family is the most acknowledged and specifically to Micol for her support, inspiration, and assistance.

---

[1] http://www.vce.at/iris/

About the Author

The author is a graduate of the University of Genoa (MS - Building Engineering and Architecture) and a licensed engineer in Italy. At the time of his Master thesis he began to investigate the technical issues related to unconventional structural morphologies and his thesis was awarded a special mention at the international contest "GUIDO NARDI" on the topic of technological innovation and complex structures in architect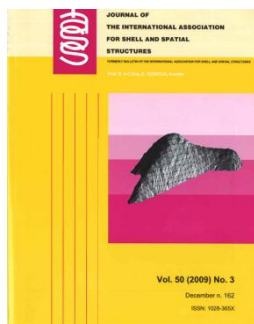ure. Since November 2008, starting date of his Doctorate, he has been developing further his research on this subject at the edge between Structural Engineering and Architecture, till in order to focus on structures having the potential to adapt their configuration to varying excitations.

Figure I – picture from the HANGAI awarded paper chosen as cover image of the IASS Journal Vol. 50 N. 3, December n.162.

The innovation and quality of the achieved results has been recognized at an international level, leading his conference papers to be selected twice for the publication on peer-reviewed journals and particularly allowing him to be awarded the 7th IASS HANGAI prize by the International Association for Shell and Spatial Structures of which he is a member since 2009.

The range of the author's research activities has been then extended by the competences gained during the PhD courses and the training abroad, specifically in the fields of performance-based design, risk analysis and structural health monitoring. These competences, the consultancy work in the civil division of the Italian engineering firm D'Appolonia S.p.A. and, more generally, the development of a very diverse educational, academic and professional background have certainly influenced part of this thesis applications and reasoning.

About the Thesis

Central to this thesis is the concept of "optimal form-finding". This concept may sound unfamiliar or even strange to the reader who is accustomed to hearing about the two fields, form-finding and structural optimization, separately. However, these two fields have also a lot to share when focusing on the structural morphology and this thesis have studied how the methods of both parts can be extended and combined to propose an effective approach to the design of innovative structures.

Specifically, the reader should be aware that this process has been carried out in two phases. In the first phase the research was targeted to solve performance and constructability issues of freeform structures by affecting their geometry and thus (often but not always) their shape. In the second phase the achievements of the first phase have been generalized till to include the design and control of variable geometry structures (i.e. adaptive structures), aiming at a holistic view – static and kinematic – of the structural form. The kinds of structures addressed belong in both cases to the family of spatial framed systems, such as grid-shells, reciprocal frames, etc. or are representable in such a way (e.g. folded shells).

For all the developed algorithms at least an application of interest is presented. Given the breadth of the presented applications, ranging across different disciplines from statics to acoustics and fluid dynamics, the results are not to be interpreted as the output of highly specialized studies but as the proof of the feasibility and potential effectiveness of the proposed methods. Since the issues dealing with the design of complex to variable structural morphologies are in fact primarily geometrical, the deepest insight is to be found in the theoretical, procedural and technical contributions to their solutions.

In assessing the quality of such an effort, it may be difficult to determine what work is original and what work is taken from other sources and applied. For this reason, the author's primary contributions to the body of knowledge are highlighted as follows:

Theoretical

- Unifying the force density based form-finding methods under a common matrix symbolism and exploiting their underlying mathematical meaning using graph theory (Chap 3)
- Introducing abstract elements in the force density method (VFDM) to address general purpose optimization problems related to free-form frameworks performance, costs and constructability (Chap 4)
- Determining a comparative limit for the quantification of the reliability gain derived from the application of the structural adaptivity concept in risk analysis (Chap 5)

Procedural

- Developing a finite state strategy (FSCS) for the design and control of adaptive structures for the building envelope (Chap 5)
- Developing a topology optimization process to minimize the number of actuators in a single-layer MDOF adaptive system (Chap 5)

Technical

- Developing a method to standardize the element typologies in freeform grid-shells and generic spatial trusses of minimal deformation energy (Chap 4, 6)
- Developing a method to design freeform meshes with planar quadrilateral elements (Chap 4, 6)
- Developing a method to design freeform spatial reciprocal frames (Chap 4, 7)
- Exploiting the relationship between the topology of a framed structure and its number of finite mechanisms and corresponding self-stress states (Chap 5)

Description of the Graduate School

Settore: **Field:**	Ingegneria Engineering
Sede Amministrativa non consortile: **Administrative location:**	Università degli Studi di PAVIA University of PAVIA
Durata del dottorato: **Duration**:	3 anni 3 years
Periodo formativo estero: **Period in external organization**:	Come previsto dal regolamento del Dottorato di Ricerca As required by the School by-law
Numero minimo di corsi: **Minimum number of courses:**	6 6

The two page description is provided first in Italian and then is repeated in English.

Italiano

Il dottorato di ricerca in Ingegneria Civile presso la Facoltà di Ingegneria dell'Università degli Studi di Pavia è stato istituito nell'anno accademico 1994/95 (X ciclo).

Il corso consente al dottorando di scegliere tra quattro curricula: Idraulico, Sanitario, Sismico e Strutturale. Egli svolge la propria attività di ricerca rispettivamente presso il Dipartimento di Ingegneria Idraulica e Ambientale o quello di Meccanica Strutturale.

Durante i primi due anni sono previsti almeno sei corsi. Il Collegio dei Docenti, composto da professori dei due Dipartimenti, organizza i corsi con lo scopo di fornire allo studente di dottorato opportunità di approfondimento su alcune delle discipline di base. Corsi e seminari vengono tenuti da docenti di Università nazionali ed estere. Il Collegio dei Docenti, cui spetta la pianificazione della didattica, si è orientato ad attivare ad anni alterni corsi sui seguenti temi:

- Meccanica dei solidi e dei fluidi
- Metodi numerici per la meccanica dei solidi e dei fluidi
- Rischio strutturale e ambientale
- Metodi sperimentali per la meccanica dei solidi e dei fluidi
- Intelligenza artificiale

più corsi specifici di indirizzo.

Al termine dei corsi del primo anno il Collegio dei Docenti assegna al dottorando un tema di ricerca da sviluppare sotto forma di tesina entro la fine del secondo anno; il tema, non necessariamente legato all'argomento della tesi finale, è di norma coerente con il curriculum, scelto dal dottorando.

All'inizio del secondo anno il dottorando discute con il Coordinatore l'argomento della tesi di dottorato, la cui assegnazione definitiva viene deliberata dal Collegio dei Docenti.

Alla fine di ogni anno i dottorandi devono presentare una relazione particolareggiata (scritta e orale) sull'attività svolta. Sulla base di tale relazione il Collegio dei Docenti, "previa valutazione della assiduità e dell'operosità dimostrata

dall'iscritto", ne propone al Rettore l'esclusione dal corso o il passaggio all'anno successivo.

Il dottorando può svolgere attività di ricerca sia di tipo teorico che sperimentale, grazie ai laboratori di cui entrambi i Dipartimenti dispongono, nonché al Laboratorio Numerico di Ingegneria delle Infrastrutture.

Il "Laboratorio didattico sperimentale" del Dipartimento di Meccanica Strutturale dispone di:

- una tavola vibrante che consente di effettuare prove dinamiche su prototipi strutturali;
- opportuni sensori e un sistema di acquisizione dati per la misura della risposta strutturale;
- strumentazione per la progettazione di sistemi di controllo attivo e loro verifica sperimentale;
- strumentazione per la caratterizzazione dei materiali, attraverso prove statiche e dinamiche.

Il Laboratorio del Dipartimento di Ingegneria Idraulica e Ambientale dispone di:

- un circuito in pressione che consente di effettuare simulazioni di moto vario;
- un tunnel idrodinamico per lo studio di problemi di cavitazione,
- canalette per lo studio delle correnti a pelo libero.

English

The Graduate School of Civil Engineering at the University of Pavia was established in the Academic Year of 1994/95 (X cycle). The School allows the student to select one of the four offered curricula: Hydraulics, Environment, Seismic engineering and Structural Mechanics.

Each student develops his research activity either at the Department of Hydraulics and Environmental Engineering or at the Department of Structural Mechanics. During the first two years, a minimum of six courses must be selected and their examinations successfully passed. The Faculty, made by Professors of the two Departments or by internationally recognized scientists, organizes courses and provides the

student with opportunities to enlarge his/her basic knowledge. Courses and seminars are held by University Professors from all over the country and abroad. The Faculty starts up in alternate years common courses, on the following subjects:

- solid and fluid mechanics,
- numerical methods for solid and fluid mechanics,
- structural and environmental risk,
- experimental methods for solid and fluid mechanics,
- artificial intelligence.

More specific courses are devoted to students of the single curricula. At the end of each course, for the first year the Faculty assigns the student a research argument to develop, in the form of report, by the end of the second year; the topic, not necessarily part of the final doctorate thesis, should be consistent with the curriculum selected by the student.

At the beginning of the second year the student discusses with his Coordinator the subject of the thesis and, eventually, the Faculty assigns it to the student. At the end of every year, the student has to present a complete report on his research activity, on the basis of which the Faculty proposes to the Rector his admission to the next academic year or to the final examination.

The student is supposed to develop either theoretical or experimental research activities, and therefore has access to the Department Experimental Laboratories, even to the Numerical Laboratory of Infrastructure Engineering.

The Experimental Teaching Laboratory of the Department of Structural Mechanics offers:

- a shaking table which permits one to conduct dynamic tests on structural prototypes;
- sensors and acquisition data system for the structural response measurements;
- instrumentation for the design of active control system and their experimental checks;
- an universal testing machine for material characterization through static and dynamic tests.

The Department of Hydraulics and Environmental Engineering offers:

- a pressure circuit simulating various movements;
- a hydrodynamic tunnel studying cavitation problems;
- micro-channels studying free currents.

Recapiti – Addresses

Dipartimento di Meccanica Strutturale
Via Ferrata, 1 – 27100 Pavia – Italia
Tel. +39.0382.985450 – Fax +39.0382.528422

Dipartimento di Ingegneria Idraulica e Ambientale
Via Ferrata, 1 – 27100 Pavia – Italia
Tel. +39.0382.985300 – Fax +39.0382.985589

Coordinatore – Coordinator

CASCIATI Fabio – Professore Ordinario – ICAR/08
Dipartimento di Meccanica Strutturale
Via Ferrata, 1 – 27100 Pavia – Italia
Tel. +39.0382.985458 – Fax +39.0382.528422
E-mail: fabio@dipmec.unipv.it

Collegio dei Docenti – Teaching Staff

CASCIATI Fabio – Professore Ordinario – ICAR/08 (Coordinatore)
CIAPONI Carlo – Professore Ordinario – ICAR/02
DEL GROSSO Andrea Enrico – Professore Ordinario – ICAR/09
FARAVELLI Lucia – Professore Ordinario – ICAR/08
GALLATI Mario – Professore Ordinario – ICAR/01
GOBETTI Armando – Professore Associato – ICAR/08
MOISELLO Ugo – Professore Ordinario – ICAR/02
PAPIRI Sergio – Professore Associato – ICAR/02
SALA Roberto – Professore Associato – ING – IND/08
MARCELLINI Alberto – Dirigente di Ricerca, CNR – Milano.

Elenco delle Tesi – Previous PhD Theses

Battaini Marco (X Ciclo)	Sistemi strutturali controllati: progettazione e affidabilità (Novembre 1998).
Mariani Claudia (X Ciclo)	Problemi di ottimizzazione per strutture bidimensionali anisotrope (Novembre 1998).
Negri Antonella (X Ciclo)	Stima delle perdite idrologiche nei bacini di drenaggio urbani (Aprile 1999).
Pisano Aurora Angela (XI Ciclo)	Structural System Identification :Advanced Approaches and Applications (Aprile 1999).
Saltalippi Carla (XI Ciclo)	Preannuncio delle piene in tempo reale nei corsi d'acqua naturali (Aprile 1999).
Barbieri Eugenio (XI Ciclo)	Thermo fluid Dynamics and Topology: Optimization of an Active Thermal Insulation Structure (Aprile 2000).
Barbolini Massimiliano (XII Ciclo)	Dense Snow Avalanches: Computational Models, Hazard Mapping and Related Uncertanties (Aprile 2000).
Espa Paolo (XII Ciclo)	Moti atmosferici generati da forze di galleggiamento: simulazioni numeriche e studio su modello fisico (Aprile 2000).

Petrini Lorenza (XII Ciclo)   Shape Memory Alloys: Modelling the Martensitic Phase Behaviour for Structural Engineering Exploitation (Aprile 2000).

Podestà Stefano (XIII Ciclo)   Risposta sismica di antichi edifici religiosi: una nuova proposta per un modello di vulnerabilità.

Sturla Daniele (XIII Ciclo)   Simulazioni lagrangiane di flussi rapidamente variati nell'approssimazione di acque poco profonde.

Marazzi Francesco (XV Ciclo)   Semi -active Control of Civil Structures: Implementation Aspects (Gennaio 2003).

Nascimbene Roberto (XV Ciclo)   Sail Modelling for Maximal Speed Optimum Design (Gennaio 2003).

Giudici Massimo (XVI Ciclo)   Progettazione in regime non lineare di strutture in CAP a cavi aderenti e non aderenti (Aprile 2004).

Mutti Matteo (XVI Ciclo)   Stability Analysis of Stratified Three-phase Flows in Pipes (Febbraio 2004).

Petaccia Gabriella (XVI Ciclo)   Propagazione di onde a fronte ripido per rottura di sbarramenti in alvei naturali (Febbraio 2004).

D'Amico Tiziana (XVI Ciclo)   Ricerca e sviluppo di metodologie diagnostiche per il recupero di edifici monumentali: prove vibroacustiche sul tufo (Febbraio 2005).

Casciati Sara (XVII Ciclo)	Damage Detection and Localization in the Space of the Observed Variables (Febbraio 2005).
Barco Olga Janet (XVII Ciclo)	Modeling the Quantity and Quality of Storm Water Runoff Using SWMM (Marzo 2006).
Boguniewicz Joanna (XVIII Ciclo)	Integration of Monitoring and Modelling in the Surface Water State Evaluation Process of a Sub-Alpine Lake Watershed (Marzo 2006).
Bornatici Laura (XVIII Ciclo)	L'impiego degli algoritmi generici per la risoluzione dei problemi di progetto di reti di distribuzione idrica (Marzo 2006).
Collivignarelli M.Cristina (XVIII Ciclo)	Trattamento di rifiuti liquidi mediante processi biologici aerobici termofili e mesofili e processi avanzati di ossidazione chimica in diversa (Marzo 2006).
Domaneschi Marco (XVIII Ciclo)	Structural Control of Cable-stayed and Suspended Bridges (Febbraio 2006).
Ráduly Botond (XVIII Ciclo)	Artificial Neural Network applications in Urban Water Quality Modeling (MArzo 2006).
Antoci Carla (XVIII Ciclo)	Simulazione numerica dell'interazione fluido-struttura con la tecnica SPH (Luglio 2006).

Cappabianca Federica (XVIII Ciclo)	La valutazione del rischio valanghivo attraverso la modellazione dinamica (Luglio 2006).
Callegari Arianna (XVIII Ciclo)	Applicazione di tecnologie di monitoraggio on-line per la gestione dei processi di trattamento reflui (Luglio 2006).
Gazzola Elisa (XVIII Ciclo)	Applicazione di processi biologici anaerobici al trattamento di acque reflue e fanghi di depurazione: aspetti tecnici ed energetici (Febbraio 2007).
Maranca Federica (XVIII Ciclo)	Valutazione del ciclo di vita (LCA): confronto tra sistemi di trasporto gas via gasdotto (Febbraio 2007).
Giuliano Fabio (XIX Ciclo)	Performance Based Design and Structural Control for Cable Suspension Bridges (Febbraio 2007).
Falappi Stefano (XIX Ciclo)	Simulazioni numeriche di flussi di fluidi viscosi e materiali granulari con la tecnica SPH (Febbraio 2007).
Zanaboni Sabrina (XIX Ciclo)	Pre-trattamento di rifiuti liquidi industriali mediante ossidazione ad umido (Febbraio 2007).
Bruggi Matteo (XX Ciclo)	Topology optimization using mixed finite elements (Febbraio 2008).
Cimellaro Gian Paolo (XX Ciclo)	Passive Control of Industrial Structures for Natural Hazard Mitigation: Analytical Studies and Applications (Febbraio 2008).

Pagliardi Matteo (XX Ciclo)	Application of PIV technique to the study of subaqueous debris flows (Febbraio 2008).
Todeschini Sara (XX Ciclo)	Il controllo degli scarichi fognari in tempo di pioggia mediante vasche di prima pioggia: aspetti progettuali e gestionali (Febbraio 2008).
Abbà Alessandro (XXI Ciclo)	Recupero dei rifiuti speciali nel settore delle costruzioni: studio delle possibilità di recupero e valutazione dei meccanismi di lisciviazione (Febbraio 2009).
Hamdaoui Karim (XXI Ciclo)	Experimental Applications on Cu-based shape Memory Alloys: Retrofitting of Historical Monuments and Base Isolation (Febbraio 2009).
Messervey Thomas (XXI Ciclo)	Integration of Structural Health Monitoring into the Design, Assessment, and Management of Civil Infrastructure (Febbraio 2009).
Ubertini Filippo (XXI Ciclo)	Wind Effects on Bridges: Response, Stability and Control (Febbraio 2009).
Fuggini Clemente (XXII Ciclo)	Using satellites systems for structural monitoring: accuracy, uncertainty and reliability (Febbraio 2010).
Raboni Massimo (XXII Ciclo)	Impiego di tecniche numeriche e sperimentali per l'analisi di fenomeni multiphysics (Luglio 2010).

AlSaleh Raed (XXIII Ciclo)

Verification of wind pressure and wind induced response of a supertall structure using a long term structural health monitoring system (Febbraio 2011).

Crotti Barbara Marianna
(XXIII Ciclo)

Verifiche di funzionalità e criteri di ottimizzazione degli impianti di potabilizzazione: alcuni casi di studio (Gennaio 2011).

Franchioli Luigi (XXIII Ciclo)

Analisi prestazionale dei sistemi di distribuzione idrica e calcolo della loro affidabilità (Marzo 2011).

Marzi Alessandro (XXIII Ciclo)

Impianti in materiale plastico per il trasporto dei fluidi nel settore navale (Febbraio 2011).

Bourdim Sidi Mohammed
El-Amine (XXIII Ciclo)

Diagnostique et Analyse Sismique d'un monument Historique à Tlemcen (Dicembre 2011).

Chen ZhiCong (XXIV Ciclo)

Structural Monitoring and System Control Using a Wireless Sensor Network (Dicembre 2011).

Cornalba Veronica (XXIV Ciclo)

Recupero energetico da biomasse:
aspetti tecnici e di impatto ambientale (Dicembre 2012).

Torti Emanuela (XXIV Ciclo)

Experimental and numerical analysis of a confined two phase turbulent jet system (Dicembre 2012).

Contents

PART I

    PART III

6.   The cost optimization of free-form grid-shells 109

xxii

List of Figures

List of Tables

Symbols

Scalars:

$\mathcal{A}$	Graph edges (arcs)
A	Element section
b	Number of framework edges
b_{int}	Number of framework internal edges
b_{ext}	Number of framework external edges (boundary)
χ	Number of redundant constraints of a framework (singularities)
E	Young modulus
f	Element force
$\mathcal{F}$	Framework
$\mathcal{G}$	Graph
k	Number of restraints for node displacement d for a reticulated system
l_0	Element unstressed length
l	Element length
m	Number of inextensional mechanisms of a framework
n	Number of framework nodes
n_{int}	Number of framework internal nodes
$\mathcal{N}$	Graph nodes (vertices)
N	Number of degrees of freedom (DOFs) for a reticulated system ($N = 3n - k$ for space systems, $N = 2n - k$ for plane systems)

ξ	Scale factor in TNA
λ	Lagrange multiplier
π	Element functional
Π	Functional
R^N	Displacement space
s	Number of self-stress states of a framework
ω	Number of loop constraints of a framework (holes in a mesh)
$rank(\mathbf{A})$	Rank of a matrix $\mathbf{A}$
$nullity(\mathbf{A})$	Nullity of a matrix $\mathbf{A}$

Vectors and **MATRICES**:

Ω	Constraints matrix
$\mathbf{C}$	Branch-node matrix
$\mathbf{C}^T$	Incidence matrix
$\mathbf{C}_{free}$	Columns of the branch-node matrix related to free nodes
$\mathbf{C}_{fix}$	Columns of the branch-node matrix related to fixed nodes
$\mathcal{C}$	Connectivity matrix
$\mathbf{d}$	External displacement vector
$\mathbf{e}$	Internal deformation vector (edge elongations, equivalent to $\mathbf{E}^T\mathbf{d}$)
$\mathbf{e}_l$	Vector of length variation coefficients, defined by $l_0(l-l_0)$
$\mathbf{E}$	Equilibrium matrix (equivalent to $\mathcal{E}\mathbf{L}^{-1}$)
$\mathbf{E}^T$	Compatibility matrix
$\mathcal{E}$	(Inner) equilibrium matrix (equivalent to $\begin{pmatrix} \mathbf{C}^T\mathrm{diag}(\mathbf{Cx}) \\ \mathbf{C}^T\mathrm{diag}(\mathbf{Cy}) \\ \mathbf{C}^T\mathrm{diag}(\mathbf{Cz}) \end{pmatrix}$)
$\mathbf{f}$	Internal load vector (equivalent to $\mathbf{Ke}$)
$\mathbf{G}$	Edge attribute matrix representing material stiffness ($G_{ii}=E_iA_i/l_{0i}$)
$\mathbf{I}$	Identity matrix
$\mathbf{J}$	Jacobian matrix
$\mathbf{J}^+$	Pseudo-inverse of the Jacobian matrix

K	Stiffness matrix (equivalent to $\mathbf{K}_E + \mathbf{K}_G$)
K$_E$	Linear stiffness matrix (equivalent to $\mathbf{E}\,(\mathbf{G} - \mathbf{Q})\,\mathbf{E}^T$)
K$_G$	Geometrical stiffness matrix (equivalent to $\mathbf{I} \otimes \mathcal{L}_{Q}$)
L	Edge attribute matrix representing lengths
$\mathcal{L}$	Laplacian matrix (equivalent to $\mathbf{C}^T\mathbf{W}\mathbf{C}$)
$\mathcal{L}_Q$	Force-density matrix (equivalent to $\mathbf{C}^T\mathbf{Q}\mathbf{C}$)
p	External load vector (equivalent to $\mathbf{E}\mathbf{f}$)
q	Force-density vector ($q_i = f_i/l_i$)
Q	Edge attribute matrix representing force densities
Λ	Diagonal matrix of eigenvalues (from spectral decomposition)
Φ	Matrix of eigenvectors (from spectral decomposition)
w	Attribute vector / Node weights
W	Attribute matrix
x	Vector of x Cartesian coordinates in the 3D space
y	Vector of y Cartesian coordinates in the 3D space
z	Vector of z Cartesian coordinates in the 3D space
diag(**A**)	Diagonal of a matrix **A**
Im(**A**)	Vectorial columnspace of a matrix **A** (dimension = *rank*(**A**))
Ker(**A**)	Vectorial nullspace of a matrix **A** (dimension = s)
Ker(**A**^{T})	Vectorial left-nullspace of a matrix **A** (dimension = m)

Operators:

$\otimes$	Kronecker product
r(.)	VFDM vectors generation rule

Abbreviations

AFDM	Adaptive Force Density Method
CGS	Complex Geometry Structure
CFD	Computational Fluid Dynamics
DOF	Degree of Freedom
EFDM	Extended Force Density Method
FDM	Force Density Method
FE	Finite Elements
FSCS	Finite State Control Strategy
GA	Genetic Algorithm
MA	Memetic Algorithm
MDOF	Multi Degree of Freedom
MSE	Mutually Supported Elements
PQ meshes	Planar Quadrilateral Meshes
SHM	Structural Health Monitoring
TNA	Thrust Network Analysis
VFDM	Virtual Force Density Method
VGS	Variable Geometry Structure

Part I
Introduction

Chapter 1

Introduction

Abstract

Firstly an introduction of the *picture* which contains and motivates this thesis is given. *Subject*, *meaning* and *purpose* of the research are then defined and the proposed *approach* is discussed. Finally, an overview of the *book organization* is given.

1.1.   Background – reasons for the progress

Reasons for the progress always come from new needs and opportunities and these two aspects are often both a consequence of innovation (good and bad respectively). With reference to the holistic design of buildings, but even in a more generic context, these reasons are today called *ecophysiological*[2] *awareness* and *new technologies*.

---

[2] **Ecophysiology** (from Greek οἶκος, *oikos*, "house(hold)"; φύσις, *physis*, "nature, origin"; and -λογία, *-logia*) or **environmental physiology** is a biological discipline which studies the adaptation of organism's physiology to environmental conditions (Wikipedia).

Starting from these two major topics, this section attempts to summarize the fundamental dynamics that today move the world of the architectural engineering research to exploit the related consequences on the design of structures.

Particularly four are the points that will be discussed in this context and their relationship is illustrated in Figure 1.1.
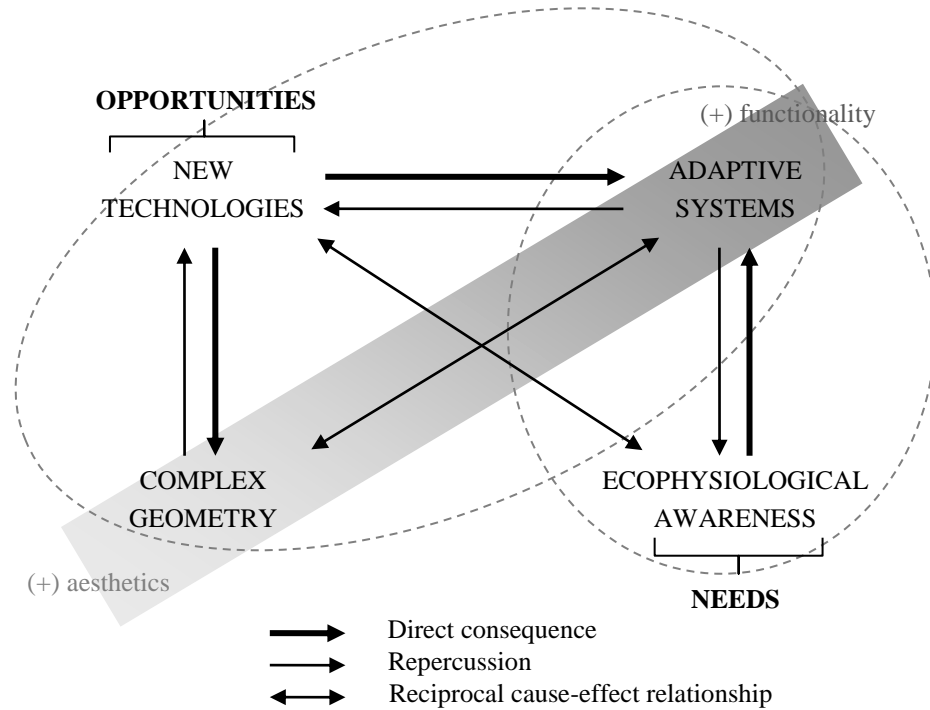
Figure 1.1 − Scheme of the relationships among the fundamental dynamics that today move the field of architectural engineering research.

These four points represent areas which are growing in a strictly connected "*cause and effect*" way. The four areas are only introduced here since the focus stays most on the relationships among them. A more detailed picture of *complex geometries* and *adaptive systems* is given in Chapter 2. *New technologies* concerning the computational design and the construction phase are further discussed in Chapter 2 while their impact on algorithms development is exploited in

Chapter 3. An insight into the matter of *ecophysiology* is instead out of the scope of this research and it won't be further discussed in the following Chapters.

1.1.1. Information technologies and complex geometries

The recent capillary diffusion of information technologies also in the building world has encouraged the birth of a recent sector of experimental research which is focused on the relationship between the new technologies and the design procedure in architecture, a relationship which should always be put into question. Back in 2003 a series of projects, belonging to this approach were displayed at the Pompidou Centre in Paris, grouped under the name "Architectures non standard" [Migayrou and Mennan, 2003]. The heterogeneity of the proposals ranged from the alteration of all compositional, static and constructive principles to the total dematerialization to get to virtual architecture, the so called "*Trans-architecture*" of Marcos Novak. Together with these experimentations new progressive designers didn't restrict themselves to using commercial software, but they personalized it managing to create the most suitable instrument to solve specific problems every time. An example of this current of thought is given by the words of John Zils[3]: *"We were used to create our own software customized for what we wanted to do… And now we are dependent of others who do things for us and that, of course, are not in the way in which we want them."* [Zils, 2006].

On one side information technology allows designers to develop their formal expression, leading to the blob as the extreme reference of their thinking, on the other side the resolution of new problems connected to free forms is approached by creating new instruments of form optimization and research which are developed "ad hoc". When forms which are not easily geometrically definable gradually replaced more regular forms, then information technologies were used to face the problems connected to representation and constructive rationality − i.e. costs. Information technologies are becoming integral part of the design procedure and the

---

[3] John Zils is Senior Engineer and Associate Partner of Skidmore Owings & Merrill LLP (SOM). The sentence is taken from his book: *Skidmore, Owings & Merrill: SOM from 1936*, Electa, Milano 2006 [Zils, 2006].

interaction between the designer and the software is no longer a mere instrumental relationship. Morphogenesis and computational optimization techniques, which draw from research on artificial intelligence and on the evolution of complex systems of biological nature (evolutionary algorithms, genetic algorithms, neural networks, etc.) as well as they draw from Operative Research, are now turning out to be strong and exceptionally powerful instruments in engineering applications, above all where the complexity of the problem makes it difficult to have a more traditional approach.

1.1.2. From complex geometry to variable geometry

…or, in other words, from the "Bilbao effect" to "dynamic architecture"[4].

Once almost all the possible shapes have been built, the new challenge in architecture is represented by buildings which can mutate their configuration. In this sense, variable geometry systems (VGSs) are interpreted as the last step in the evolution of "form experimentation".

Visionary designers have always pushed forward the limit of organic form as it happened in 2008 at the Venice Biennale[5] where an impressive amount of new proposals involved the concept of interactivity. However the position of such ideas is still mainly at the research level where technology and engineering are trying to add the necessary performance improvement to make the resulting system convenient.

---

[4] The term "Bilbao effect" refers to the trend of free form architectures which have been proposed after the huge impact of the Guggenheim Museum in Bilbao by Frank Gehry in 1997. The museum is globally referred as the icon of the, so called, *free form architecture* and a product of the period's technology. Similarly the "dynamic architecture" is the symbol of a new trend firstly proposed by David Fisher with the rotating towers, the first important example of mechanism-like structure to be built.

[5] Venice Biennale of Architecture in 2008 was titled: "Out there – architecture beyond building". The topic aimed to reflect on the relationship of the building with the environment and concepts like "interactivity" and "sustainability" were consequently considered by the most of the proposals.

From a different point of view, the reasons behind the concept of variable geometries in architecture come from the aerospace and transportation industries where systems with such a feature are studied since years ago. In this case the possibility of a building to adapt to changing situations is considered an opportunity to define a new limit for performances where energy efficiency, structure lightness, etc. can all be improved. This concept is echoed and further discussed in the following section.

1.1.3. Free forms, adaptive systems and ethic thinking

The morphogenesis has given new freedom to designers, but such a freedom claims for new responsibilities with respect to society. Technical responsibilities must be satisfied without forgetting the social responsibilities: ethical, economic and environmental requirements which must be at all times considered and respected by current designers.

Computers and morphology have given extraordinary potentiality to designer's task: from a technical point of view, today it is possible to represent, to analyze, and to build any kind of structural form, but from a social point of view not every form become necessarily a genuine architectural or engineering work. Sometimes very complicated designs look as a demonstration of the designer's skills to cope with sophisticated software as well as an exhibition of their personal vanity, more than a sincere expression led to satisfy technical and social requirements. This feeling has led more and more designers to explore the freedom of the form with performances enhancement in mind. In this sense "complexity" has often become a synonymous of "optimization" when the boundary conditions (e.g restraints) are not symmetric. Let's think for instance at the design process for the crematorium of Kakamigahara by Toyo Ito and Matsuro Sasaki (Figure 1.2). As shown by Pugnale and Sassone [2007], the asymmetric boundary conditions (Figure 1.3) imposed by the architectural design force the best structural solution – in terms of deformations – to be geometrically unconventional. The form-finding process, leaded by a genetic algorithm, is reported in Figure 1.4.

Figure 1.2 – The crematorium of Kakamigahara, Japan, by Toyo Ito and Matsuro Sasaki (© Toyo Ito and Associates).

(a)   (b)
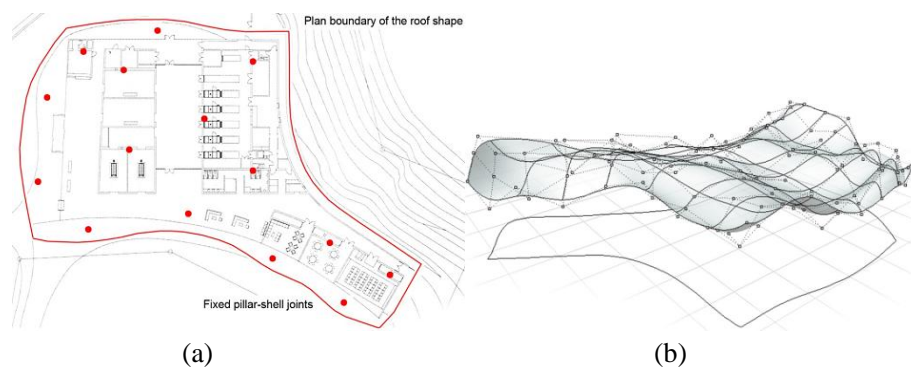
Figure 1.3 – (a) Boundary conditions of the form-finding process; and (b) NURBS representation of the roof. Courtesy of Pugnale and Sassone.
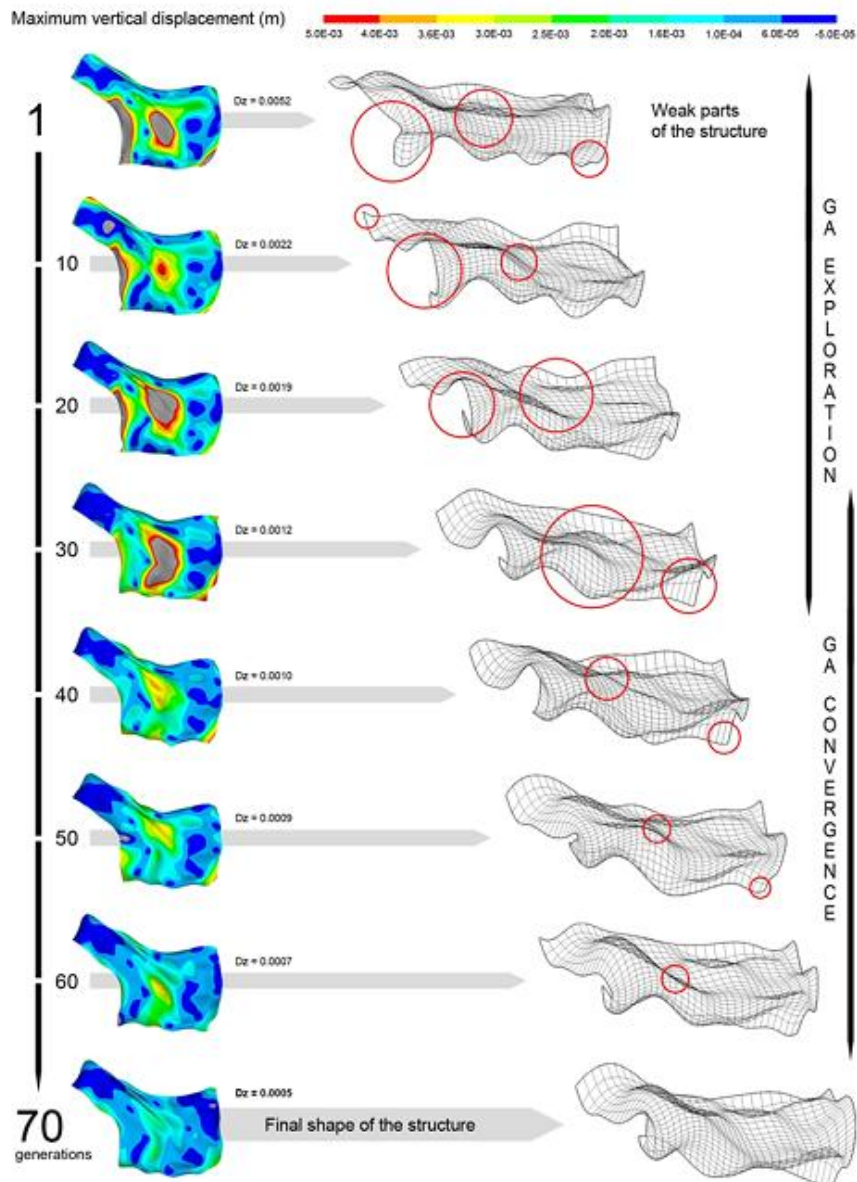
Figure 1.4 – Evolution phases of the morphogenetic process. Courtesy of Pugnale and Sassone.

9

VGSs, as already mentioned before, can be seen as the last step in the evolution of "form experimentation" but also as a new possibility to improve the limits of structural performances. In this second case VGSs can be combined with a sensing system and an actuator system to build the, so called, adaptive structures.

Other terms with more or less equivalent meaning and often used when referring to this kind of structures are "interactive", "responsive", "morphing", etc. Dealing with the subtle differences among these terms is out of the scope of this research therefore the terms have to be considered equivalent hereafter. However it is worth noting how the terms grew up according to the evolution of the idea they are associated to (Table 1.1).

Table 1.1 – Alternative definitions associated to Variable Geometry Structures.

System	Definition
Deployable	Implies the change of shape of the system. Few possible stable configurations (generally two) with at least one "open" and "closed" state.
Morphing	Implies the change of shape of the system. Several possible stable configurations, very often associated to truss structures and structures in the aerospace field (e.g. morphing wing).
Interactive	The term mainly comes from the information technology field and is sometimes preferred when the human input is involved.
Dynamic	Like *morphing*, basically introduced with the rotating tower project by Fisher.
Adaptive	These two are the most generic definitions. The change of the
Responsive	system, which is supposed to happen automatically depending on a specific input, may be independent of its shape.

Adaptive structures can answer the clear need to develop new technologies and strategies to address energy efficiency with appropriate procedures and building techniques, while taking account of the social acceptance by the buildings' users and the return on investment.

For instance, in a building, adaptive structures could be used to replace those elements of the envelope which have a higher potential contribution to reducing the

energy demand. Consequently, the roof and façade elements seem to be first to be addressed, both externally and internally.

In the first case, structural adaptivity is currently investigated as an innovative and effective solution leading to the, so called, "responsive skins". The aim is the performance enhancement of those facade elements which are subject to variable actions and, consequently, which could take advantage of changes in their configurations. Such elements are, for instance, solar panels and sliding shutters which behavior depends on the position of the sun or, also, wind turbines which on the other hand, rely on wind intensity and direction. As random, pseudo-random or just time dependent inputs are quite always associated to actions which are variable in space other than in intensity, it is straightforward the necessity for devices able to face such variability, that's to say it becomes a problem of inverse kinematics and optimization over some kind of VGS. The best solution, in terms of VGS, obviously depends on the particular faced problem because every VGS has its own characteristics. This concept is further exploited in Chapter 2.

1.2.   Background – drivers of the project

At the reduced scale of the project, the contribute of innovative solutions is readable according to three main parameters: performance, costs and constructability. Their mutual relationship determines in fact the goodness of the project. Figure 1.5 symbolically represents the quality of the project through a triangular area and the greater the area the better.
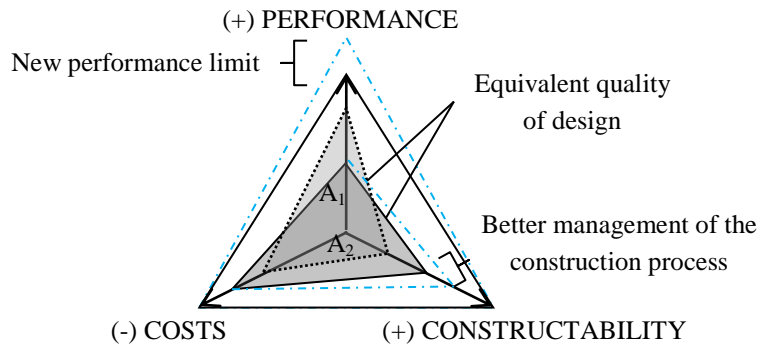
Figure 1.5 – Diagram of the relations among the three main aspects of design.

Usually once an optimal design solution is achieved (greatest area) the triangle can still change its shape according to possible compromises achievable among the three parameters but is unlikely to get better results if the boundary conditions (instruments, technology, knowledge, etc.) don't vary. Innovative solutions ''improve'' the area of the inner triangle (better use of available resources) or the shape of the outer triangle (new limits for performance, costs, constructability), or both.

The applications reported in this thesis focus on one or more of these three parameters in different contexts.

1.3.   Motivation

The scenario depicted by the current research and experimentation in architectural engineering is defined by many and varied design drivers. Among these, the aesthetic component is undoubtedly one of the most considered and the designer's desire to impress inevitably falls primarily on what is the main component in the appearance of a building: ***the form***.

Form also influences and, in turn, is influenced by various aspects of design (Figure 1.6). While in the past, with a more limited range of possible geometries, aspects such as size, the tones, materials, decoration, etc. could be referred to as the major figure of discrimination in architecture, now they are again secondary parameters. The ability to model and visualize any kind of volume or surface, thanks to CAD/CAE and constructive possibilities given by the "file to factory" and CNC technologies have allowed designers to propose a new kind of geometry called "complex" or "free form" which is quickly became the symbol of the major brands.

Again the tools and their growing computational simplification have played a key role in the more recent introduction of the concept of "interactivity" in architecture. But in the most cases *interactivity* still plays almost exclusively a role of scenic effect, like a new frontier in the current experimentation of complex shapes. Following the trend of organic architecture, it could be said that shapes are preparing to evolve their last step, becoming natural not only because of their appearance but also because of their behavior.

12
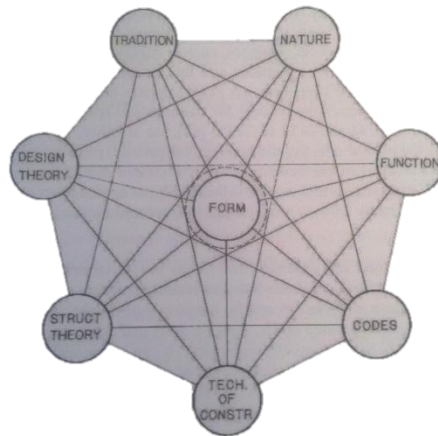
Figure 1.6 – Circle of influence on Form (*Bulletin of the IASS* 70, 1979, p.43, [Medwadowski, 1979]).

If, on the one hand, the phenomenon of *complex* shapes and the one of *interactive* shapes represent the ultimate steps of evolution of the geometrical experimentation in architecture, on the other hand they have inevitably had an impact on the work of the engineer and, more generally, on the approach to engineering design.

The engineer mainly cares of the performance of the structure and always tries to choose a solution on a rational basis. Since the number of possible solutions is increasing, the engineer needs then to consider more and more design variables such that its final choice could be determined by optimum criteria.

As a consequence, questions about the methods are arising:

- Do the currently available tools and methods have to be redesigned?
- How to deal with always more multidisciplinary activities?
- What is the role of form-finding, morphogenesis and optimization in today structural design?

and the main motivation of the current research places in this context.

1.4.   Problem Statement

From every point of view it is not suitable to waste natural resources and human efforts, therefore, recalling the words of F. Otto [1996]: *"Structures cannot be designed arbitrary"*.

From the previous discussion, one is still the key problem to outline and it can be briefly expressed through the "not-new" question:

<p style="text-align:center;"><u>*how to better control the structural form*</u>?</p>

However, it is worth noting that the novel perspective from within the above statement is considered herein, involves both the concepts of complex and variable geometry.

1.5.   Scope of the Research

Recalling the few questions arisen at the end of section 1.3, the stated problem is faced with emphasis on the methods development in the form-finding field.

The scope of this research is then to first recognize the new issues in the form-finding field and to understand the limits of applicability of the available methods to the new structural and architectural context.

A specific issue to investigate is considered the extension of the concept of form-finding to VGSs. This in turn means to propose a flexible approach based on a unique suitable representation model to manage not only different purposes but also different input structural systems.

Besides the generic approach, the development of algorithms to tackle specific design issues is expected as a proof of concept.

1.6.   Methodology

The way the stated problem is approached is with in mind the current architectural trend and structural variety. Since the number of structural morphologies is increasing the available methods to control the form may not always be suitable. New methods are therefore needed and proposed every day. As a consequence the number of available methods is increasing too, leading to a messy scenario for the designer. There are plenty of different methods to solve almost every kind of problem but there is still an acute need for methods which are flexible enough to tackle several different tasks at a time.

In the developed methods the concepts of *flexibility* and *clarity* are proposed both in term of applicability to different purposes and to different structural systems apparently quite different.

For instance, as discussed in section 1.1 the relationship between complex geometry structures and variable geometry structures can be seen as a continuous process of evolution towards more organic forms. The same approach is proposed in this thesis when dealing with form-finding and optimization methods. Since the variation in the configuration of a variable geometry structure is basically still a variation of form, then a method which applies to static structures is still potentially suitable if the kinematics is treated separately.

The proposed methods are then built according to the above principle such that they can be flexibly adapted to work the same both when only statics and when statics and kinematics are involved.

Table 1.2 – Scheme of the optimization process for a "static" structure and for a VGS. The process can be the same if kinematics is considered separately for the VGS case.

Input structural system	Optimization process	Solution(s)
Static structure	⇨	Only one solution (average optimum)
Variable geometry structure	Kinematics compatibility restraints	Two or more solutions (local optimum)

15

To prove the *effectiveness* of the proposed approach a wide range of applications is proposed concerning:

- Structural performance
- Building physics
- Constructability and costs

Every proposed case study deals with a current issue in the design of complex or variable geometry structures and exemplifies how the new possibilities in terms of shapes/configurations can enhance performance.

1.7.   Organization of the book

The dissertation is divided into four parts. In Part I, the motivation and goals of the research are defined and framed within the current state of the art.

Chapter 2 reviews the relevant literature and discusses the current state of representation for both complex geometry and variable geometry structures both in terms of structural systems and mathematical models.

Part II introduces the concept of optimal form-finding and, after reviewing the most recent advances in this field, proposes two novel algorithms.

Chapter 3 groups the existing form-finding methods into three main categories using a unified symbolism. Previous methods for the form-finding of three-dimensional framed structures are then reviewed and assessed, and a critical overview is given of the approaches and the main features which have influenced the development of the algorithms proposed in chapters 4 and 5.

Chapter 4 introduces the VFDM method. It states the assumptions, fundamentals and key concepts; outlines the method in an overview of the main steps in the methodology; sets up the equilibrium constraints of the framework model; formulates the problem using the generality of graph theory; and explains the solving procedure.

Chapter 5 proposes a strategy where the use of the VFDM is in combination with a general evolutionary algorithm to extend the optimal form-finding approach to mechanism-like structures (adaptive structures). The resulting procedure is presented with the name of Finite State Control Strategy (FSCS).

Part III presents applications and results of the proposed algorithms.

Chapter 6 shows the results of using the VFDM for the enhancement of free-form grid-shells geometry in order to validate the method and point out its versatility. Firstly how to approximate generic complex-shape geometry by means of a limited range of frame typologies is discussed. A second problem concerns the generation of planar-quadrilateral free-form meshes. A multi-objective procedure that involves static analysis combined with the discussed geometrical optimization is finally proposed.

Chapter 7 analyzes the problem of the design of an adaptive ceiling for the enhancement of a concert hall acoustics. The case study demonstrates the power of the FSCS for the design exploration of different variable geometry systems considered for the main structure of an adaptive envelope.

Chapter 8 presents a fluid-structure interaction problem where the potential of controlling the adaptive skin (façade) of a high-rise building in order to minimize the wind induced vibrations on the structure is investigated. The case study is again presented within the FSCS framework.

In Part IV, Chapter 9 provides general conclusions and outlines the future work.
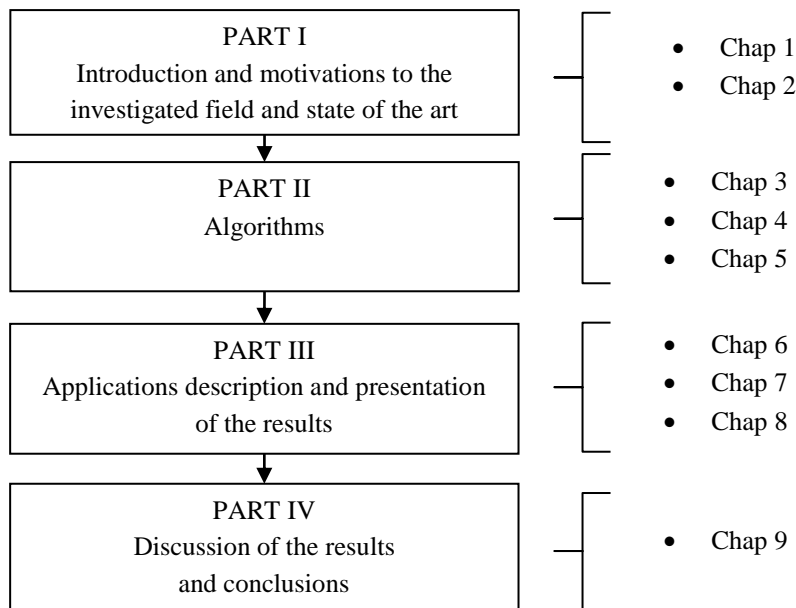
Figure 1.7 – Visual representation of the organization of the book.

Chapter 2

Complex to variable geometry systems in structural design

Abstract

First an overview of the state of the art of *complex geometry structures* (CGSs) and *variable geometry structures* (VGSs) is presented.

Several possible different representations of complex geometry are then illustrated and one of these is chosen to be as a reference in this thesis. According to the selected geometry representation model, a convenient matrix procedure for the kinematic analysis is then defined.

2.1. Free-Form Structures

> *"…And thus it is possible to build successfully forms so varied…that is only the announcement and proclamation of the revolution that is approaching in the field of architecture, whose vocabulary of plastic forms is opening and widening with rapidity and imaginative fecundity unknown in all the history of Construction."*

(Translated from the Spanish original text, Torroja [1960]).

19

The above words were written by EduardoTorroja in 1957 and they are an expression of his visionary thought about the future of construction. Torroja most famous work was in the field of concrete thin shells (e.g. Figure 2.1) and together with the contribution of other remarkable designer like Le Corbusier, Felix Candela (Figure 2.2), Pier Luigi Nervi, Heinz Isler, etc. he put the basis, between the '50s and the '60s, for the development of complex shapes in architecture.
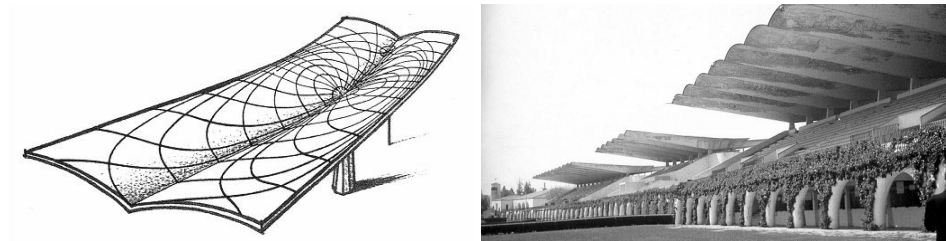
Figure 2.1 – Zarzuela Hippodrome by Eduardo Torroja, Madrid, 1935.
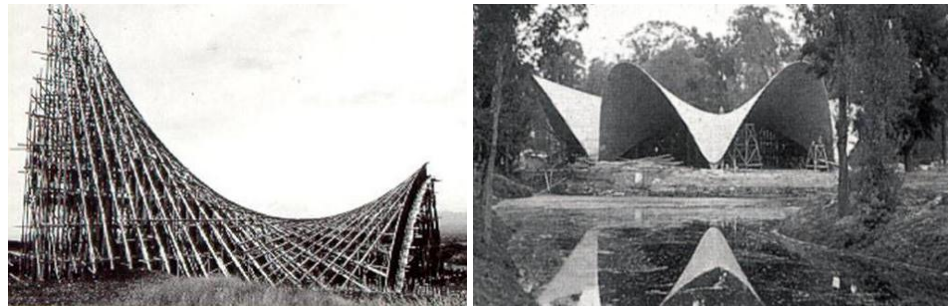
Figure 2.2 – Restauramt at Xochimilco by Felix Candela, Mexico City. 1958.

Quite obviously, in fact, the first free form structures were all made using reinforced concrete for a set of reasons but mainly because of the difficulties of building a smooth and organic shape by means of any other material. Regarding the construction material itself, masonry is generally still today not suitable to build a freeform structure because of the compression-only behavior, even if recent advances in the analysis and design of masonry vaults [Block, 2009] make this sentence less true and masonry structures like the one in Figure 2.3 are possible.

Figure 2.3 – Free-form Catalan Thin-tile vault, project by the Block Research Group, ETH Zurich, (http://block.arch.ethz.ch/projects/freeform-catalan-thin-tile-vaulting).

Regarding the modeling and constructability, the complications due to the design of nodes in the three dimensional space are limited compared to an equivalent steel or wooden structure thanks to the process of setting and hardening of the concrete. Moreover in the '50s it is unlikely that the manufacturing offered a customized range of element typologies both referring to the structure and the cladding. It is unlikely, as well, that the lack of computational tools allowed the effortless calculation and verification of whatever static scheme. In this sense, in fact, also many of the first freeform concrete structures were calculated using equivalent strut-and-tie schemes, thus neglecting the concrete shell contribute in terms of static performance, but only accounting it in terms of dead load, using its plastic and pleasant way of filling an empty space. This is for example the case of the Longuelo Church by Pino Pizzigoni, as testified both by the conception sketches (Figure 2.4c) and by the building process (Figure 2.4e,f).

In Italy Pino Pizzigoni was a pioneer of freeform design and with him also Sergio Musmeci and Luigi Moretti are worth to be remembered. Figure 2.5, Figure 2.6 and Figure 2.4 show three representative works respectively made by the three designers in the 1950s.
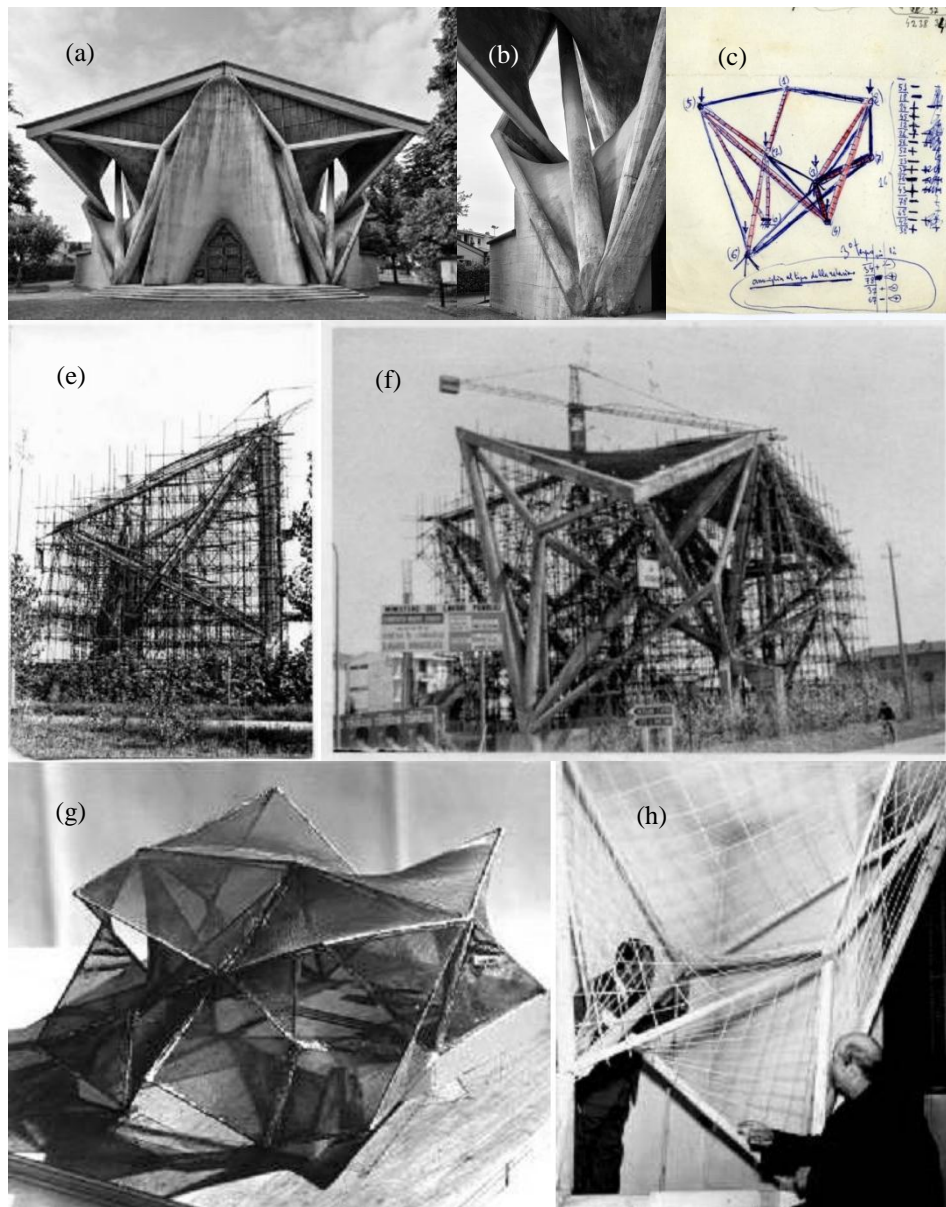
Figure 2.4 – Church of Longuelo, physical models and realization by Pino Pizzigoni (1965).
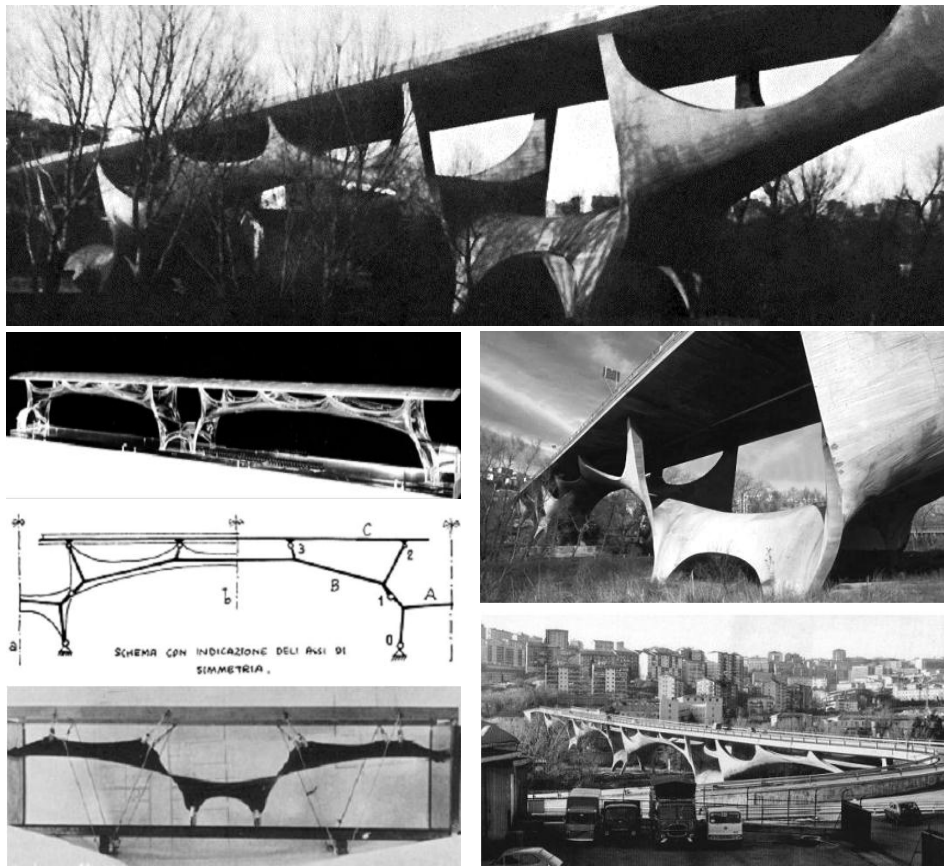
Figure 2.5 – Bridge on the Basento river, physical models and realization by Sergio Musmeci (1967 -1976).
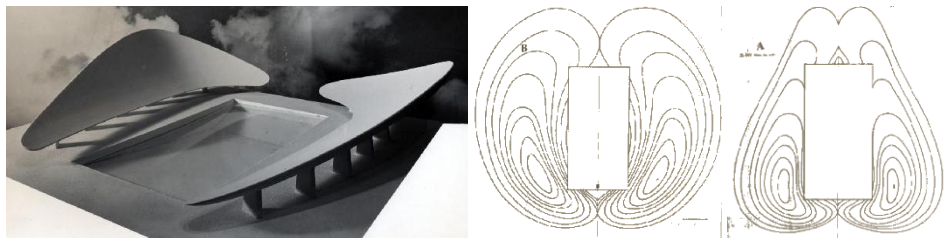
Figure 2.6 – Parametric model of a stadium for swimming by Luigi Moretti (1960).

Later in the 1970s, the impact of the computer allowed for the first numerical modeling and simulation of membrane structures which represent a second step towards free forms. However is when the first important steel structure was built with a non-conventional form that the term *freeform* really got its actual meaning. This structure is almost globally recognized to be the Guggenheim museum in Bilbao by Frank Gehry in 1997.

Passed more than ten years from the Guggenheim in Bilbao, today freeform structures are built using a variety of systems and materials as shown in the Figure 2.7 and Figure 2.8. The rising of free forms has then led to significant changes to the entire architectural engineering scenario, from concept to detail design, from production to construction and so on, the *mass customization*[6] to be one of the most important. The design issues related to this type of structures have been such as to justify the creation of specialized groups within engineering companies, namely the Advanced Geometry Unit (AGU) of Ove Arup, the Black Box of Skidmore Owings and Merrill (SOM) and the SMART group at Buro Happold.

Together with this trend, a number of research studies have also begun focusing on this topic. For instance, it is worth noting the recent attempt to categorize free forms made by the TU Delft[7]. Categories are based on the operations like bending, scaling, twisting, etc. by which a base geometry is transformed into a freeform one. The most of the studies, included the present one, have instead been targeted at making both iconic and ethic the role of freeform structures, allowing the design of unconventional geometries with a very low waste of resources or even leading to an enhancement of the overall performance. However, regardless of the years of research and the use of the latest technologies, the icon role remains often predominant and the ethic of structure like the Beijing Bird's Nest (US$423 million cost, more than 110.000 tons of steel, 10 casualties during the construction – Figure 2.9) is still questionable.

---

[6] **Mass customization**, in marketing, manufacturing, call centres and management, is the use of flexible computer-aided manufacturing systems to produce custom output. Those systems combine the low unit costs of mass production processes with the flexibility of individual customization (from Wikipedia).

[7] http://www.free-d.nl

Figure 2.7 – Walt Disney concert hall, Los Angeles, US, by Frank Gehry.

Figure 2.8 – Docks de Paris, Jakob and MacFarlane, 2009.

Figure 2.9 – Bird's Nest Stadium by Herzog & de Meuron, Beijing, China, 2008.

2.2.   **Variable Geometry Structures**

The concept of structural adaptivity has been introduced in Section 1.1.2. Since its intended meaning herein is specifically related to the morphological variation of the structure, it is useful to look at adaptive structures as the combination of two major components, i.e. the *structural system* and the *control system*. Both components are fundamental but, while for the latter devices are the same of those used in active control practice, it is in the former that the concept of structural adaptivity mainly emerges.

An adaptive structure requires the whole structural system or at least some of its elements to be able to change their geometry. This requirement leads to the field of mechanism-like structures or, in other words Variable Geometry Structures (VGSs).

VGSs have the function to respond to changing situations in their use, operation or location, by modifying their configuration. The mechanism is driven by actuators composed by smart materials [e.g. Sofla et al., 2007] or more traditional hydraulic engines. Another important aspect, always cited when dealing with such kind of structures, is stability. A discussion about stability is outside the present scope but a few references on multi-stable mechanisms are mentioned [Guest and Pellegrino, 2006; Seffen, 2007; Briccoli Bati et al., 2009].

VGSs can be classified according to their structural system. In doing so, four main groups can be distinguished: spatial bar structures consisting of hinged bars,

foldable plate structures consisting of hinged plates, strut-cable (tensegrity) structures and membrane structures. These structural systems have been classified by their morphological and kinematic characteristics by Hanaor and Levy [2001]. This classification is presented in Figure 2.10.

In this paper the focus is on kinematics, consequently such structures, according to their process of transformation, can be distinguished into only two main categories. The first category – *deformable* – includes those that rely on the intrinsic property of their material to change configuration, like engineering balloons that are blown up with hot air, whereas the second category – *rigid links* – consists of those that rely on the geometric inter-linking of their elements to change configuration; this latter category usually contains a number of essentially resistant bodies, which are connected by hinges employed to enable movement along one or more degrees of freedom. In the next paragraphs, according with the two mentioned categories, some of the most recent significant applications in architecture and some of the most promising ideas are presented.
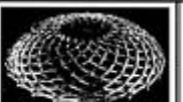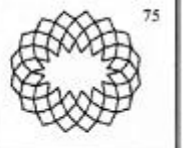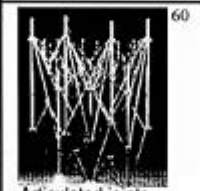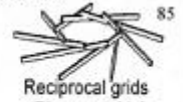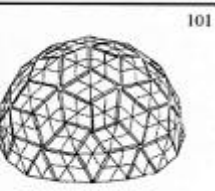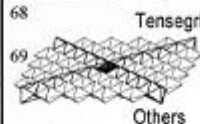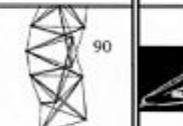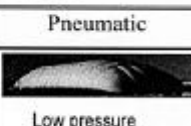
		Morphology			
		Lattice			Continuous
		DLG	SLG	Spine	Plates
Kinematics	Rigid links	Pantographic (scissors)			Folded Plates
		Peripheral Scissors 19 / Radial scissors 22 / 55 / Others	Angulated scissors 74 (retractable roofs) 75	Masts and arches 16 / 98	Linear deployment 110 / Radial deploymemt 5
		Bars			Curved surface
		Articulated joints 60	Ruled surface 83 / Reciprocal grids 85 (Dismountable)	93	101
	Deformable	Strut-cable systems	Tensioned membrane		
			Fabric		Pneumatic
		Tensegrity 68 / 69 / Others 90 / 97	120 / Hybrid 88 / Ribbed		Low pressure 124 / High pressure

Figure 2.10 – Classification of VGSs on the basis on their morphological and kinematic characteristics by Hanaor and Levy [2001].

28

2.2.1. Deformable

a)   Compliant mechanisms

Due to the hingeless nature, compliant mechanisms offer numerous advantages over traditional mechanisms. The ability to store strain energy in compliant mechanism eliminates the need of return springs and can be used to design bi-stable mechanisms such as in [Golabchi and Guest, 2009]. The monolithic feature reduces the number of joints and fasteners in the assembly, leading to weight savings. Furthermore, the absence of joints in compliant mechanisms eliminates the backlash seen in kinematic joints, thus providing high precision and highly repeatable motion. The noise and wear associated with kinematic joints are also eliminated, which further reduces the cost for maintenance and enhances performance.
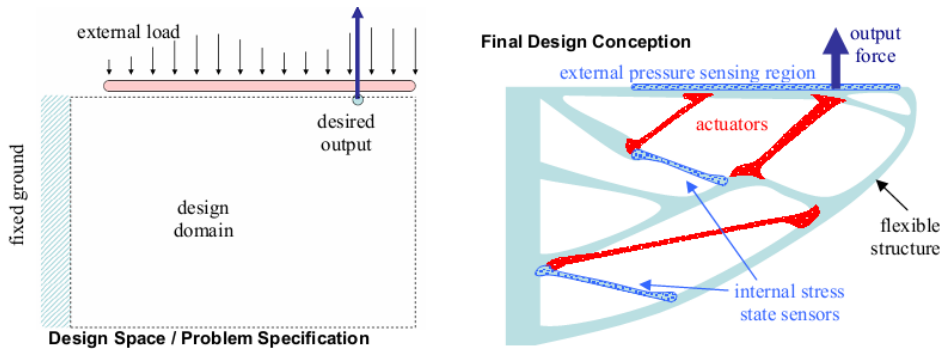
Figure 2.11 – Design of a fully-compliant system with embedded and distributed actuators and sensors, given a specified design space, external loading conditions, and desired mechanical task (Trease and Kota, 2006).

If the compliant mechanism is a "fully distributed" one, there is also a sensible reduction in stress concentration and a smooth deformation throughout the structure is possible and particularly attractive to shape morphing applications [Kota et al., 2001]. Moreover, due to the absence of backlash and wear, a compliant mechanism is particularly effective to work with small displacements (1-100 μm) usually provided by smart actuators [Lu, 2004].

Despite the potential advantages and a consistent number of studies and applications in fields like precision engineering and aircraft engineering, there are no relevant studies related to applications in architecture.

b) Tensegrity structures

Tensegrity structures have a long history [Buckminster Fuller, 1978] and, being composed by rigid bars and cables as bones and nerves in the body, they are also belonging to the class of bio-inspired structures. Acting on the cables it is possible to modify and optimize the shape of the structure and even obtain fully deployable systems [Skelton and de Oliveira, 2009]. Figure 2.12 illustrates a prototype of an actuated tensegrity type space structure. Different types of applications have been proposed in aerospace engineering and robotics. Small and large structures have also been proposed in the civil engineering field. A large scale example is described in [Pedretti, 1998]. The study of the shapes is one of the crucial aspects in the design of tensegrity structures and in some cases instabilities can arise. These situations can be overcame by adding active control, as proposed in [Del Grosso et al., 2000]. Tristan d'Estree Sterk of The Bureau for Responsive Architecture and Robert Skelton of UCSD have been working on shape-changing "building envelopes" using "actuated tensegrity" structures, i.e. a system of rods and wires manipulated by pneumatic "muscles" that serve as the building skeleton, forming the framework of all its walls [d'Estree Sterk, 2006]. Within the project sensor/computer/actuator technologies are used to produce a series of intelligent building envelopes that seek fresh relationships between 'building' and 'user'. These responsive buildings are covered by skins that have the ability to alter their shape as the social and environmental conditions of the spaces within and around each building change. Figure 2.13 represents one of the first for such kind of buildings.

Although extensively studied for application to architecture and subject of different patents, no significant realizations with or without 'adaptive properties' have been performed to date.

Figure 2.12 – Actuated tensegrity prototype by Tristan d'Estree Sterk and ORAMBRA, 2009.
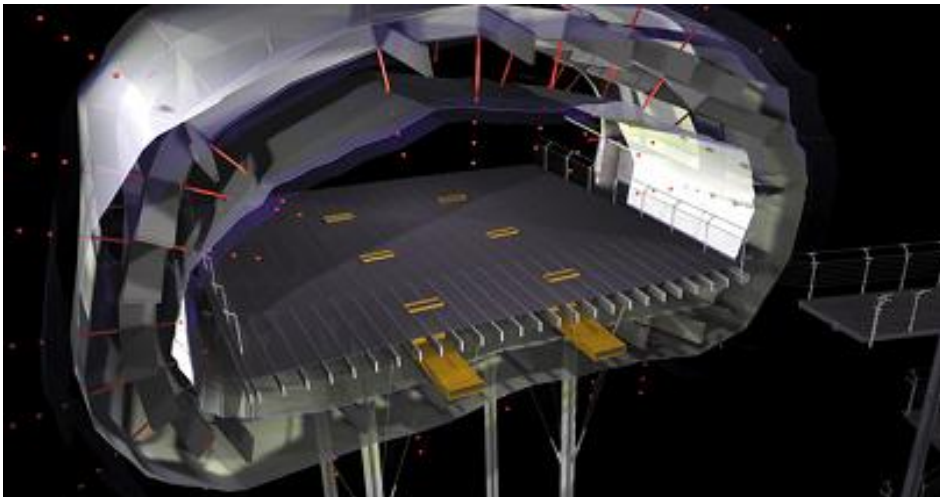
Figure 2.13 – Responsive envelope by Tristan d'Estree Sterk at The Office for Robotic Architectural Media & The Bureau for Responsive Architecture, 2003.

c) Pneumatic structures

31

The lighter the structure the easier and the more precise can be movement. If the proper movement can also be achieved by air pressure, i.e. if costly and heavy mechanisms can be avoided, literally light-weight movements can be achieved. Pneumatic structures fulfill these requirements of light weight and flexibility. In structural engineering pneumatic structures are known as air-inflated and air-supported structures. While in air-supported structures the air pressure is applied between the surface and the ground, in air-inflated structures the air pressure is enclosed in a cushion or a tube.

The development of pneumatic structures started with air-supported structures, but they have to deal with several problems like a big air volume and a comparable low air pressure, which is restricted because the interior is used by people. On the other side the air-inflated structures enclose the pressure with a continuous membrane so that the interior is decoupled from the pressure. Looking at the adaptive potential of pneumatic structures, air-inflated structures seem to be more suitable [Wang and Johnson, 2003] as there will be a smaller amount of air volume which has to be handled, a wider range of different air pressures are possible and no compatibility with human restrictions, i.e. influence of air pressure to the human body, is necessary. Hence the pressure difference is both the stabilizing and the form giving parameter. The structure is therefore very sensible to pressure changes. The above mentioned need for regulation of pneumatic structures leads to the idea of implementing the desired motion by the same mechanism without any extra motors or cable pulls. Ideas like this go back to designs from the '70s when T.Oki & Associates designed in 1969/70 a flexible umbrella with a central movement and are today the focus of several research projects as the movable roof in Figure 2.14 from Böegle et al. [2009].

One more interesting aspect we just want to mention here is the possibility, given for example by materials as ETFE films, to allow transparency, which consequently and very easily drives to lighting and energy considerations.

32
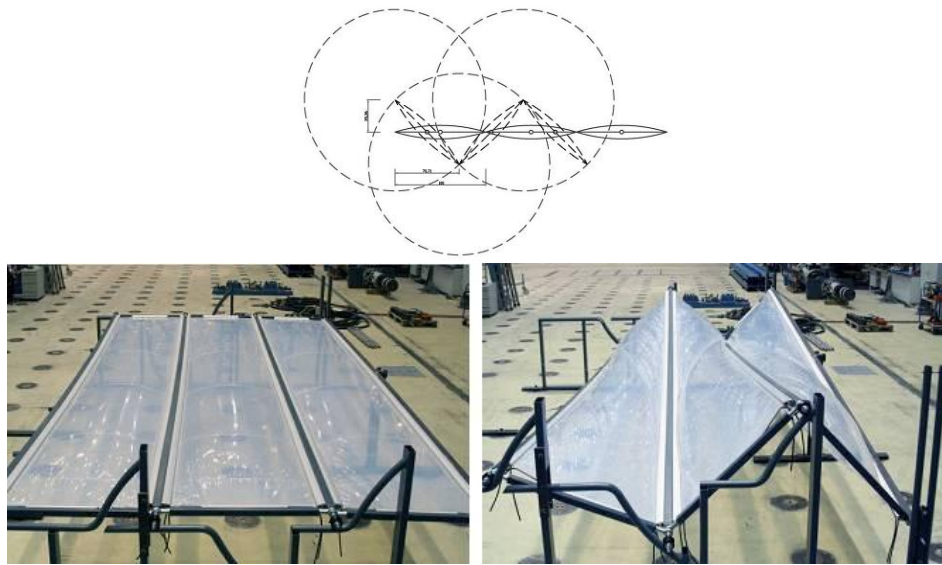
Figure 2.14 – Kinematic scheme and two different configurations of an adaptive pneumatic structure prototype model (courtesy of A. Böegle et al.).

2.2.2. Rigid Links

a) Mutually supported elements

Mutually supported elements (MSE) arranged in closed circuits create MSE modules. These modules are also known as reciprocal frames [Popovic, 1996] or nexorade fans [Beverel, 2000]. MSE circuits may be connected one to another to generate much larger space structures. Such configurations are generally 3-dimensional and non-traditional in form and differ from better known truss assemblies because elements join each other not only at the ends but even at intermediate points. There are various ways of connecting circuit elements together, bolting being one of the most simple and effective methods [Rizzuto, 2006]. Space structures assembled and connected in this way have the potential advantage of eliminating complex ball-joint type connectors traditionally used in lattice type assemblies. One of the most interesting aspects of this structural system is the possibility to manage restraints in order to allow a frame to change the position of

its supporting point by sliding on another frame (Figure 2.15). This particular kinematic behavior of MSE is fascinating for many researchers [Parigi et al., 2009] who consider such structural system promising for applications in the field of adaptive structures.

However available studies involve mainly the static behavior of MSE and no significant realizations in the field of adaptive systems have been performed to date.
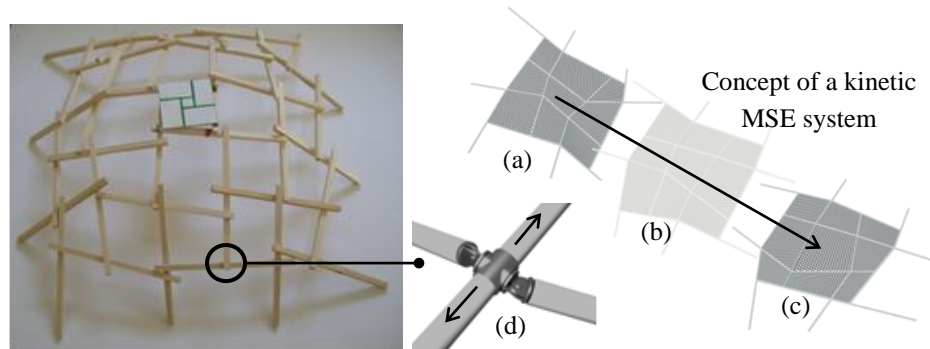
Figure 2.15 – (a, b, c) Different spatial configurations of MSE obtained by sliding frames one on another and (d) a node detail.

b) Rigid foldable origami

Several applications of folded surfaces can be found in architecture (Figure 2.16). However, only in the last years the kinematic behavior of origami has been taken into consideration for adaptive architectural envelopes [Heinzelmann, 2009]. Non-static examples of origami structures mainly come from space engineering where deployable surfaces have been studied since a long time ago. A particular kind of origami is the so called 'rigid foldable origami', extensively studied in mathematical theory [Belcastro and Hull, 2002; Balkcom et al., 2004] and also successfully applied in space engineering [Miura, 2009]. A rigid-foldable origami is a piecewise linear developable surface that can realize a deployment mechanism if its facets and fold lines are substituted with rigid panels and hinges, respectively. Such a deployment mechanism looks interesting also in an architectural context because its structure, based on watertight single surfaces, is suitable for constructing an envelope of a space, and because its purely geometric mechanism does not rely

on the elasticity of materials. A well-known developable double corrugation surface, which is rigid foldable as well as developable and flat-foldable, is the Miura-ori [Miura, 1970] and it is for example utilized in the packaging of deployable solar panels for use in space or in the folding of maps. The rigid-foldability of Miura-ori is due to the singularity in its pattern, where a single vertex is repeated but it has been demonstrated by Tachi [2009] that it is possible to achieve rigid-foldability in quadrilateral mesh origami without the trivial repeating symmetry. The resulting one-DOF finite rigid motion which characterizes this kind of opening mechanism is suitable for low-energy actuation while the possibility to switch between general shapes allows an unconstrained design. A generalized controlled finite rigid motion with more than one-DOF is one of the next steps to be investigated but still a today unachieved result.

Figure 2.16 – Origami structures in architecture – from left to right: (a) Air Force Academy Chapel by Skidmore Owings & Merril in Colorado Springs, USA, (b) Theatre Lelystad by UNStudio, The Nederlands (picture by Hans Veneman, 2007), (c) International Cruise Terminal by Foreign Office Architects+Arup in Yokohama, Japan.
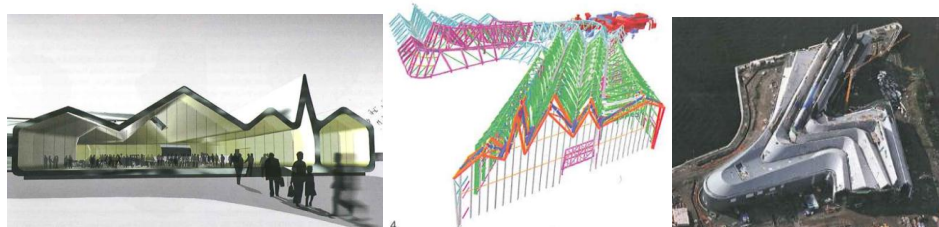
Figure 2.17 – Glasgow Museum of Transport, 2004-2011.
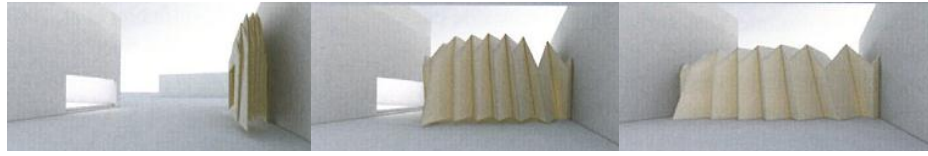
Figure 2.18 – Model of 1DOF deployable rigid-foldable quadrilateral origami envelope, courtesy of T. Tachi.

c) Morphing truss structures

A space truss is defined as a three-dimensional system of bars connected at their nodes by frictionless hinges or joints which is subjected to forces applied only at the joint centers. The conventional fixed shape space trusses consisted of tetrahedral truss units, which provide high stiffness and strength to weight. They can be designed as doubly curved structural systems such as the roof of the Eden Project's structure and Buckminster Fuller's geodesic dome in Montreal. The high specific stiffness of space trusses also makes them well suitable for large space structures, where the high cost of orbital insertion drives the design of mass efficient concepts.

Shape morphing can be easily fabricated from well-known traditional truss structures by replacing some of the trusses with linear displacement actuators [Sofla et al., 2009]; on the other side joints represent one of the main challenges [Sofla et al., 2007]. The first application of an adaptive structure using a Variable Geometry Truss (VGT) mechanism is showed at the International Expo 2005, Aichi, Japan [Inoue, 2008]. The presented movable monument (Figure 2.19), composed of three identical movable towers; each tower comprises four actuating truss members and the monument's shape can be changed variably by controlling the length of each of its extensible actuators.
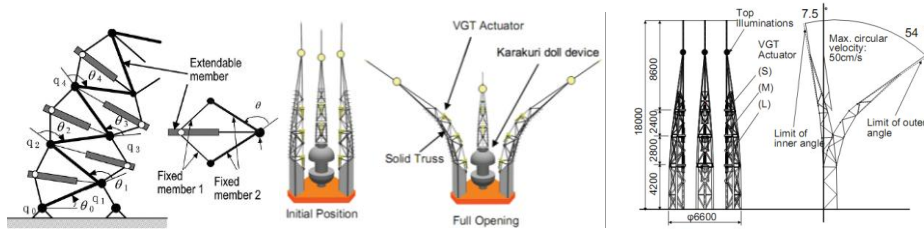
Figure 2.19 – Scheme of the three morphing towers showed at the International Expo 2005, Aichi, Japan (courtesy of F. Inoue).

d) Scissor-like mechanisms

Most of the already developed kinetic structures have 'open-closed' or 'extended-contracted' body shapes based on scissor-like elements [Piñero, 1962; Calatrava, 1981; Hoberman, 1993; Pellegrino and You, 1997, Del Grosso et al., 1999]. Recently, proposals for adaptive kinetic structures using scissor-like elements have been given, i.e. structures where transformations occur between more than two different shapes to constitute more flexible shape alternatives [d'Estree Sterk, 2006].

Scissor hinge structures possess unique extension and rotation capabilities, and the modified scissor unit developed by Akgün, et al. [2007 and 2010] greatly increases the form possibilities for the structure. This modified scissor unit differs from common scissor units in the addition of two joints at a specific point in the mechanism. With the development of this modified unit, it is possible to change the shape of the whole system without changing the dimensions of the struts or the span. The proposed scissor structure is two-dimensional (Figure 2.20), but it is also possible to combine structures in groups to create three-dimensional systems.

Recent proposals (Barents at al., 2011; Guest et al., 2011) concern scissor-like mechanisms coupled with springs to achieve "zero stiffness" (energy free) systems as the one reported in Figure 2.21.
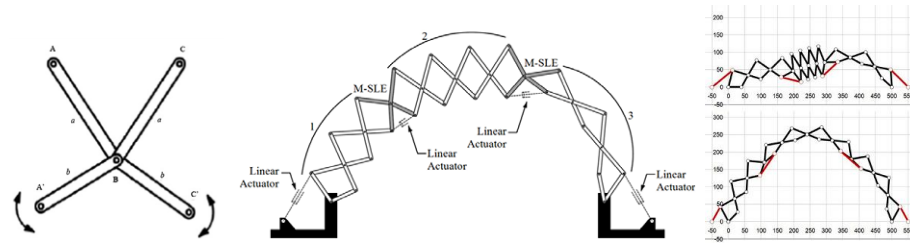
Figure 2.20 – From left to right: (a) – modified Scissor-Like Element (M-SLE), (b) – locations of M-SLEs and actuators on a scissor-hinge structure at a random geometric configuration and (c) – successive geometric configurations of the structure (courtesy of Y. Akgun et al.).

Figure 2.21 – Practical implementation of a gravity equilibrator using the parallelogram storage spring principle with zero-free-length spring (Barents et al., 2011).

38

2.3. Geometry and topology representation

A key step in the design process is the choice of a suitable representation for the structure geometry and topology. Since the research deals with complex geometries, this usually restricts the choice to one of the following two models:

- *Mesh*
- *NURBS*

In free-form structures, where the shapes cannot be generally described in terms of simple geometries, the desired surface could be approximated by a discrete mesh, composed by triangular or quadrilateral elements. The mesh is simply described by a set of nodal coordinates and the map of nodal connectivity (e.g incidence matrix or adjacency matrix).

Some advantages in free-forms representation are brought by NURBS, that is an acronym for "Non Uniform Rational B-Splines"[8]. This mathematical parametric formulation of surfaces has its antecedents in the Rational and Non-Rational B-Splines and in the Bézier curves and surfaces, used since the Sixties to solve engineering problems related to the representation of suitable 'free' curves in automotive design, and based on the Bernstein basis polynomials[9]. At present, NURBS could be considered as the standard way of describing and modeling free-form shapes in Computer-Aided Design (CAD) and, more in general, in computer graphics.

The surfaces represented by means of NURBS are defined by a control polyhedron and its vertices are called control points. Compared to the mesh representation, the NURBS control points (i.e. nodes) encapsulate more information than only the Cartesian coordinates. In fact, there are other parameters that affect

---

[8] The more complete manual of NURBS curves and surfaces is [Piegl and Tiller, 1995].

[9] The engineer Pierre Etienne Bézier was the first in developing parametric curves and surfaces during his work at Renault. A detailed biography with a description of his activity and inventions is provided in [Rogers, 2001].

the final surface shape and its mathematical definition, such as the degree and the knot matrix. The mathematical definition of a NURBS surface is given by Eq. 2.1 where *m* and *n* are the number of control points in the *u* and *v* direction respectively, *N* is a basis function which contains information on the degree (*p*) along a direction (*u* or *v*), $P_{i,j}$ is a control point and $w_{i,j}$ is its corresponding weight.

$$S(u,v) = \frac{\sum_{i=0}^{m}\sum_{j=0}^{n} N_{i,p}(u)N_{j,q}(v)w_{i,j}P_{i,j}}{\sum_{i=0}^{m}\sum_{j=0}^{n} N_{i,p}(u)N_{j,q}(v)w_{i,j}} \tag{2.1}$$

A graphical representation with highlighted the main components is instead shown in Figure 2.22.
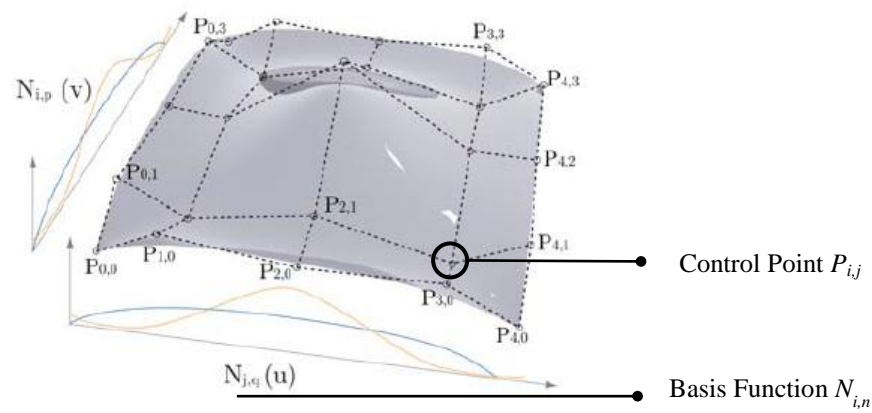
Figure 2.22 – NURBS representation of a free-form surface.

On the other hand the control polyhedron shows a much less flexible structure if compared to the mesh one. Moreover, a major drawback is that NURBS must be approximated by meshes in order to accomplish any kind of Finite Element Analysis (FEA). For further insight in the NURBS representation the interested reader may refer to Piegl and Tiller [1995].

Current research in this field looks with interest at hybrid approaches which can combine the advantages of both NURBS and meshes. A promising one is based on the so called *subdivision surfaces* [Shepherd and Richens, 2011]. Subdivision

Surfaces are well established surface modeling tools for computer gaming and animation, but have been overlooked by the construction industry despite presenting many benefits over more widespread techniques such as Splines or NURBS. By starting from a relatively coarse triangulated or quadrilateral mesh, each edge of the mesh is split into two by introducing a new vertex at the middle, and each facet is then be re-meshed to incorporate these new vertices.

Successive "subdivisions" of this type lead to finer versions of the mesh in a recursive manner, which eventually converge onto a single "limit surface".
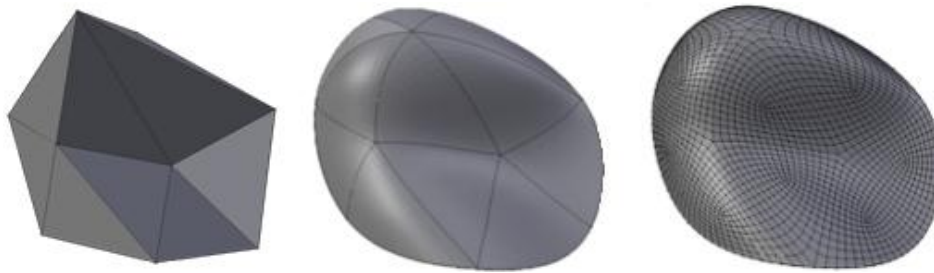
Figure 2.23 – From left to right: The rough mesh, the rough mesh projection on the final surface and the equivalent final mesh subdivided by means of the Catmull-Clark subdivision algorithm.

The inherent recursive level of detail which subdivision surfaces provide can be exploited in a number of ways for building design. The mesh facets can be used to represent cladding panels, or the mesh edges to represent structural members. The user can then sample the limit surface at any desired level of detail to result in panels or members of the desired size.

This readily-available hierarchy of multiple levels of detail is even more useful when combining geometric modeling with multi-disciplinary engineering analysis. Finite element analysis for example may require particularly small mesh elements in order to calculate the structural behavior of a proposed building structure to a reasonable degree of accuracy. However, the thermal or acoustic performance of the same structure might be calculable from a much coarser mesh. By using a subdivision surface as the basis for the model, the proposed building geometry can be sampled separately from a single definition, at exactly the right level of detail for each individual analysis, with very little extra overhead in terms of geometry

processing. Subdivision Surfaces can also be constrained to lie along a specified boundary, thereby allowing the designer more control over the resulting form.
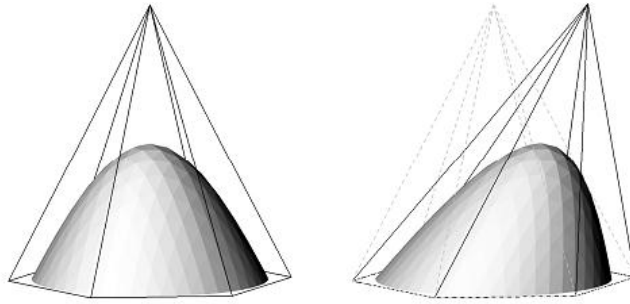
Figure 2.24 – The final subdivision surface shape is controlled by the rough mesh.

Another powerful but quite abstract representation takes advantage of the concept of *graph*. Graphs are widely used in literature but not so often associated to structures in the architectural engineering research where more specific representations are usually preferred. A derivation of the graph representation named as *framework* has been chosen here as the basis to describe the developed algorithms and the advantages of this approach are further explained in the following sub-section.

42

2.3.1. Frameworks

Edge $\mathcal{A}$

Node $\mathcal{N}$
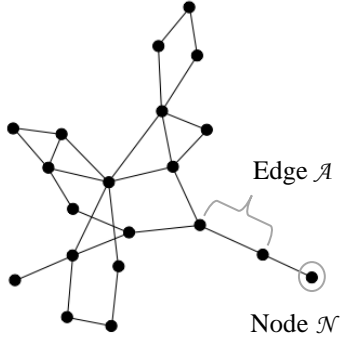
Figure 2.25 – Framework.

A framework (Figure 2.25), from the structural engineering point of view, can be defined as a discrete set of one-dimensional elements in the three-dimensional space, connected at their ends to points called nodes. As long as one can associate frameworks to meshes, then frameworks can represent a huge variety of structural systems (e.g. trusses, cable-nets, tensegrity, membranes, folded plates, etc.).

The basic properties of a framework can be derived from graph theory, which is the study of "*mathematical structures used to model relations between objects from a certain collection*" [Diestel, 2010]. In this context a framework is equivalent to a weighted graph $\mathcal{G} = (\mathcal{N}, \mathcal{A})$ – usually simple, i.e. a graph with no loops and no more than one edge between any two different nodes – where the nodal coordinates are weights associated to each node.

Definition 1. A framework $\mathcal{F} = (\mathcal{N}, \mathcal{A})$ is a weighted graph where:

- each node $i \in \mathcal{N}$ has associated with it a weight $w_i = f(x_i, y_i, z_i)$
- each edge $(i,j) \in \mathcal{A}$ has associated with it a weight $w_{ij} = f(l_{ij})$.

where $\mathcal{N}$ represents the nodes (vertices) of the framework, $\mathcal{A}$ represents the edges (arcs) of the framework and w_{ij} and l_{ij} represent the weight and the length of the edge $(i,j) \in \mathcal{A}$ respectively.

Therefore a graph and a framework share two fundamental characteristics: the *topology* and the *attributes*. Theoretically, everything in a framework could be described as a function of these two elements. The former is usually represented by the branch-node matrix $\mathbf{C}_{bxn}$, where b is the number of edges and n is the number of nodes. Other common ways of describing the topology make use of the transpose of $\mathbf{C}$ – i.e. the incidence matrix – or of the adjacency matrix $\mathbf{A}_{nxn}$. Attributes instead

43

are associated values belonging to a framework, vertices or edges. If these values can be represented by a real number, then attributes are equivalent to weights. Referring to edges, for example, attributes can be seen as a vector $\mathbf{w}_b$ (attribute vector) of weights or as the corresponding square diagonal matrix $\mathbf{W}_b$ (attribute matrix).

A further important element often associated to a framework is the *Laplacian* matrix $\mathcal{L}_{nxn}$ which can be described as a combination of $\mathbf{C}$ and $\mathbf{W}$ in the following way:

$$\mathcal{L} = \mathbf{C}^{\mathrm{T}}\mathbf{W}\mathbf{C} \qquad (2.2)$$

It should be noted that, if the weights of the edges are seen as a set of force densities $\mathbf{q}$ ($q_i = f_i/l_i$, $f_i = i$-th element force, $l_i = i$-th element length) [Shek, 1974], such that $\mathbf{W} = \mathbf{Q}$, then $\mathcal{L}$ becomes a very famous matrix in the classical form-finding literature, known with the name of force-density matrix [Tibert and Pellegrino, 2003; Estrada et al., 2006; Tran and Lee, 2010] or (small) stress matrix [Connelly, 1999; Guest, 2006] or equilibrium matrix [Zhang and Ohsaki, 2006]. Since this particular Laplacian is recalled several times in the next session, it is useful to define:

$$\mathcal{L}_Q = \mathbf{C}^{\mathrm{T}}\mathbf{Q}\mathbf{C} \qquad (2.3)$$

as the force-density matrix.

Leaving the abstractiveness of graph theory it is possible to bring the described elements into a structural analysis context. In particular, assuming small strains and small displacements, the three basic equations of structural analysis can be linearized and rewritten as a combination of $\mathbf{C}$ and $\mathbf{W}$. The system of static equilibrium equations for a structure is given by:

$$\mathbf{E}\mathbf{F} = \mathbf{p} \qquad (2.4)$$

where $\mathbf{E}$ is the *equilibrium* matrix, $\mathbf{f}$ is the internal force vector and $\mathbf{p}$ is the external load vector.

44

The system of kinematic compatibility equations is given by:

$$\mathbf{E}^{\mathrm{T}}\mathbf{d} = \mathbf{e} \tag{2.5}$$

where $\mathbf{E}^{\mathrm{T}}$ is the *compatibility* matrix, $\mathbf{d}$ is the external displacement vector and $\mathbf{e}$ is the internal deformation vector (edge elongations). The stress-strain relationship is given by:

$$\mathbf{K}\mathbf{e} = \mathbf{f} \tag{2.6}$$

where $\mathbf{K}$ is the *stiffness* matrix.

From the definition of attributes it is obvious that all the vectors – i.e. $\mathbf{d}$, $\mathbf{e}$, $\mathbf{f}$ and $\mathbf{p}$ – can be seen as a specific case of $\mathbf{w}$. Defining $\mathcal{E}$ as

$$\mathcal{E} = \begin{pmatrix} \mathbf{C}^{\mathbf{T}}\mathrm{diag}(\mathbf{Cx}) \\ \mathbf{C}^{\mathbf{T}}\mathrm{diag}(\mathbf{Cy}) \\ \mathbf{C}^{\mathbf{T}}\mathrm{diag}(\mathbf{Cz}) \end{pmatrix} \tag{2.7}$$

where $\mathbf{x}$, $\mathbf{y}$ and $\mathbf{z}$ are node attribute vectors representing the nodal coordinates, it is then possible to write $\mathbf{E}$ as

$$\mathbf{E} = \mathcal{E}\,\mathbf{L}^{-1} \tag{2.8}$$

where $\mathbf{L}$ is an edge attribute matrix representing lengths. $\mathbf{K}$ can be written as the sum of two contributions [Przemieniecki, 1968; Guest, 2006]:

$$\mathbf{K} = \mathbf{K}_{\mathrm{E}} + \mathbf{K}_{\mathrm{G}} \tag{2.9}$$

where $\mathbf{K}_{\mathrm{E}}$ is the *linear stiffness* matrix:

$$\mathbf{K}_{\mathrm{E}} = \mathbf{E}\,(\mathbf{G} - \mathbf{Q})\,\mathbf{E}^{\mathrm{T}} \tag{2.10}$$

45

with **G** and **Q** edge attribute matrices representing material stiffness ($G_{ii} = E_i A_i / l_{0i}$, $E_i = i$-th element Young modulus, $A_i = i$-th element section, $l_{0i} = i$-th element unstressed length) and force densities respectively, while **K**$_G$ is the *geometrical stiffness* matrix:

$$\mathbf{K}_G = \mathbf{I} \otimes \mathcal{L}_Q \qquad (2.11)$$

where $\mathbf{I}^{dxd}$ is the identity matrix and d the dimension of the space.

2.4.   Mechanism representation

A raw definition of mechanism could correspond to a structure which has a number of degrees of freedom greater than zero (DOFs > 0).

This leads to, at least, two considerations: firstly, in order to represent a mechanism, a representation of the structure has to be chosen. Secondly, the first problem to face when dealing with the representation of a mechanism is to correctly describe its DOFs.

Matrix structural analysis is the classical approach to describe both the statics and the kinematics of a structure [Przemieniecki, 1968] and can be effectively applied to this context. Particularly matrix analysis of pin-joint structures [Pellegrino and Calladine, 1986] is based on a representation of the structure geometry and topology which works well with the previously given definition of framework.

Therefore, taking advantage of this approach, the next sub-sections illustrate the basis of the matrix analysis of frameworks. The focus will be on the identification of those mechanisms which are to be considered in the design of a VGS.

2.4.1. Kinematically indeterminate frameworks

The concept of kinematical indeterminacy is center to an understanding of the mechanisms of a framework. This information can be obtained by analyzing the four fundamental subspaces of the equilibrium matrix $\mathbf{E}$ of the framework. Particularly a framework is considered to be kinematically indeterminate if:

$$m = rank(\mathbf{E}) - 3n > 0 \tag{2.12}$$

where n is the number of nodes of the framework and m (≥ 0) is the number of independent inextensional mechanisms. m is also equal to the number of vectors which span the nullspace of $\mathbf{E}$. Besides, the analysis of each vector composing the basis of the nullspace of $\mathbf{E}$ gives further insight into the mechanisms behavior as explained by Pellegrino and Calladine [1986].

2.4.2. Infinitesimal and finite mechanisms

Once a framework is known to be kinematically indeterminate it is then important to distinguish *infinitesimal mechanisms* from *finite mechanisms*.

Infinitesimal mechanisms practically correspond to displacements which are not relevant compared to the structure dimensions, i.e. don't allow a real change of the framework configuration and are therefore not suitable to build a VGS.

According to Koiter's definitions [Koiter, 1984] "*an infinitesimal mechanism of the first order is characterized by its property that any infinitesimal displacement of the mechanism is accompanied by second-order elongations of at least some of the bars. An infinitesimal mechanism is called of second (or higher) order, if there exists an infinitesimal motion such that no bar undergoes an elongation of lower than the third (or higher) order*".

A more precise definition of the order of mechanisms can take advantage of the formulation submitted by Tarnai (1984), formulation extended to multiparametered

case by Vassart et al. ([2000](#)), and which is similar to the one submitted by Salerno ([1992](#)). An internal mechanism is called mechanism of order "r" ($r \geq 1$) if there exists infinitesimal node displacement d (of the first order) such as member length variations are equal to zero until order r , but there does not exist infinitesimal node displacement s such as member length variations are equal to zero at order $r + 1$.

Mechanism of order $r \Leftrightarrow$

$$\begin{cases} \exists \mathbf{d} = O_1 \ (i.e.\ \mathbf{d} \neq \mathbf{0}): \mathbf{e}^{(1)} = 0, \mathbf{e}^{(2)} = \mathbf{0}, \dots, \mathbf{e}^{(r)} = \mathbf{0} \\ \qquad \forall \mathbf{d} = O_1: \mathbf{e}^{(r+1)} \neq \mathbf{0} \end{cases} \tag{2.13}$$

Where $\mathbf{d}$ is a vector of node displacements related to reference configuration and $\mathbf{e}$ is a vector of member length variations evaluated in respect to the reference configuration.

A mechanism is called *finite mechanism* if there exists a displacement which does not generate length variations of any order.

Many authors have worked on mechanism's order determination for kinematically indeterminate systems.

Calladine and Pellegrino ([1991a](#), [1992](#)) submitted a test, which was based on energetical computations and which allows to establish a distinction between mechanisms of the first order and of higher order.

Kuznetsov ([1988](#), [1991a](#), [1991b](#), [1991c](#)) developed a method based on the decomposition of the system in sub-systems. Tarnai ([1989](#)) used a geometrical method, with which he tested all the possible displacements in order to find (by a max (min) research) those which are associated with the least length variations. But this method can only be used for simple or periodic reticulated systems.

Salerno ([1992](#)) gave a numerical method based on energetic properties of systems. The corresponding algorithm is based on the calculation of deformation energy of system supposed to be in zero self stress state, and length variations for members appear in a quadratic form. In this method after a parametring operation, energy is developed as a series, whose increasing order terms are minimized. These

calculations are done in the vicinity of mechanisms, but without explicit decomposition of displacements in two orthogonal vectorial subspaces of R^N ($R^N = Im(A) \otimes Ker(A^T)$). Corresponding results, given in numerical form, give only an inferior limit of mechanism's order, certainly because of calculation complexity.

Vassart et al. (2000) describe an analytic method for which only geometrical properties of kinematically indeterminate systems are taken into account. With this method order of infinitesimal mechanisms can be evaluated without limitation for order's level. A stop criterion is also given so as to detect possible finite mechanisms of a kinematically indeterminate system.

However, dealing with the mechanism's order to determine if a mechanism is finite or not, it is not proved to be a safe method. The following alternative approaches are instead more effective:

- Symmetry identification;
- Simulation;
- Self-stress states avoidance ($s = 0$).

The *analysis of framework symmetries* has been successfully used by several authors [Tarnai, 1980; Guest, 2000; Tachi, 2010b] in order to recognize finite mechanism. The drawback of this method is the limited range of possible applications.

The *simulation of motion* proves that a mechanism is finite if at every step, provided that the step is small enough, the number of inextensional mechanisms m remains constant. In other words, the finite motion is ensured by keeping the degrees of freedom (DOFs) of the mechanism positive throughout the transformation. If any part of panels (faces) is not touching each other, in the three-dimensional space the DOFs are only given by the Jacobian matrix:

$$\text{DOFs} = m = b_{int} - 3n_{int} - 6\omega + \chi \qquad (2.14)$$

49

where b_{int} is the number of internal edges, b_{int} is the number of internal nodes, ω is the number of loop constraints of the framework (holes) and χ is the number of redundant constraints of the framework (singularities).

The method has been discussed by Tachi [2009a, 2009b] and successfully used to deal with origami foldability. However sometimes it may be preferable to avoid the simulation process which may be computationally expensive.

The third approach takes advantage of the fact that a framework with *no self-stress states* and $m > 0$ has exactly m finite inextensional mechanisms.

The extended Maxwell's formulation [Pellegrino and Calladine, 1986] states that:

$$s - m = b - 3n + k. \tag{2.15}$$

where b is the number of edges of the framework, n is the number of nodes, k is the number of external constraints, s (≥ 0) is the number of independent states of self-stress and m (≥ 0) is the number of independent inextensional mechanisms. If the structure is unconstrained and in the three-dimensional space (2.15) becomes:

$$m = m_i + 6 = 3n - b + s. \tag{2.16}$$

where m_i is the number of *internal* independent inextensional mechanisms.

The m_i mechanisms are finite then if:

$$s = b - \text{rank}(\mathbf{E}) = 0. \tag{2.17}$$

where $\mathbf{E}$ is the equilibrium matrix of the framework.

This method works the best if (2.17) is satisfied, otherwise further investigation of the nullspace of $\mathbf{E}$ is required to determine which mechanisms are stiffened by the self-stress states – e.g. by means of a simulation.

50

2.4.3. Simulation of motion

To simulate the motion of a framework there are at least two possible approaches in literature depending on the chosen set of variables: the *unstable truss model* or the *rotational hinges model*. The former represents the configuration of the structure by the positions of vertices. The change in the configuration is constrained by length preserving rigid bars along edges (creases and foldlines) and diagonals of facets ($2(k - 3)$ bars for a planar k-gonal facet); this model is used by Resch and Christiansen [1970], and it is suitable for directly using the points positions in a non-singular state. The latter represents the configuration by the rotational angles of edges and asserts the constraints so that closed loops cannot separate. This approach is for example used by Tachi [2009b] to simulate the rigid folding of origami.

Here it is straightforward to associate a framework to an *unstable truss model*. The inverse kinematics of the framework is then controlled by the Moore-Penrose generalized inverse, or pseudo-inverse of the Jacobian of the non-linear vector equation (constraints matrix):

$$\mathbf{\Omega}\,(x,y,z)\ = [\mathbf{l} - \mathbf{l}_0] = \mathbf{0} \tag{2.18}$$

where $\mathbf{l}$ is the vector of the edge lengths at the current step and $\mathbf{l}_0$ is the vector of the initial edge lengths. Equation (2.18) can be written in terms of the Cartesian nodal coordinates:

$$\mathbf{\Omega}\,(x,y,z) = (diag(\mathbf{Cx})^2\ + diag(\mathbf{Cy})^2\ + diag(\mathbf{Cz})^2\,)^{\,1/2} - \mathbf{l}_0 = 0 \tag{2.19}$$

where $\mathbf{C}$ is the incidence matrix of the framework and $\mathbf{x}, \mathbf{y}$ and $\mathbf{z}$ are the vectors of the nodal coordinates.

Equation (2.19) yields an underdetermined system, by exploring the solution space of which it is possible to obtain variations in the configuration. Valid shapes are found by perturbing the nodal coordinates according to the nullspace of the

51

Jacobian $\left[\frac{\partial \mathbf{\Omega}}{\partial \mathbf{x}} \mid \frac{\partial \mathbf{\Omega}}{\partial \mathbf{y}} \mid \frac{\partial \mathbf{\Omega}}{\partial \mathbf{z}}\right]$. The solution is calculated using the pseudoinverse $\left[\frac{\partial \mathbf{\Omega}}{\partial \mathbf{x}}\right]^{+}$ of the Jacobian as follows:

$$dx = \left(\mathbf{I} - \left[\frac{\partial \mathbf{\Omega}}{\partial \mathbf{x}}\right]^{+} \left[\frac{\partial \mathbf{\Omega}}{\partial \mathbf{x}}\right]\right) d\mathbf{x}_0 \tag{2.20}$$

where $d\mathbf{x}_0$ represents the initial perturbation and $\mathbf{I}$ is the identity matrix.

Equation (2.20) finds the valid perturbation closest to $d\mathbf{x}_0$ by orthogonal projection to the solution space. Euler integration of this infinitesimal motion is executed. For each step, the residual has to be eliminated by the Newton-Raphson method or any other equivalent method.

It is worth noting that considerations are limited to geometric ones and elastic or plastic behavior of the structure with specific materials is not analyzed.

52

Part II
Algorithms

Chapter 3

Optimal form-finding

Abstract

A definition of *form-finding* is given together with some considerations about the *design space* in order to clarify the context.
A selected set of methods is then reviewed to both illustrate the state of the art, the specific design problems and to introduce a basis for the understanding of the developed methods proposed in Chapter 4 and Chapter 5.

3.1.   Classical form-finding

Classically form-finding is defined as an inverse mechanical problem, compared to static analysis, where stresses in the structure elements are known and a final equilibrium shape is sought.

A number of authors have been reported to date back to Galileo Galilei in the 15th century as precursors of this field. However the term finds its origins at the beginning of the 19th century with the first experimentations of a pioneer like Antoni Gaudì. Gaudì used the hanging model principle, previously studied by Robert Hooke, to find compression only surfaces for several of his Churches (Figure 3.2).

Figure 3.1 – Hanging model by Heinz Isler.
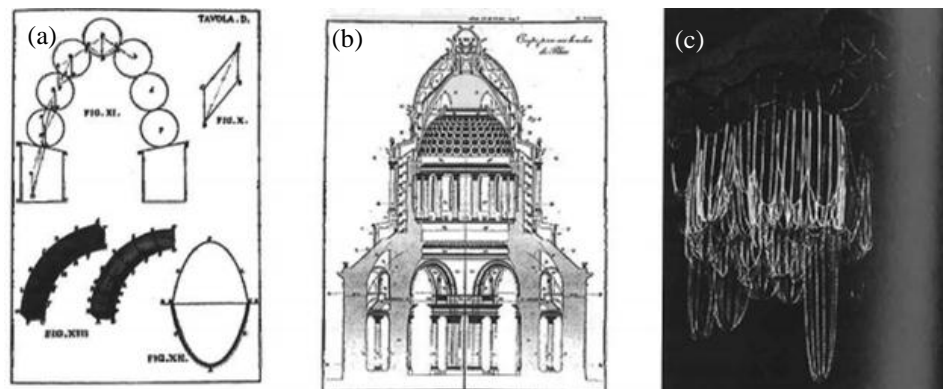
Figure 3.2 – The hanging model principle, famous examples: (a) Poleni, 1743; (b) Rondelet, 1802; (c) Gaudì (reconstruction of his hanging model for the Church in Colonia Guell).

However it was only after more than 150 years that form-finding became an established discipline with the first applications of tensile structures by Frei Otto.

Structures made by textiles or cable-nets must be pre-stressed; because they are not able to carry loads by compressive forces or bending, the interaction between the internal tensile stresses and the structure's geometry becomes crucial and cannot be deduced from standard geometries. The breakthrough can be identified by the German garden exhibition in Cologne 1957 and the famous Tanzbrunnen roof (Figure 3.3). The generation of structural shape and cutting patterns had been done experimentally with physical models because of the complexity of the three-dimensional shape.

Figure 3.3 – Tranzbrunnen roof in Cologne (1957).

With the work on the cable-net of the Munich stadium for the 1972 Olympic games (Figure 3.4) the situation changed dramatically since the dimensions had become too large for analysis by methods based on physical models.

The problem was solved thanks to the invention of a computational simulation method by Linkwitz and Shek: the Force Density Method (FDM) [Linkwitz and Schek, 1971]. Until the present, small scale experimental techniques are an important first step for the preliminary design of these structures, but the detailed form-finding and analysis is now completely based on numerical simulation.

Figure 3.4 – Olympic Stadium in Munich, 1972.

Figure 3.5 – Some possible combinations of suspended nets by Frei Otto.

3.2.   Optimization and form-finding

The classical definition of form-finding is mostly related to pre-stressed structures like cable-nets, membranes or tensegrity and, in general, to all those structures which have not a trivial equilibrium solution. Alternatively the problem can be stated as a particular case of structural optimization, since optimization is the mathematical generic tool for facing inverse problems. However, the edge between optimization and form-finding is not always precisely set and the term form-finding is extensively used to describe all those optimization problems which involve the mutation of the shape of a structure [Bellés et al., 2009; Bletzinger, 2001]. This "extended" meaning of the term has more than one reason but finds its roots in the implicit mechanical optimization of membrane structures where the material is optimally used since it is subjected to membrane forces rather than bending. The implicit optimization makes possible, for example, to apply classical form-finding processes to improve the behavior of concrete structures by affecting their shape, accordingly with physical principles which also inspired hanging models or the soap film analogy [Bletzinger, 2001]. As a consequence form-finding methods have often been modified or extended for adaptation to more general optimization purposes but still involving control of the shape. The shape, in structural analysis, is defined by a mesh which, in turn, is a combination of nodes and edges.

Therefore a form-finding method, in its "extended" meaning, can be defined as *a structural optimization process which uses the nodal coordinates as variables or can be reduced to such a process*.

This "extended" definition of form-finding is assumed hereafter.

3.3.   The infinity of the design space

The main challenge in form-finding is to define the mechanical criteria. The most famous are the hanging form and the soap film analogy which define form as equilibrium of applied dead load with stresses of given material or surface stresses with edge cable forces, respectively. Still, however, for every clearly defined criterion there exist an almost infinite number of solutions of equivalent quality

which reflects the natural multitude and physical non-uniqueness of design as the inverse of analysis (Figure 3.6). As a consequence, although the methods are explained very rationally, form-finding as such and the application of form-finding methods remains an art.

It is up to the insight and imagination of the designer about how to define a procedure of pre-selection, regularization or pre-filtering. There are no limitations for intuition and creativity to develop other experimental or numerical techniques for the exploration of the design space. A list of references which tries to sample the most significant contributions in the last 50 years can be found in [IASS, 2011][10].

Then, numerical methods of form-finding which share a common purpose mainly distinguish one from the other because of the regularization method applied. This point is further discussed in the next section where a classification of methods based on the regularization criteria is given.

---

[10] Book in celebration of the 50th Anniversary Jubilee of the IASS (1959-2009).

NO BENDING ALLOWED

a piece of paper used as "bridge"

coarse stiffening pattern

fine stiffening pattern

random stiffening pattern
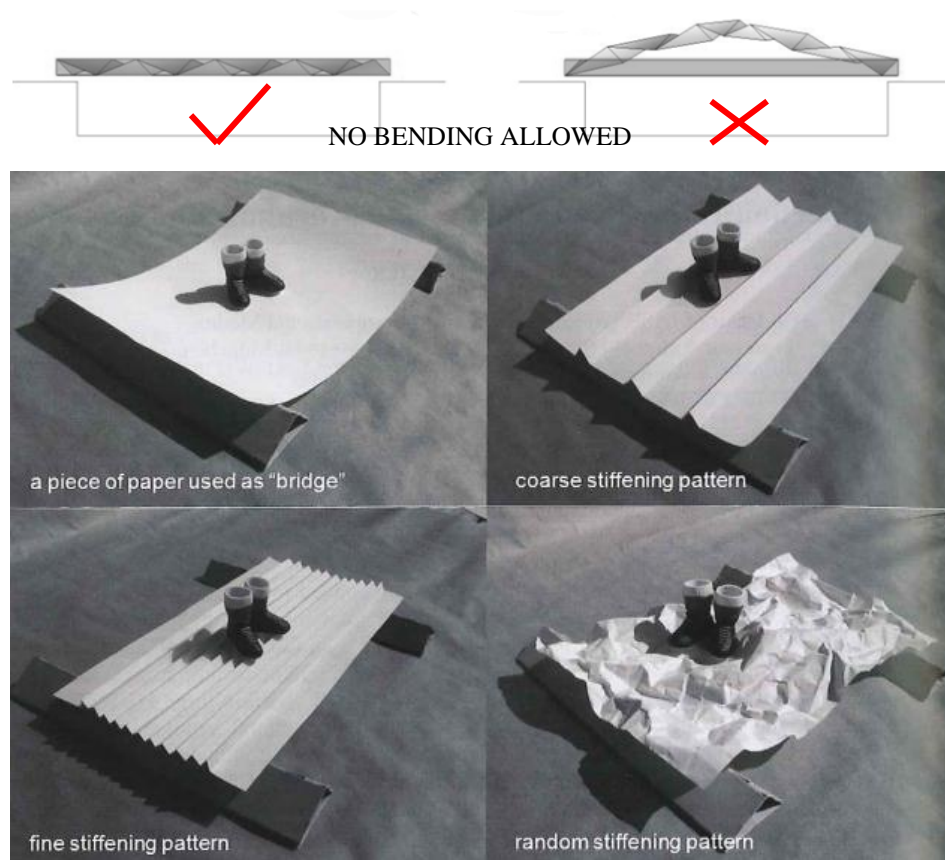
Figure 3.6 – Stiffened shell structures made from folded paper, courtesy of K-U Bletzinger. Because the paper is unable to act in bending, stiffeners have to be introduced by folding the paper. However there exist an infinite number of solutions of at least similar quality that is by far better than the quality of the initially flat piece of paper. Surprisingly enough, even a randomly crinkled paper appears to be a possible solution. The problem has been investigated also by Del Grosso and Basso [2010b].

3.4.   State of the art and recent advances

The state of the art includes an increasing number of form-finding algorithms. Many of these algorithms pursue partially overlapping goals or are defined as extensions of previously developed methods. Interesting reviews of the different methods have been presented by a number of authors [Tibert and Pellegrino, 2003; Miki and Kawaguchi, 2010b] in order to give a comprehensive overview of the problem.

However there have been recent developments not previously reviewed but which present some novelties deserving to be included in the picture. Moreover the previously reviewed methods were compared referring to the "classical" meaning of form-finding, hence the applications of these methods exclusively referred to pre-stressed or self-stressed structures (e.g. membranes and tensegrity).

This section proposes a new review of form-finding methods, particularly focusing on the most recent developments and relating them to the generic framework definition given in Chapter 2. With reference to the assumed "extended" form-finding definition it would be possible to include a large variety of methods in the picture, ranging from meta-heuristic ones to mathematical programming, analytical methods and so on. A further selection is therefore necessary not to digress.

Focusing on gradient-based methods only (the reader may consult the following references for analytical methods [Masic et al., 2005] and meta-heuristic methods [Chandana et al, 2005; Li et al, 2010]) and according to Veenendaal and Block [2011], three main categories of gradient-based form-finding methods can be recognized:

- Force Density based
- Dynamic Relaxation based
- Stiffness Matrix based

Of these three categories, only the first is pertinent to the understanding of the next Chapters. The following sub-section introduces then a selection of methods coming from the first of these three categories and specifically relevant to the

development of the algorithm in Chapter 4. The reviewed methods are presented using, as much as possible, a unified symbolism.

3.4.1. Force Density based methods

The scenario depicted by the large number of modifications and extensions which can be related to the Force Density Method (FDM) [Linkwitz and Shek, 1971; Shek, 1974] is particularly interesting. The reason of so many proposals related to the FDM is probably its linear behavior which makes it a special case of more general approaches (e.g. Bletzinger, 2001; Miki and Kawaguchi, 2010a; Connelly, 1982; Pauletti and Pimenta, 2008). Table 3.1 shows an incomplete list of recently developed methods which follow this trend. Some information regarding each method is reported and further relationships among the methods are exposed.

Table 3.1 – List of recently developed form-finding methods based on the FDM.

Method's name	Derivation/Similarities	Authors	Year	University (State)
Multi-step FDM	FDM	Sanchez at al.	2006	Navarra (Spain)
Natural FDM	FDM (URS)	Pauletti	2006	Sao Paulo (Brazil)
-	FDM (Adaptive FDM)	Estrada et al.	2006	Stuttgart, Munchen (Germany)
Adaptive FDM	FDM (Energy Meth.)	Zhang and Ohsaki	2006	Kyoto (Japan)
Thrust Network Analysis	FDM (Force Network Meth.)	Block, Ochsendorf	2007	MIT (MA – USA)
Virtual FDM	FDM	Basso et al.	2009	Pavia, Genoa, PoliTo (Italy)
Extended FDM	FDM (Energy Meth., NLP)	Miki , Kawaguchi	2010	Tokyo (Japan)
-	FDM (Adaptive FDM,)	Tran and Lee	2010	Sejong (South Korea)
Constrained FDM	FDM (Natural FDM, URS)	Descamps et al.	2011	Libre de Bruxelles (Belgium)

The Force Density Method plus three other methods derived from the former are presented hereafter. All these methods, together, cover a whole range of different form-finding problems.

3.4.1.1. Force Density Method (FDM)

Since the method is extensively investigated in literature, only its main characteristics are reported here as a basis to be recalled during the discussion of the other methods. For a detailed description one can refer to [Shek, 1974]. Basically

the method has been applied to find equilibrium configurations of pre-stressed cable-nets solving the system of equations:

$$\mathcal{E}\,f\,L^{-1} = p \tag{3.1}$$

which is non-linear. The idea is to substitute $\mathbf{q}$ to the product $\mathbf{f}\,\mathbf{L}^{-1}$ so that (3.1) becomes linear. Exposing the nodal coordinates and assuming a three-dimensional framework, the equilibrium problem can then be rewritten as

$$\mathcal{L}_Q\,x = C^T Q C\,x = p_x \tag{3.2a}$$

$$\mathcal{L}_Q\,y = \mathbf{C}^T\mathbf{Q}\mathbf{C}\,\mathbf{y} = \mathbf{p}_y \tag{3.2b}$$

$$\mathcal{L}_Q\,z = \mathbf{C}^T\mathbf{Q}\mathbf{C}\,\mathbf{z} = \mathbf{p}_z \tag{3.2c}$$

It is useful to separate the columns of $\mathbf{C}$ referring to the classification into free and fixed nodes

$$\mathbf{C} = [\mathbf{C}_{free}, \mathbf{C}_f] \tag{3.3}$$

so that (3.2a,b,c) becomes:

$$\mathbf{C}^T_{\text{free}}\mathbf{Q}\mathbf{C}_{\text{free}}\,\mathbf{x}_{\text{free}} = \mathbf{p}_x - \mathbf{C}^T_{\text{free}}\mathbf{Q}\mathbf{C}_{\text{fix}}\,\mathbf{x}_{\text{fix}} \tag{3.4a}$$

$$\mathbf{C}^T_{\text{free}}\mathbf{Q}\mathbf{C}_{\text{free}}\,\mathbf{y}_{\text{free}} = \mathbf{p}_y - \mathbf{C}^T_{\text{free}}\mathbf{Q}\mathbf{C}_{\text{fix}}\,\mathbf{y}_{\text{fix}} \tag{3.4b}$$

$$\mathbf{C}^T_{\text{free}}\mathbf{Q}\mathbf{C}_{\text{free}}\,\mathbf{z}_{\text{free}} = \mathbf{p}_z - \mathbf{C}^T_{\text{free}}\mathbf{Q}\mathbf{C}_{\text{fix}}\,\mathbf{z}_{\text{fix}} \tag{3.4c}$$

where $\mathbf{x}_{free}$, $\mathbf{y}_{free}$ and $\mathbf{z}_{free}$ are the unknowns.
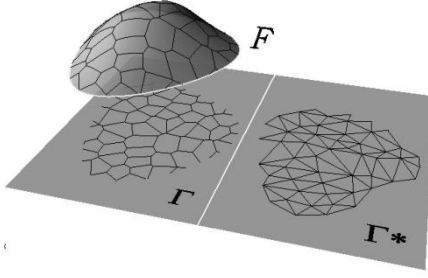
Figure 3.7 – Framework representation of a vault F, framework projection Γ and its dual graph Γ*.

3.4.1.2. Thrust Network Analysis (TNA)

The method, mainly inspired by [O'Dwyer, 1999], has been proposed by Block and Ochsendorf [2007] for the analysis and generation of compression-only vaulted surfaces and networks. The main elements considered in the method are a three-dimensional framework $\mathcal{F}$ representing the vault or the network, its projection Γ on the *xy*-plane and the dual graph of Γ, Γ* (Figure 3.7). It is pointed out that Γ and Γ* are also frameworks, consequently matrices and vectors associated with them will appear with the subscripts $_\Gamma$ and $_{\Gamma*}$ respectively.

Γ* can be derived from the *cyclespace* of Γ – i.e. the nullspace of $\mathbf{C}_\Gamma$ – as described in [Micheletti, 2008]. A property of Γ* is that it graphically represents the static equilibrium of $\mathcal{F}$ and this is the key element of the method. Practically, assuming that the framework is loaded only by vertical loads at the nodes, the forces $\mathbf{f}$ in $\mathcal{F}$ can be represented by the lengths $\mathbf{l}_{\Gamma*}$ of the reciprocal edges in Γ* scaled by a scalar ξ:

$$\mathbf{f} = \mathbf{l}_{\Gamma*}\,\xi \tag{3.5}$$

Therefore equation (3.4c), which represents the equilibrium of the framework, can be modified taking advantage of Γ* and becomes:

$$\mathbf{C}^{\mathrm{T}}_{free}\,(\mathbf{L}_\Gamma^{-1}\,\mathbf{L}_{\Gamma*})\mathbf{C}_{free}\,\mathbf{z}_{free} = \xi^{-1}\mathbf{p}_z - \mathbf{C}^{\mathrm{T}}_{free}\,(\mathbf{L}_\Gamma^{-1}\,\mathbf{L}_{\Gamma*})\mathbf{C}_{fix}\,\mathbf{z}_{fix} \tag{3.6}$$

At this point, since the interest is in the range of equilibrium configurations of $\mathcal{F}$ that fit within a given envelope, the method becomes a linear programming (LP) problem where the objective function is 1/ξ. The boundary conditions are (3.6) and

a set of upper and lower limits on $\mathbf{z}_{free}$ – i.e. $\mathbf{z}_{lb} \leq \mathbf{z}_{free} \leq \mathbf{z}_{ub}$ – and $1/\xi$ – i.e. $0 \leq 1/\xi <$ $+\infty$. The introduction of Γ^* makes it possible that the optimisation problem remains linear and provides a useful graphical output for the distribution of the forces in the framework. Note that, contrary to the FDM, the horizontal force densities in TNA cannot be chosen randomly but are related to the choice of Γ. Some care is therefore necessary when defining the topology and the geometry of the framework. So called "spider web" configurations have been shown to work well in this sense [Block, 2009].

Since TNA is mainly proposed for applications related to continuous compression-only structures, it goes against the tide with respect to the most classical form-finding methods and, consequently, it also presents a great novelty in the field.

3.4.1.3.   Adaptive FDM (AFDM)

The method has been proposed by Zhang and Ohsaki [2006] for the finding of feasible equilibrium configurations of tensegrity structures. The main idea is to force the nullity of the Laplacian $\mathcal{L}_Q$ associated to the d-dimensional framework, weighted with respect to the assigned edge force densities $\mathbf{q}_0$, to have dimension:

$$\text{nullity}(\mathcal{L}_Q) = d + 1 \qquad\qquad (3.7)$$

while constraining $\mathcal{L}_Q$ to be positive semi-definite at the same time.

Satisfying the two conditions above leads to the *super stability* of the framework [Connelly, 1999]. To this aim, the spectral decomposition of $\mathcal{L}_Q$ is first performed:

$$\mathcal{L}_Q = \Phi \Lambda \Phi^T \qquad\qquad (3.8)$$

Then the diagonal elements $\{\lambda_1, \lambda_2, \ldots, \lambda_n\}$ of Λ – i.e. the eigenvalues of $\mathcal{L}_Q$ – are analysed and modified if needed. Since the number of non-zero eigenvalues is

68

equal to the rank of $\mathcal{L}_Q$ the proposed strategy is simply to set to zero the smallest $d + 1$ eigenvalues.

The so modified Λ' leads to a modified Laplacian $\mathcal{L}_Q'$ which, in turn, is used to derive a feasible set of force densities $\mathbf{q}$. The step from $\mathcal{L}_Q'$ to $\mathbf{q}$ can be briefly summarised as the least square solution of the system:

$$q = B^{-}g \tag{3.9}$$

where the columns of $\mathcal{L}_Q'$ are stacked in the vector $\mathbf{g}^T = (\mathcal{L}_Q'{}_1{}^T, \mathcal{L}_Q'{}_2{}^T, \ldots, \mathcal{L}_Q'{}_n{}^T)$, ζ denotes the set of members connected to the i-th node of the framework and $\mathbf{B}^T = (\mathbf{B}^{1T}, \mathbf{B}^{2T}, \ldots, \mathbf{B}^{nT})$ with:

$$\mathbf{B}^i_{(j,k)} = \begin{cases} 1 & \text{if } i = j \text{ and } k \in \zeta \\ -1 & \text{if nodes } i \text{ and } j \text{ are connected by member } k \\ 0 & \text{other cases} \end{cases} \tag{3.10}$$

$\mathbf{B}$ can also be used to set constraints on specific force densities. Then $\mathbf{q}$ is used to rebuild $\mathcal{L}_Q$ and the process is iteratively repeated until (3.7) holds. Finally, a unique and non-degenerate configuration of the structure can be achieved by specifying a set of independent nodal coordinates. Note that the method could lead to asymmetric configurations even for a given set of symmetric force densities.

Estrada et al. [2006] almost simultaneously presented a method with a very similar approach. Compared to the method proposed by Zhang and Ohsaki, this method only requires the topology and the types of members to be initially defined, avoiding the choice of a set of independent nodal coordinates. The idea is still to control the rank deficiency of $\mathcal{L}_Q$ and, to this aim, the spectral decomposition of $\mathcal{L}_Q$ is used as well. However no modification of Λ is made this time and a set of d eigenvectors $\mathbf{S} = [\boldsymbol{\Phi}_1, \ldots, \boldsymbol{\Phi}_d]$ is used instead as the candidate set of final nodal coordinates. The proposed criteria for the selection of $\mathbf{S}$ aim at achieving a configuration that dominates all the other equivalent ones [Connelly, 1999] and

satisfies (3.7) at the same time. Once **S** is selected, referring to the case of *d*=3, the following further condition needs to be satisfied:

$$\mathcal{E}\,\mathbf{q} \approx 0 \tag{3.11}$$

where **S** = [**x**, **y**, **z**]. A set of force densities **q** which results as the least square solution of (3.11) and agrees with the signs of $\mathbf{q}_0$ can be found by the *singular value decomposition* of $\mathcal{E}$. Then **q** is used to rebuild $\mathcal{L}_Q$ and the process is repeated iteratively till both (3.7) and (3.11) hold. The method seems capable to find tensegrities satisfying either stability (i.e., the tangent stiffness matrix is positive definite) or super stability (i.e., the geometrical stiffness matrix is positive definite) even if only examples of this second type are reported in [Estrada et al., 2006]. Examples of the former type can be found in [Tran and Lee, 2010] where a method which is strongly based on the previous two (especially [Estrada et al., 2006]) is presented.

For all the three methods the main way of affecting the shape is by changing the force densities. Compared to [Miki and Kawaguchi, 2010b] none of the three methods can have direct and exact control over the geometrical and properties of the framework.

3.4.1.4. Extended FDM (EFDM)

The method has been proposed by Miki and Kawaguchi [2010a, 2010b] for the finding of feasible equilibrium shape of pre-stressed structures made by any composition of cables, membranes and struts. The main novelty of the method lies in the problem statement: starting from a variational principle associated to the FDM, it can be derived a generalized functional which stationary solution leads to a non-singular equilibrium configuration of the structure. The stationary problem related to the total potential energy functional was first studied by other authors (e.g. [Connelly, 1982]). The EFDM generalises that functional, building it according to the method of Lagrange multipliers in order to include also the necessary boundary conditions. For a structure that consists of cables, membranes and struts, the generalised functional reads:

$$\Pi(\mathbf{u},\boldsymbol{\lambda}) = \sum_i \pi_i\left(l_i\left(\mathbf{u}\right)\right) + \sum_j \pi_j'\left(S_j\left(\mathbf{u}\right)\right) + \sum_k \lambda_k\left(l_k\left(\mathbf{u}\right) - l_{0k}\right) \rightarrow \text{stationary} \qquad (3.12)$$

where $\mathbf{u}$ is a vector of nodal coordinates, $\boldsymbol{\lambda}$ are the Lagrange multipliers, π and π' are named elements functional, l_i represents the length of the i-th cable, S_j represents the area of the j-th triangle and l_i, l_{0i} represent the length and the objective length of the k-th strut respectively. Specifically it has been shown that suitable values for π and π' are $q_i\, l_i^4(\mathbf{u})$ and $q_i\, S_i^2(\mathbf{u})$ respectively, where q_i is the force-density related to the i-th cable. Traditional non-linear programming (NLP) techniques can then be adopted to solve the constrained minimisation problem as previously proposed by Pellegrino [1986]. The form-finding problem for a tensegrity can then be stated as:

$$\min_{\mathbf{x\,y\,z}} \ \mathbf{q}_c^{\mathrm{T}} \left(\mathrm{diag}(\mathbf{C}_c\mathbf{x})^2 + \mathrm{diag}(\mathbf{C}_c\mathbf{y})^2 + \mathrm{diag}(\mathbf{C}_c\mathbf{z})^2\right)^2 \quad \text{s. t.} \quad \mathbf{l}_s - \mathbf{l}_0 = 0 \qquad (3.13)$$

where the subscript c is for *cables* and s is for *struts* (i.e. $\mathbf{C}^{\mathrm{T}} = [\mathbf{C}_c^{\mathrm{T}}, \mathbf{C}_s^{\mathrm{T}}]$).

The resulting shape can be affected by changing the functional, the force-densities or the constraints (e.g fixed nodes, element lengths, etc.).

For tensegrity form-finding, compared to the NLP approach proposed by Pellegrino, the EFDM formulation has the advantage to include the force-density coefficients in the objective function, giving a better control on the variation of the pre-stressing state. Moreover the formulation remains extremely simple and the parallelism with the FDM is straightforward since there is a one-to-one relation between each set of cable force-densities and the corresponding equilibrium configuration. A drawback compared to [Estrada et al., 2006] is the need to predefine element lengths.

3.4.1.5.   Algorithms discussion

Several form-finding methods based on the FDM and concerning structures that underlie the given definition of framework have been discussed. The use of a unified symbolism helps to evaluate the relationship among them and to investigate specific features on a common basis. Besides, the proposed point of view relates the description of all the presented methods to the two basic elements of a framework −

71

i.e. topology and attributes. Under the light of this approach, rather different methods reveal similar formulations.

The presented methods have introduced several remarkable novelties in the field of form-finding and together they cover a wide range of purposes and deal with a wide range of structural systems. TNA has proved to be an effective way to analyze and generate compression-only vaulted surfaces and networks and makes an interesting use of reciprocal figures. EFDM proposes an abstraction of physical concepts with benefits in terms of problem statement clarity and flexible formulation. EFDM and AFDM (and related variations) together offer exhaustive solutions to classical form-finding problems concerning pre-stressed and self-stressed structures.

Chapter 4

Virtual Force Density Method

Abstract

The proposed method is a generalization of the FDM. The main point is the *abstraction* of the elements of the FDM such that the method can apply to a much wider range of problems. Possible applications of this method are further discussed in 0.

4.1.   Main concept

The method has been initially proposed by Basso et al. [2009a] to optimize the geometry of free-form grid-shells.

Essentially it is based on the abstraction of the main elements of the FDM, seen as an optimization problem. The abstraction is the key and makes it possible to use a FDM-like approach to solve problems where no force field is involved.

The great abstraction makes the problem flexible and suitable for a large range of applications. For instance, a new application of the method has been recently presented by Del Grosso and Basso [2010] concerning the field of the variable geometry structures.

4.2. Fundamental elements

Four main elements are recognized for the problem (plus the objective function) and their abstraction is reported in Table 4.1:

Table 4.1 – Main elements of the VFDM.

FDM		VFDM
(node coordinates) $\mathbf{x}$, $\mathbf{y}$, $\mathbf{z}$	$\xrightarrow{\textit{variables}}$	$\mathbf{w}$ (node weights)
(branch-node matrix) $\mathbf{C}$	$\xrightarrow{\textit{topology}}$	$\mathcal{C}$ (connectivity matrix)
(*forces*) $\mathbf{f} = f\,(\mathbf{C}, \mathbf{x}, \mathbf{y}, \mathbf{z}, \mathbf{q})$	$\xrightarrow{\textit{rule}}$	$\mathbf{r} = \mathrm{f}\,(\mathcal{C}, \mathbf{w}, ..)$ (virtual forces)
(node constraints, applied loads)	$\xrightarrow{\textit{boundary conditions}}$	(framework/edge/node attributes)
(equilibrium)	$\xrightarrow{\textit{objective function}}$	(equilibrium)

Practically the two main abstractions are $\mathbf{r}$ and $\mathcal{C}$.

Since $\mathbf{r}$ losses its physical meaning of force, it is possible to state a fictitious equilibrium problem. This is the case of the problem presented in section 6.2. Moreover, the connectivity matrix $\mathcal{C}$ extends the meaning of the branch-node matrix $\mathbf{C}$ so that the idea of connection is no longer limited to a physical one. Therefore the relations among the nodes of the framework can be set depending on the problem at hand. The *planarity* problem presented in section 6.4 well explains this concept.

On the other hand, this flexibility implies also that $\mathbf{r}$ and/or $\mathcal{C}$ may have to be rebuilt to face new problems.

A more detailed description of these two main elements, along with a comparison with the corresponding elements of the FDM, is provided in the following sub-sections.

4.2.1. Connectivity matrix

FDM is essentially based only on one kind of connectivity matrix (C) that is an nxe matrix where n is the number of nodes and e is the number of connections (edges). It is important to point out that, in this case, a connection is always intended as a link between two nodes. Consequently the calculation of the resultant vector in each point is dependent only by the position of the other points which are connected to this through a frame.

This has been obviously the more suitable choice since the aim was the static optimization of structures where stress is strictly connected to frames/cables but, on the other side, the method could be applied for several others purposes by changing the 'classical' connection matrix with a more effective one. Figure 4.1 shows, for example, a comparison between a classical connection and an alternative connection we have used to apply the method to the planarity problem (see section 6.4).

(a)   (b)
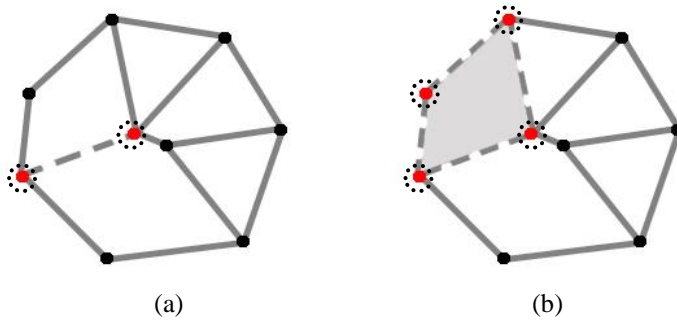
Figure 4.1 – from left to right – a) connection between two vertices of the mesh - the connector is a frame; b) a possible alternative connection among more than two vertices - the connector is a face.

4.2.2. Vector's generation rule

Vector generation in the traditional FDM is due to the interaction between a force field applied over the structure and the stress state of the structure itself. So, in this case, vectors which are generated in each node are essentially the result of a vectorial sum of forces. From the mathematical point of view the concept can be resumed with a function like:

$$r = f(\mathbf{w}, C, \mathbf{t}, \mathbf{f}) \qquad\qquad (3)$$

where:
- $\mathbf{w}$ and C have been already defined,
- $\mathbf{t}$ is the 1xe array describing the stress state of the net and t_i is the tension value associated to the i element (connection), for i = 0, 1.. , e
- $\mathbf{f}$ (optional) is a 3xn array of forces with $\mathbf{f}_k$ the force vector applied on the net node k, for k = 0, 1.. , n .

Assuming $\mathbf{t}$ and $\mathbf{f}$ as parameters confined inside f makes it possible to replace or simply avoid them.

For instance, with reference to our problems, where there is no presence of force fields but only geometry is involved, the function for vector generation will read:

$$r = f(\mathbf{w}, C, \dots) \qquad\qquad (4)$$

In this case vector generation on each node of the framework could be dependent on the geometry only. Vectors generated in such a way can be seen as fictitious forces and this is the reason why the method is referred as "virtual". In Chapter 6 two application of the VFDM with different vectors generation rules and different connectivity matrices are presented.

4.3.   General scheme

The flowchart of Figure 4.2 briefly resumes the iterative optimization procedure.
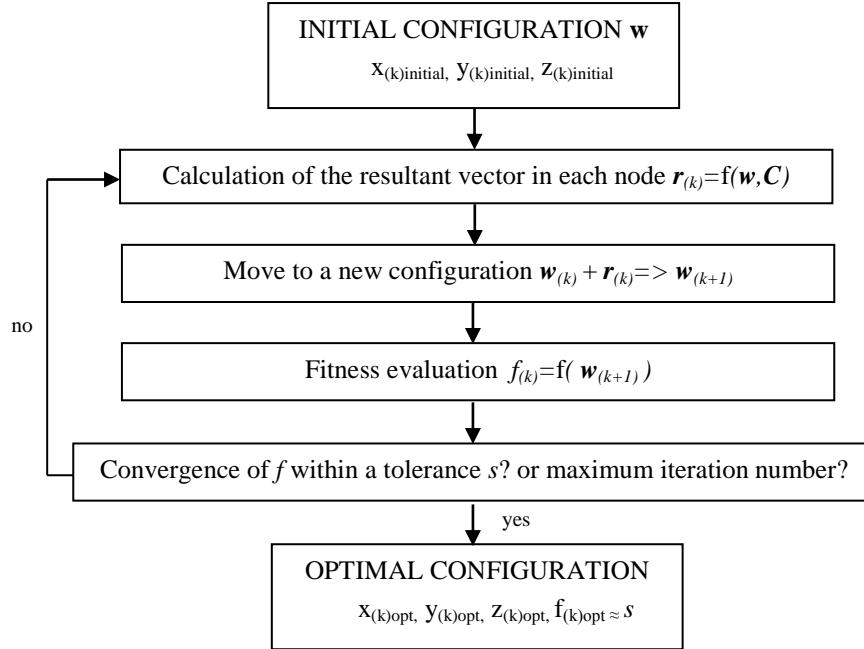
Figure 4.2 – Scheme of the VFDM.

Chapter 5

Finite State Control Strategy

Abstract

The proposed method is a combination of an *evolutionary optimization technique* and the VFDM. The main point is the interpretation of the optimization problem of a VGS as a *static problem* – i.e. optimal configurations (*finite states*) are found without explicit care of the kinematics of the system. Possible applications of this method are further discussed in Chapter 7 and Chapter 8.

5.1. Context and potential

5.1.1. Issues and potential of adaptive structures in civil engineering

Specific issues when dealing with adaptivity in the field of civil structures are the scale factor and the time. Contrary to what happens in mechanical engineering, automotive engineering or space engineering where structures are often much lighter and considered to be in motion, it is unlikely that a civil structure is able to change its configuration in a very short time. Dimensions, mass and the presence of people are typically going to constrain the possible range of accelerations and

velocities, not to mention displacements and trajectories of the moving elements. The human threshold of motion perception is a consistent example of such a limitation[11]. Because of these reasons, the adaptive behavior cannot belong to nor can come from all the elements of the structure at the same time. Specifically referring to buildings, the existing proposals involving structural adaptivity are in fact usually focusing on the internal and/or external envelope – i.e. the "building skin". Shells and grid-shells, where the distinction between walls and roof becomes weaker or even disappears, are probably the kind of structure which more easily could be tailored to fit the concept of adaptive skins and with the greater potential. Other immediate applications may relate to roof structures and façades.

   Restricting adaptivity to the building skin means that mechanisms are developed exclusively at the boundary, thus reducing kinetic inconsistencies with the internal space and possibly allowing a main static structure to be the core of the building. This, in turn, implies that adaptivity tends to come from mechanisms *distributed* all over the envelope in order to provide a better change of shape. A consequent distribution of sensors and actuators is also expected, which may contribute to easily satisfy the previously mentioned redundancy requirements.

   The envelope plays then an *interface* role towards the most of the environmental actions, both externally (e.g., wind – Figure 5.1) and internally (e.g. people walking).
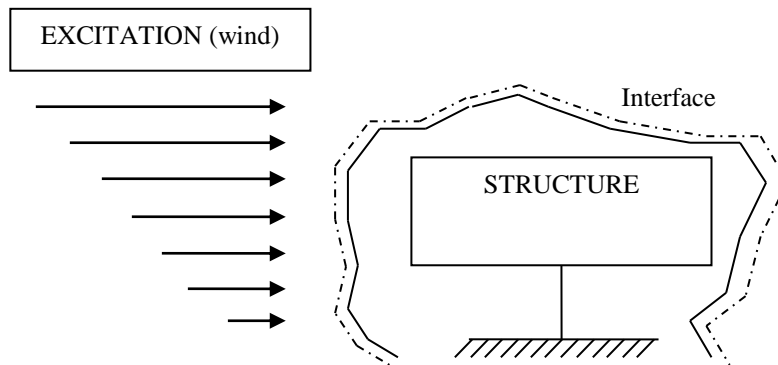
Figure 5.1 – The "building skin" as the interface to the external excitation by wind.

---

[11] http://www.cppwind.com/support/papers/papers/structural/PEAKvsRMS.pdf

Moreover, this *interface* role is exploited with respect to "shape-dependant" actions other than loads, which makes adaptive skins suitable for a wide range of purposes. Figure 5.2 gives an example of two possible fields of application.
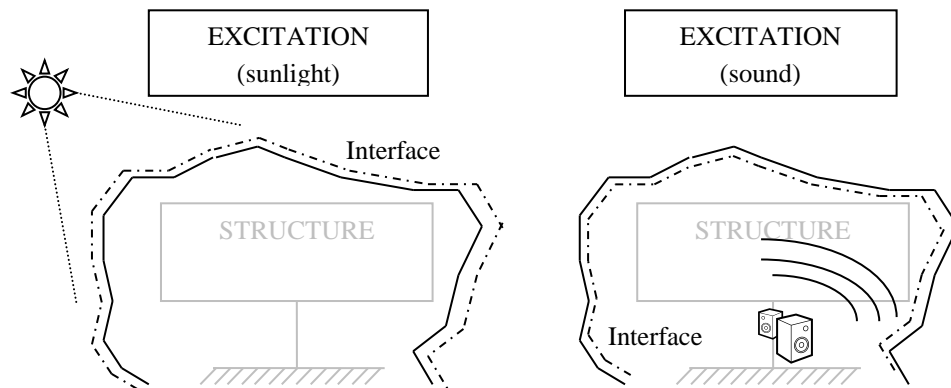
Figure 5.2 – The "building skin" as the interface to non-structural external and internal design drivers.

This aspect makes possible to take advantage of the same adaptive system to improve different performances of the building and it perhaps represents the most relevant feature when comparing structural adaptivity with more traditional control approaches.

Besides the main functionality aspects, it is also worth noting the potential of adaptive structures to well match the aesthetics and the organic nature criteria of modern architecture and thus providing contextual motivations to their implementation. These considerations are not of secondary importance to the context of structural reliability because they indirectly enforce the role of sensing and actuation devices in buildings and make their costs more attractive to contractors and stakeholders. This additional potential can find one of its today best representations in the dynamic architecture by David Fischer[12]. Referring to the Fisher project in Figure 5.3, the system, made of superimposed rotating storeys, can achieve astonishing free-form configurations, is able to produce enough energy for

---

[12] http://www.dynamicarchitecture.net/

the building needs and for vending outside 20% of it thanks wind turbines between each floor (Figure 5.4) and the control of the movable parts has been proposed as a form of energy dissipation or, in a wide sense, of controllable additional damping [Casciati et al., 2009].

Figure 5.3 – The Rotating tower project in Dubai (UAE) by David Fisher.

Figure 5.4 – Vertical axis wind turbines between each floor for energy harvesting; the building aims to be sustainable and self-powered other than aesthetically pleasant (Fischer, 2008).

Another specific aspect in the civil field, which is quite neglected in many others, is related to the morphology of the adaptive "skin", implicitly associated to the definition of building envelope. Considering the generic case of the free-form mesh in Figure 5.5, then a responsive skin associated to such an envelope translates into a multi degrees of freedom (MDOFs) system. A MDOFs structure turns out to be quite complicated to design and even more complicated to control since the number of actuators needed and their positions should be known and, possibly, optimized according to the morphing requirements. Moreover a MDOFs envelope generally shows reciprocal kinematic relations among its parts and it is consequently not a trivial structure to be real-time controlled.

(a)   (b)   (c)
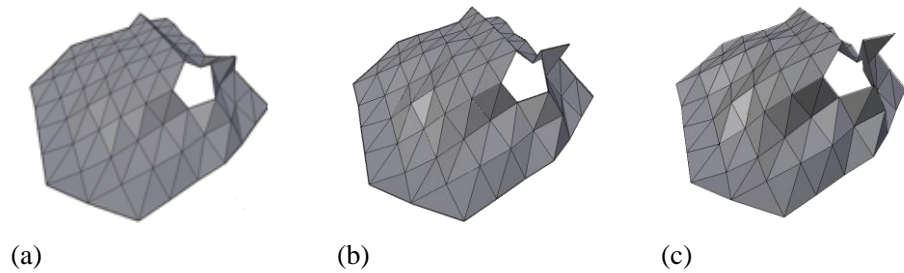
Figure 5.5 – (a), (b) and (c): three different configurations of a MDOFs mesh.

5.1.2. Risk reduction through structural adaptivity

Evolution has resolved many of nature's challenges leading to lasting solutions. Nature has always inspired human achievements and has led to effective materials, structures, tools, mechanisms, processes, algorithms, methods, systems, and many other benefits [Bar-Cohen, 2005].

The concept of adaptivity, as many others in history, is still once inspired by nature. It may be found in the behavior of plants like the Mimosa Pudica (Figure 5.6), whose leaves have the capability to display thigmonasty (touch-induced movement). In the sensitive plant, the leaves respond to being touched, shaken, heated or rapidly cooled. The speed of the response depends on the magnitude of the stimulus. Hitting the leaf hard with the flick of a finger will cause the leaf to

close in the blink of an eye whereas a gentle touch or modest heat source applied to leaflets at the tip of a leaf will result in a slower response and the propagation of the stimulus along the leaf can be observed. The phenomenon is made possible by osmosis, the flow of water in and out of plants' cells. Triggers such as touch cause water to leave certain plant cells, collapsing them. Water enters other cells, expanding them. These microscopic shifts allow the plants to move and change shape on a larger scale.

Figure 5.6 – The Mimosa plant, which folds its leaves when they're touched, is among the plant varieties that exhibit specialized "nastic motions", i.e. large movements you can see in real time with the naked eye.

While bio-inspired materials and structures may or may not employ biological constructs directly, they do tend to be inherently multifunctional, adaptive, and hierarchical. In this context, an adaptive structure is typically defined as a structure which is able to adapt, evolve or change its properties or behavior in response to the environment around it. Harbour cranes [Del Grosso et al., 2002], for instance, represent an interesting field of research and application for this kind of structures because of their light weight and flexibility and the necessity of preventing vibration during operations. Morphing aircrafts are another result of the adaptive structures research[13]. The morphing ability of such structures yields benefits far beyond those afforded by more traditional approaches, such as variable sweep wings, by allowing two or more degrees of freedom to be controlled simultaneously, resulting in independent control of a number of wing geometric parameters such as aspect ratio, chord length, and planform area (Figure 5.6).

---

[13] http://www.nextgenaero.com/

83
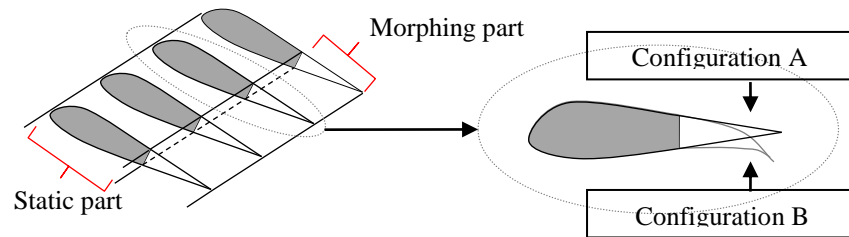
Figure 5.7 – Concept of a morphing wing made by four two-dimensional variable geometry sections.

As the example of the morphing aircrafts may highlight, some confusion still exists concerning the term "adaptive" and its exact meaning, particularly when compared to the term "morphing". Although, on one side, the etymology of the word would suggest an even closer relationship with other terms like "interactive" or "responsive" and the generic definition would imply a wider range of applications than those only dependent on the morphology of the structure, on the other side the term adaptive has long been linked to studies where the "change of shape/configuration" played the most important role (e.g. compliant mechanisms, multi-stable surfaces, aeroelastic and aerospace structures, lightweight airfoils, etc.). Other representative examples of such a dualism may be found in books [Adaptive Structures: Engineering Applications, 2007; Clark et al., 1998] as well as in conference proceedings in recent years (IASS Symposia, ICAST) [14].

Within the field of structural engineering, depending on the context and the focus, the meaning of adaptivity may therefore become inherent to the

---

[14] The International Conference on Adaptive Structures Technologies (ICAST) is a good example of how the concept of adaptivity can be intended at different scales (from material level to structural level) and how well it couples with control theory. On the contrary, the latest (2009 and 2010) Symposia of the International Association for Shell and Spatial Structures (IASS) had special sessions named "Adaptive Systems" and "Adaptive Structures" respectively, which mainly focused on the shape variation of a structure in response to "design drivers".

morphological change of the structure; this specific meaning is the intended meaning herein.

   Some clarification is then required to correctly contextualize this concept of adaptivity in the field of structural reliability. At first, the concept of structural adaptivity is indeed very closed to the concept of active structural control since, in both cases, some actuation force is expected in response to an occurring excitation in order to improve the behavior of the structure. As already said, however, the term adaptivity implies here that the improvement of the structural behavior comes specifically from a change in the morphology (shape) or in the system configuration (i.e. the actuation force is responsible of this change).

   It is possible to qualitatively estimate the benefit in terms of safety coming from structural adaptivity by making a comparison between Figure 5.8 and Figure 5.9. The model parameters considered, θ_f (excitation model – "factor") and θ_m (system model – "mechanism"), are derived from the IRIS paradigm [Del Grosso et al., 2012]. Figure 5.8 represents the case of a system without any kind of control device on it while Figure 5.9 shows the case of an adaptive structure.
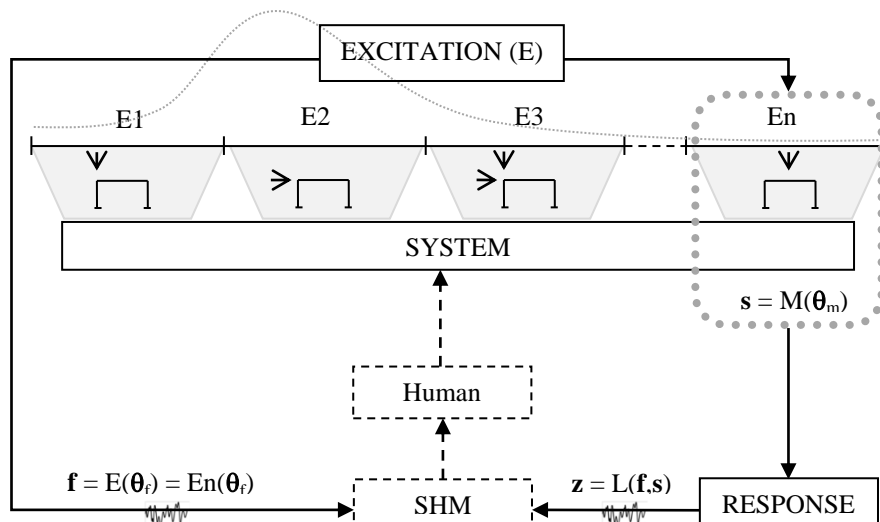
Figure 5.8 – Block diagram of system without control. Dashed arrows and boxes are to be considered optional components of the flow chart.
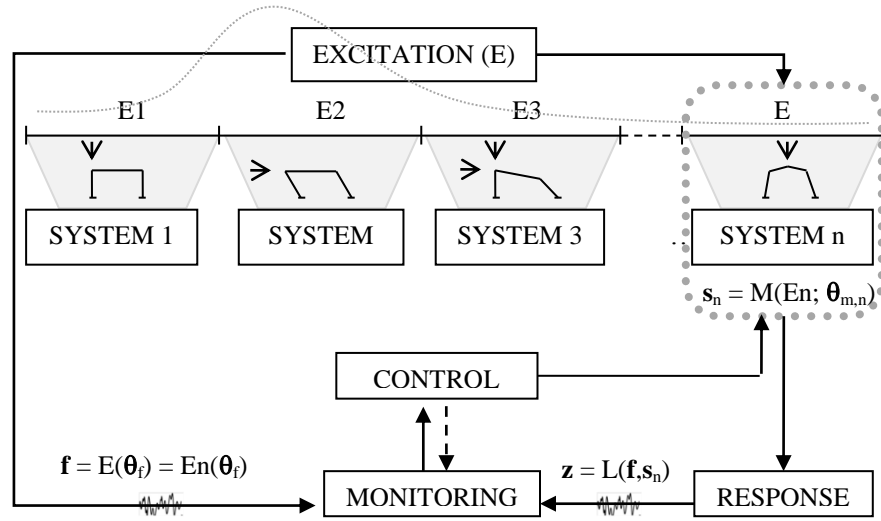
Figure 5.9 – Block diagram of Active Control through Structural Adaptivity. Dashed arrows are to be considered optional components of the flow chart.

Assuming a simplified limit state function

$$g(R, L) = R(\mathbf{s}) - L(\mathbf{f}, \mathbf{s}) = R - L \tag{5.1}$$

where R represents the system carrying capacity and L represents the load effect on the system, if we refer to Figure 5.8 we can divide the excitation range into *n* incompatible sub-ranges E1, E2, …, En, such that

$$g_i(R, L) = R(\mathbf{s}) - L(\mathbf{f}_i, \mathbf{s}) = R - L_i \quad \forall i \in [1, n] \; in \; \mathbb{N} \tag{5.2}$$

Then the failure probability of the system can be expressed as

$$p_{fail,1} = \sum_{i=1}^{n} p(R - L_i \leq 0 | E_i) \, p(E_i) \tag{5.3}$$

Analogously, in the case of an adaptive structure (Figure 5.9) the limit state functions would read

$$g_i(R, L) = R(\mathbf{s}_i) - L(\mathbf{f}_i, \mathbf{s}_i) = R_i - L_i \quad \forall i \in [1, n] \; in \; \mathbb{N} \tag{5.4}$$

86

leading, in turn, to the following probability of failure

$$p_{fail,2} = \sum_{i=1}^{n} p(R_i - L_i \leq 0|E_i) \, p(E_i) +$$

$$\sum_{i=1}^{n} p(\overline{R_i} - L_i \leq 0|E_i \cap MCD) \, p(MCD|E_i) p(E_i) \tag{5.5}$$

where MCD represents the event of *malfunction of the control devices*. Assuming that MCD and E are statistically independent events then Eq. 5.5 can be rewritten as

$$p_{fail,2} = \sum_{i=1}^{n} p(R_i - L_i \leq 0|E_i) \, p(E_i) +$$

$$\sum_{i=1}^{n} p(\overline{R_i} - L_i \leq 0|E_i \cap MCD) \, p(MCD) p(E_i) \tag{5.6}$$

When comparing Eq. 5.3 and Eq. 5.6 we should assume that, for the specific sub-range of events E_i, the corresponding optimal configuration of the adaptive structure performs equally or better than a static system which is designed to support the whole range of events E. In other words:

$$\sum_{i=1}^{n} p(R_i - L_i \leq 0|E_i) \leq \sum_{i=1}^{n} p(R - L_i \leq 0|E_i) \tag{5.7}$$

We shall call adaptivity gain (Ag) the difference

$$Ag = \sum_{i=1}^{n} p(R - L_i \leq 0|E_i) - \sum_{i=1}^{n} p(R_i - L_i \leq 0|E_i) \tag{5.8}$$

According to Eq. 5.7 is then obvious that

$$p_{fail,2} < p_{fail,1} \Leftrightarrow Ag > p(MCD) \cdot \sum_{i=1}^{n} p(\overline{R_i} - L_i \leq 0|E_i \cap MCD) \, p(E_i) \tag{5.9}$$

and it is reasonably expected that

$$Ag < \sum_{i=1}^{n} p(\overline{R_i} - L_i \leq 0|E_i \cap MCD) \, p(E_i) \tag{5.10}$$

From Eq. 5.9 and Eq. 5.10 the important conclusion to remark is that the reliability of the whole system is heavily determined by the control system.

Consequently an important design objective to make the adaptive structure convenient should be

$$p(MCD) \ll Ag \tag{5.11}$$

The malfunction of the control system may happen when the actuators fail but also when the sensor are unable to detect the excitation/response of the system or because of a wrong interpretation of it. This means that the safety level of the monitoring system is also involved in determining $p(MCD)$.

From the considerations above it seems reasonable that the main concepts of robustness have reason to migrate from the design of the structure to the design of the control system, redundancy being the most important among them. Of course, this doesn't mean that the design process is allowed to ignore the structure capacity in terms of energy absorption, redundancy and ductility but it becomes of primary importance to ensure the reliability of a control system which is in charge to manage the structural form since it plays the major role in contributing to robustness [Agarwal et al., 2012]. To this aim it would be feasible, for instance, to take advantage of the installed monitoring system to check also the state of the control devices, as suggested in Figure 5.9 (dashed arrow). The design should also provide, if possible, a safe configuration, i.e. an intermediate state among the possible configurations, in case of malfunction of the control devices.

On the other hand, a redundant and reliable control (and monitoring) system is sensibly beneficial with respect to other fundamental aspects in a risk assessment like, for instance, the human role in failures [Vrouwenvelder et al., 2012]. Generally, human error is considered as the main cause of structural failures; estimates range from 50% to 90%[Ellingwood, B.,1987], mainly distributed among the below listed foreseeable sources:

- Design error;
- Material flaw;
- Construction error;
- Misuse;
- Lack of maintenance;
- Miscommunication.

The most part of the risk coming from these human errors could be greatly reduced by an integrated monitoring system. However, a SHM system alone has a quite long return time on investment with no immediate tangible benefits which makes it barely suitable for small to medium size structures. The cost of such a system could be instead mitigated if included in a structural adaptivity approach which has the potential to immediately give better performance at competitive costs (e.g. by saving on the material weight)[15].

5.1.3. Introduction of the strategy

In the present section a Finite State Control Strategy (FSCS) is proposed for the design and control of MDOFs adaptive envelopes. The main advantage of the FSCS is that a set of optimal configurations (finite states) are investigated during the design phase to partially or totally avoid the computational cost of the real-time control. It is worth noting, however, that the finite states, being them a limited number of achievable configurations, influence the possibility of mutation of the structure in service. Particularly, the configurations will always or almost always be sub-optimal since the structure remains in a given state for a whole range of possible excitations, but these limitations are expected to be negligible in the context of civil structures, especially when compared to the advantages in terms of easiness of design integration, energy gain to energy consumption ratio and real-time control simplification.

The strategy can handle any kind of VGSs which can be associated to the framework representation defined in Chapter 2. The framework representation is central to the strategy development, mainly because the matrix analysis of the framework is used to control the kinematic properties of the envelope.

---

[15] http://engd-usar.cege.ucl.ac.uk/project/view/idprojects/18

5.2.   Main concept

The Finite State Control Strategy (FSCS) is basically a general procedure for the design of adaptive structural envelopes, i.e. VGSs.

The proposed procedure is applicable to every structural envelope which can be associated to a single-layer framework (Figure 5.10a). So, although the civil-architectural engineering context remains as a reference, the application of the proposed procedure is not limited to it.

The procedure is basically a combination of two main parts: a *meta-heuristic optimization process*, which aims at discovering new optimal configurations – i.e. *finite states* – according to some defined purpose, and *gradient-based optimization process* which acts as a constraint for the kinematic compatibility maintenance.

A *topology optimization process,* which aims at decreasing the number of DOFs of the structure while retaining its ability to achieve the optimal configurations, is proposed if the structure is pin-jointed.

In principle any meta-heuristic technique and gradient-based algorithm could be coupled according to the defined scheme. However, specifically the choice here is to use an evolutionary algorithm, which leads the search for optimal solutions, and the VFDM to ensure the compatibility of the resulting configurations.

5.3.   General scheme

Figure 5.11 represents the flowchart of the FSCS.

The initial framework to optimize G_0 has to be equivalent to a triangular mesh. The choice of this initial mesh is determinant to achieve a good result. In this sense the most depends of the density of the defined mesh – i.e. how many nodes and edges are needed. A coarser mesh has fewer possible configurations compared to a denser one but more DOFs to manage. Moreover the mesh should represent a real envelope made with real panels which always come with a limited range of possible measures.

The topology of the initial mesh – i.e. how the edges are connected – is another important factor because it constraints the "folding" process. It is for instance important to start with a symmetric pattern if the mesh is expected to fold

90

symmetrically. Topology and density of the initial mesh may then be part of the whole optimization process but, on the other hand, these two elements are also fundamental to the definition of the envelope appearance. Consequently, thinking at a building façade, roof or internal ceiling, these turn to be architectonical parameters the most of the times. Topology and density of the initial mesh are therefore left outside the optimization process here since they are considered directly a designer choice.

Pin-jointed single-layer framework

Linear
Actuator

(a)   (b)

Kinematically indeterminate   **Kinematically determinate**
15 finite mechanisms
(6RBM + 11 internal mechanisms)

Different compatible configurations (finite states) of the system
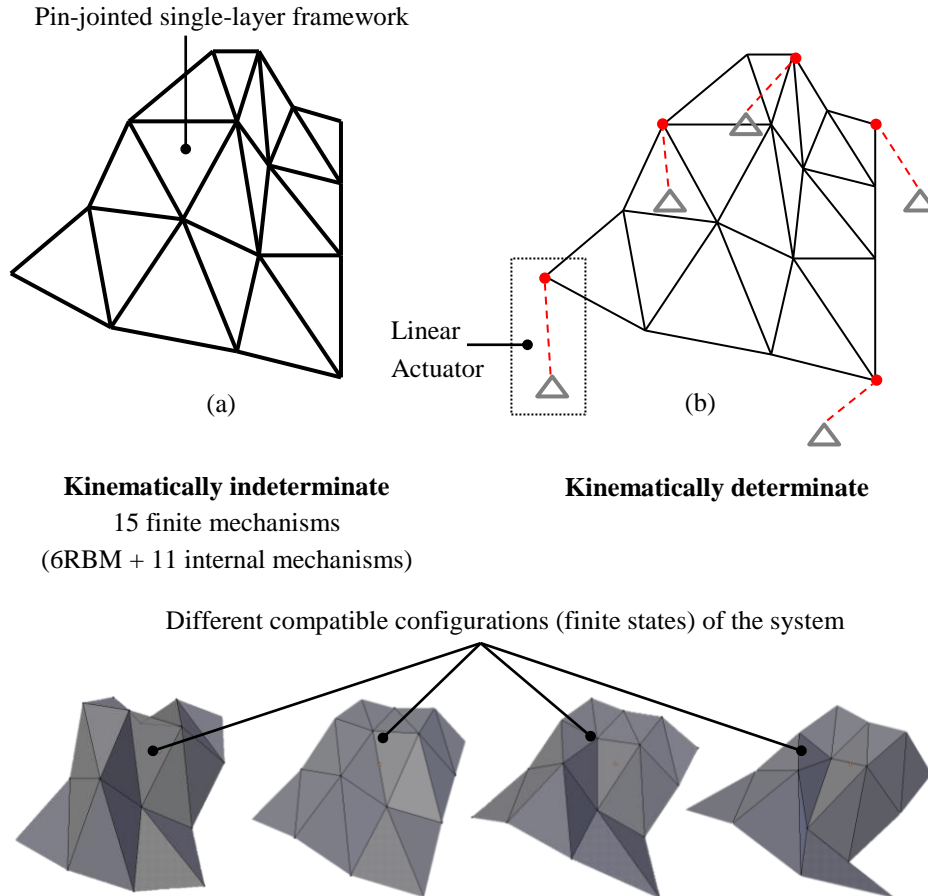
Figure 5.10 – MDOF Single Layer Framework.

91
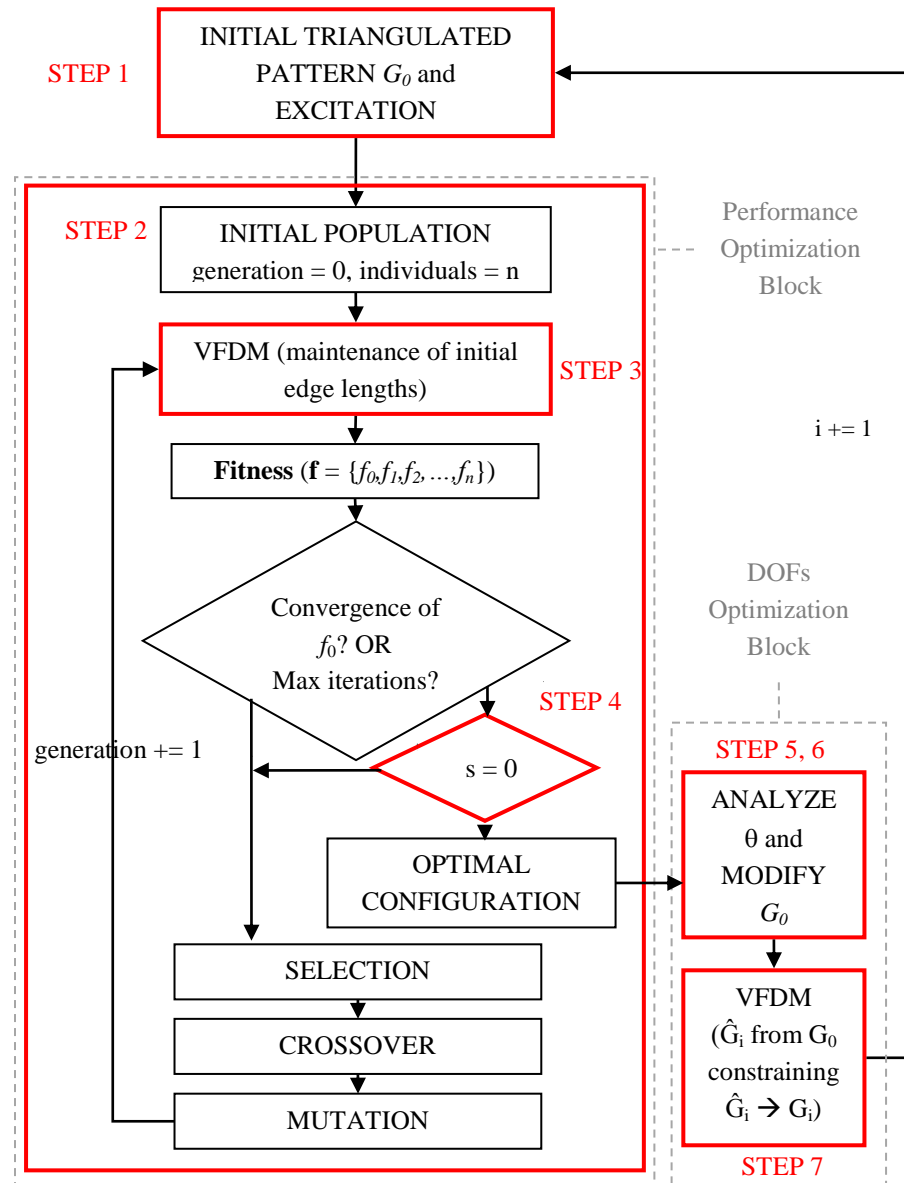
Figure 5.11 – Flowchart of the optimization procedure.

The *performance optimization* block, which involves steps 2 to 4, is basically an evolutionary algorithm where complex constraints for the compatibility maintenance among the solutions are managed by the VFDM. Solutions are equivalent to optimal configurations geometrically compatible one with the other. These are called here *finite states* because of the "static" approach used. The block is further explained in sub-section 5.4.

The *topology optimization* block, which involves steps 5 to 7, is only applicable with the assumption that the framework nodes are equivalent to pin-joints. The block is further explained in sub-section 5.5.

A step by step description of the whole algorithm is given in sub-section 5.6.

5.4.   Optimal states selection

The optimal states selection is made by means of an evolutionary technique. Specifically a Memetic Algorithm (MA) [Elbeltagi et al., 2005] is used.

The MA is based on the better known Genetic Algorithm (GA) which is a search algorithm inspired to the mechanics of natural evolution[16]. At present GAs provide an effective tool to find optimal or sub-optimal solutions when dealing with complex problems, such as air-traffic programming, weather forecasts, share portfolios balance and electronic circuits design. Several applications of this technique are specifically developed to face structural and constructive problems in architecture [Pugnale and Sassone, 2007; Sassone and Pugnale, 2008].

---

[16] In contrast with many others evolution-inspired algorithms that were studied starting from the 1950s for the optimization and machine learning, the theoretical and mathematical framework of Genetic Algorithms was developed by John Holland [1992] and his team in the 1960s, and finally formalized in 1975, as the result of a more general study on the phenomenon of natural adaptation in order to simulate the biological evolution under computer systems. Originally defined by Holland as "genetic plans" they were soon renamed by his doctoral students, replacing the term "plan" with "algorithm", in order to focus the attention on the role of computation. Only in the 1980s genetic algorithms received an increasing recognition by scientists and studies ranging from biology, A.I., engineering and business to social sciences became to appear.

Any clearly defined problem can be formulated in genetic terms following the four major steps defined by Koza [1992]:

- Determining the representation scheme;
- Determining the fitness measure;
- Determining the parameters and variables for controlling the algorithm;
- Determining the way of designating the result and the criterion for terminating a run.

In GAs the generation and selection of neighbourhood solutions are performed through biologic evolutionary concepts as genetic coding, mutations and crossover recombining and a scheme of the conventional procedure, derived from Mitchell [1998], is shown in Figure 5.12.
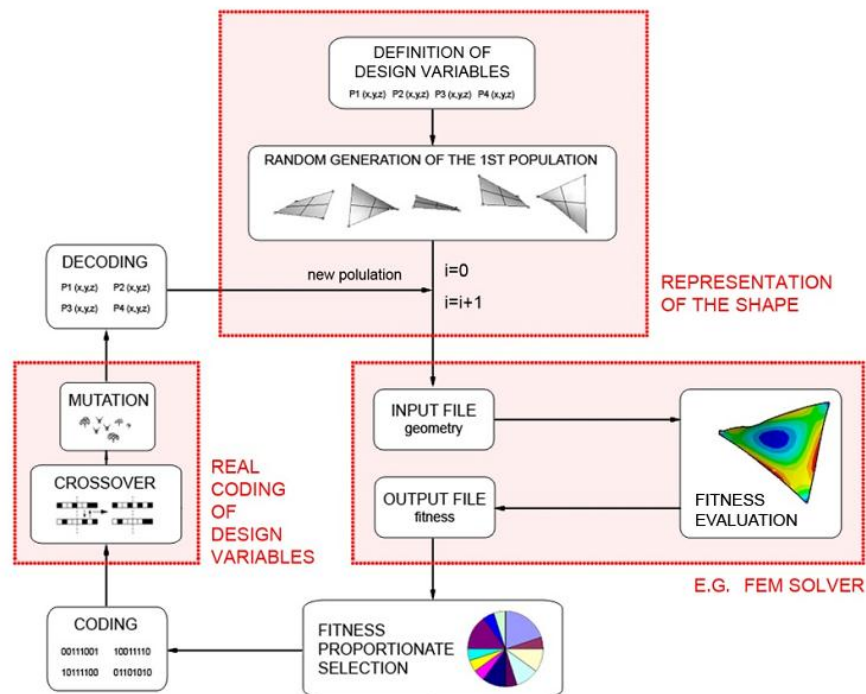
Figure 5.12 – GA scheme.

The main scheme is still valid for the MA. The difference between GA and MA is limited to the management of the three main operators: selection, crossover and mutation. While the classical GA uses the three operators on the whole population in the same way, the MA instead implements the concept of "local search" as illustrated in Figure 5.13.

Anyway, as already mentioned, the MA is briefly illustrated here because it has been the choice for the forthcoming applications but any other meta-heuristic method could be adapted to the proposed approach.

(a)

(b)
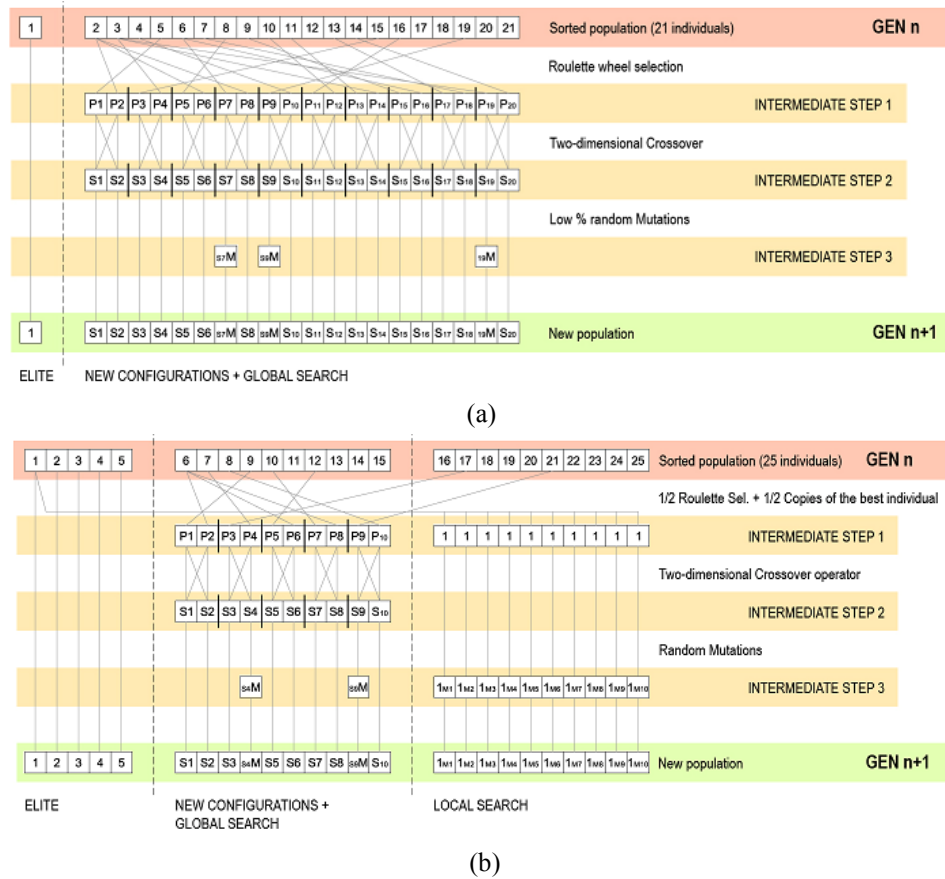
Figure 5.13 – Comparison between (a) the classical GA scheme and (b) the MA scheme.

The fundamental aspect to underline here concerns instead the kinematics compatibility maintenance. Two precautions are taken to this aim:

- The VFDM applies in order to maintain the system geometry constraints;
- An initial planar configuration is chosen as a reference.

The compatibility maintenance among different configurations can be translated in a geometrical optimization problem with a very low tolerance. This means that it cannot be tackled effectively by the evolutionary process only. The VFDM, already introduced in Chapter 4, is therefore integrated inside the MA loop to accomplish this task. Depending on the problem at hand, is still within the setting of the VFDM that the type of structure is taken into account while the exploration of the design space by the MA remains unaffected. This concept is better exemplified by the applications proposed in Chapter 7.

The second precaution is not strictly necessary but it is useful to avoid possible *snap-through* behavior between two configurations when the envelope is allowed to vary bi-directionally. An alternative to the assumed precaution could be to verify the existence of the path "a posteriori", e.g. by interpolating between the configurations as explained by Tang et al. [2010].

It is worth noting that, since the kinematic simulation is not involved, this way of looking for the optimal states potentially allows changing both topology and geometry on the fly with a very robust behavior.

5.5.   Topology optimization

A single-layer pin-joint framework can be associated to what is called a "rigid-foldable origami structure". Since this relationship exists and the rigid-origami foldability is a quite intuitive concept and a well-known research topic in literature [Tachi, 2009b and 2010a], it is useful to illustrate a few preliminary concepts about the topology effect on kinematics using an "origami-based" approach.

$$\begin{pmatrix} 0 & 1 & 0 & 1 & 0 & 0 \\ 1 & 0 & 1 & 0 & 1 & 0 \\ 0 & 1 & 0 & 0 & 0 & 1 \\ 1 & 0 & 0 & 0 & 0 & 0 \\ 0 & 1 & 0 & 0 & 0 & 0 \\ 0 & 0 & 1 & 0 & 0 & 0 \end{pmatrix} - - - - \rightarrow \begin{pmatrix} 0 & 1 & 0 & 1 & 0 & 0 \\ 1 & 0 & 1 & 0 & 1 & 0 \\ 0 & 1 & 0 & 0 & 0 & 1 \\ 1 & 0 & 0 & 0 & 0 & 0 \\ 0 & 1 & 0 & 0 & 0 & \mathbf{1} \\ 0 & 0 & 1 & 0 & \mathbf{1} & 0 \end{pmatrix}$$

Figure 5.14 – Topology modification can be represented by differences in the adjacency matrix of the framework.

5.5.1. Preliminary considerations

The foldability of a rigid origami is defined by the pattern topology and geometry. For instance, considering the topology first, it is known that a triangulated pattern usually allows several mechanisms while a quadrilateral pattern

Figure 5.15 - From left to right - singular quadrilateral pattern (Miura-Ori) with one DOF and a non-foldable variation of the former.

is generally not rigid-foldable. However, when the geometry of a quadrilateral pattern presents some singularities a one DOF mechanism can be achieved (e.g Miura Ori pattern – Figure 1) [Miura, 1970, 2009]. This result is interesting for a wide range of

applications in the field of deployable structures and many recent researches focus on the quadrilateral pattern singularities to find new one DOF mechanisms. On the other side, it is sometimes preferred to leave more than one DOF in order to allow multiple paths for the structure transformation. This could be the case of architectural adaptive skins which have to change their configuration according to external inputs like wind or light. It is however always necessary to precisely define a number of finite mechanisms to accordingly set a proper system of actuators. The actuators can be smart materials or more traditional hydraulic engines but a comprehensive analysis of these would be out of the scope of this section. Actuators are generally to be considered as an important part in the whole cost of the system and their number has therefore to be limited to a minimum, according to the sought purpose.

97

Starting from these considerations the idea is to look for a pattern which is a combination of triangular and quadrilateral panels, using the quadrilateral ones to stiff the structure but leaving the desired number of DOFs. A procedure which allows the design of a rigid foldable origami envelope based on this principle is proposed in the next sub-section.

Note that, in principle, not only quadrilateral panels can be used to decrease the number of DOFs but every kind of polygon with four or more edges. However convergence tolerance may be a non trivial problem for polygons with a high number of edges.

5.5.2. DOFs management

A rigid foldable origami can be related to a single-layer pin-joint framework [Resch and Christiansen, 1970]. The topology of the origami pattern can then be represented by the adjacency matrix of the framework and the kinematics can be analyzed by investigating the four fundamental subspaces of the equilibrium matrix of the framework. In particular the left-nullspace of the equilibrium matrix is the one which defines all the inextentional mechanisms of the framework. Referring to the extended Maxwell's rule [Pellegrino and Calladine, 1986], the number of internal independent inextensional mechanisms m for an unconstrained framework in the three-dimensional space can be derived as follows:

$$m = 3n - b + s - 6 \tag{5.12}$$

where b is the number of frames, n is the number of nodes and s is the number of self-stress states of the framework. It has been shown by Tachi [2009a, 2009b, 2010a] that ensuring a positive number for m during the transformation from one configuration to another is an effective way to prove the foldability of a pattern. However it is possible that m is a combination of both infinitesimal and finite mechanisms. This, in turn, means that the hypothetical number of actuators needed to transform the structure to all its possible configurations would be less than m. A way to ensure that all the m mechanisms are finite is to keep $s = 0$ which practically

98

is the most common case for a randomly generated triangular pattern associated to an envelope in the three-dimensional space. In other words $s = 0$ if the triangular pattern is not planar neither presents other singularities. Therefore two configurations of a rigid foldable origami which share a triangular pattern with these characteristics (i.e. $s=0$) can be transformed into each other by means of (maximum) m actuators. The compatibility of the two configurations – i.e. the fact that they share exactly the same triangular pattern – can be ensured by constraining the lengths of the frames to remain constant during the transformation.

The number of finite mechanisms m can then be managed by affecting the topology of the pattern. An increment of m can be trivially achieved by a further discretization of the pattern while decreasing m it is possible by replacing two triangles with a quadrilateral face. Precisely, assuming a non-singular triangular pattern, it is known that the replacement of two adjacent triangles by a quadrilateral panel results in the loss of a DOF such that $m \rightarrow m - 1$. With reference to the framework representation based on only nodes and frames, it is possible to simulate this substitution by adding a frame connecting the two disconnected nodes of two adjacent triangles. With the additional frame, every transformation of the pattern, made by constraining the lengths of the frames to remain constant, would then maintain the quadrilateral panel. Figure 5.16 shows several variations of a generic triangular pattern by addition of frames (yellow colored) to simulate quadrilateral panels (red colored).
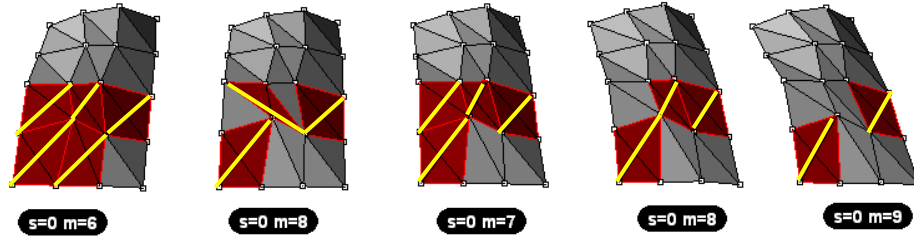
Figure 5.16 – Variations of the framework kinematic properties when different combinations of triangular and quadrilateral panels are considered. Under each configuration both the number of self-stress states and the number of internal (finite) mechanisms is reported.
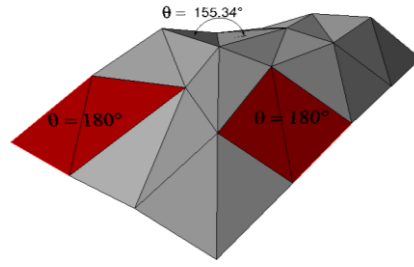
Figure 5.17 – Dihedral angles.

A proposed criterion for making this substitution is based on the analysis of the dihedral angles θ (Figure 5.17) of the pattern. When θ is close to 2π then the folding of the two associated triangles can be considered as marginal in the whole transformation process. The closer θ to 2π, the less the replacement of triangles by quadrilateral panels will affect the resulting configuration. The choice of a limit for the θ values to be considered can be made by iteratively checking how each value affects the performance of the analyzed configuration.

5.6. Design procedure

A procedure to design rigid foldable origami envelopes with an optimal number of DOFs is defined by the following steps:

- define a planar triangulated pattern G_0;
- transform G_0 to find k optimal configurations $G_1, G_2, …, G_k$ according to the set purpose (performed via MA);
- $\forall\ G_i\ |\ i = 1,2,…k$, constrain G_i to be compatible with G_0 (performed via VFDM);
- $\forall\ G_i\ |\ i = 1,2,…k$, if $s = 0$ and $m > 0$ continue, else modify G_i (return to step 2);
- $\forall\ G_i\ |\ i = 1,2,…k$, analyze the dihedral angle $\theta_{i,j}$ between each couple j of adjacent triangles;
- $\forall\ j$, if   max $\theta_{i,j}\ ––> 2\pi\ |\ i = 1,2,…k$, substitute the j-th couple of triangles in G_0 with a quadrilateral panel and check that $m > 0$;
- $\forall\ \hat{G}_i\ |\ i = 1,2,…k$, build $\hat{G}_i$ from G_0 constraining $\hat{G}_i$ to be as closed as possible to G_i (performed via VFDM) and check that the performance requirements are maintained.

100

It is worth to be noted that the initial planar (developed) configuration has mainly the scope to avoid possible "snap-through" mechanisms which may otherwise happen passing from one configuration to another.

5.7.   Actuation process

The actuation process is simulated as explained in section 2.4.3. The simulation has the double purpose to check the feasibility and to investigate the kinematics of the transformation.

Once the number of DOFs is determined, so is the number of actuators needed. The actuators are then assumed to be linear and to be linked both to the adaptive envelope and to the supporting structure through pin-joints as shown in Figure 5.18.

(a)   (b)
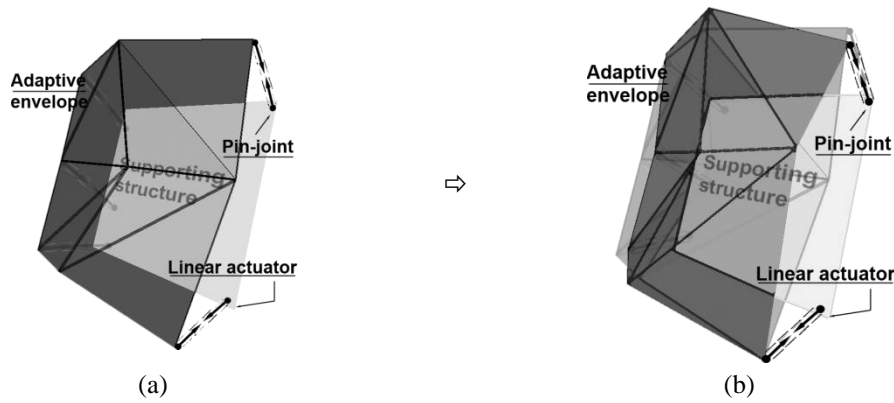
Figure 5.18 – (a) Scheme of an adaptive envelope linked to the supporting structure and (b) a different configuration of the same envelope when actuated. The envelope is represented by a triangular mesh (9 nodes and 16 edges) which is linked to the supporting structure by 5 linear actuators. Actuators are pin-jointed both to the supporting structure and to the envelope.

The location of the actuators cannot be chosen arbitrarily in order to control all the mechanisms. This concept is better illustrated by comparing Figure 5.19a and Figure 5.19b. Note that the two frameworks have the same number of nodes, the

same number of edges and also the same edge lengths. Moreover the number of mechanisms is exactly the same when an equal number of actuators/restraints is assumed, no matter which are their locations. But in Figure 5.19b, if no actuators are placed at node 7 and neither node 7 is constrained, it is not possible to manage the face 4-7-8 rotation around the edge 4-8. This doesn't happen instead in Figure 5.19a because of the different topology of the pattern.

(a)   (b)
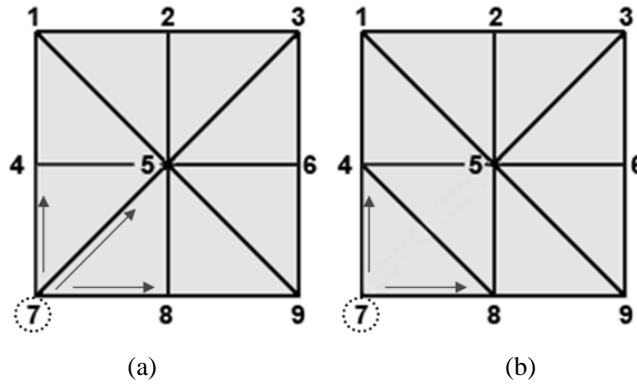
Figure 5.19 – Different pattern topologies and consequences on the possible actuator locations. Node 7 has connectivity ≤ 2 and needs to be controlled directly.

The above example leads to the first important conclusion that no nodes with connectivity ≤ 2 can be left unconstrained or not actuated.

The second important observation is that actuators and constraints should be placed first on nodes which are not directly connected one to the other. For instance, still looking at Figure 5.19, it turns out that a minimum of four actuators/restraints are needed to control the 11 mechanisms and at least one self-stress state is expected (3 DOFs $\times$ 4 actuators $-$ 11 mechanisms = 1). The only group of four nodes which can be selected avoiding nodes inside the same group to be connected to each other is the one composed by nodes 1, 3, 7 and 9. Controlling these four vertices through pin-joint restraints or actuators results in zero mechanisms and only one self-stress state of the framework. Assuming the same kind of restraints/actuators, every other combination of four nodes would end up with more self-stress states.

Inverse kinematics can then be used both to plan and to verify the actuation process, as already explain in Chapter 2. The inverse kinematics of the framework can be controlled by the Moore-Penrose generalized inverse of the Jacobian of the non-linear vector equation representing the geometry constraints (constraint equation). The constraint equation for a pin-joint framework reads:

$$\mathbf{\Omega}(\mathbf{x}, \mathbf{y}, \mathbf{z}) = [\mathbf{l} - \mathbf{l}_0] = \mathbf{0} \tag{5.13}$$

where $\mathbf{l}$ is the vector of the edge lengths at the current step and $\mathbf{l}_0$ is the vector of the initial edge lengths. Eq. (5.13) can be written in terms of the Cartesian nodal coordinates:

$$\mathbf{\Omega}(\mathbf{x}, \mathbf{y}, \mathbf{z}) = (\text{diag}(\mathbf{Cx})^2 + \text{diag}(\mathbf{Cy})^2 + \text{diag}(\mathbf{Cz})^2)^{1/2} - \mathbf{l}_0 = \mathbf{0} \tag{5.14}$$

where $\mathbf{C}$ is the incidence matrix of the framework and $\mathbf{x}$, $\mathbf{y}$ and $\mathbf{z}$ are the vectors of the nodal coordinates.

Eq. (5.14) yields an underdetermined system, by exploring the solution space of which it is possible to obtain variations in the configuration. Valid shapes are found by perturbing the nodal coordinates according to the nullspace of the Jacobian $\mathbf{J} = \left[\frac{\partial \mathbf{\Omega}}{\partial \mathbf{x}} \mid \frac{\partial \mathbf{\Omega}}{\partial \mathbf{y}} \mid \frac{\partial \mathbf{\Omega}}{\partial \mathbf{z}} \right]$. The solution is calculated using the pseudoinverse $\mathbf{J}^+$ of the Jacobian as follows:

$$d\mathbf{u} = (\mathbf{I} - \mathbf{J}^+ \mathbf{J}) d\mathbf{u}_0 \tag{5.15}$$

where $d\mathbf{u}_0$ represents the initial perturbation and $\mathbf{I}$ is the identity matrix.

Eq. 5.15 finds the valid perturbation closest to $d\mathbf{u}_0$ by orthogonal projection to the solution space. An integration of this infinitesimal motion has to be executed and, for each step, the residual has to be eliminated (e.g. Newton-Raphson method).

It is worth noting that considerations are limited to geometric ones and elastic or plastic behavior of the structure with specific materials is not analyzed.

With reference to Eq. (5.15) the perturbation vector $\Delta \mathbf{u}_0 = [\Delta x_1, \Delta x_2, \ldots, \Delta x_n]^T_{1 \times n}$ is then built from the zero vector $[0, \ldots, 0]^T_{1 \times n}$ by substituting the zero values

corresponding to the "actuated" nodes with the distance between the node at the current position and the node at the target position.

5.8. Discussion

Differences concerning the applicability of adaptive structures to engineering problems of different fields have been discussed. Of particular interest for potential civil applications are MDOFs envelopes which are generally characterized by a high reciprocity in the behavior of their parts. The resulting constrained MDOFs kinematics is not trivial to be real-time controlled in order to achieve optimal configurations. The proposed FSCS is based on the "a priori" exploration of the design space in order to reduce the computational cost during the real-time control of the structure. A finite number of optimal compatible configurations, called finite states, are found during the design stage, where the exact number is a function of the excitation, of the performance target and of the structure morphology. FSCS can handle the design of any adaptive envelope which can be associated to a single-layer framework. The possibility to manage the DOFs number is also considered in the special case of pin-joint frameworks. Further investigation will be focused on the possible integration of the finite states with classic control methods in cases where it is preferable or not possible to determine all the necessary optimal configurations a priori.

Part III
Applications and Results

Chapter 6

The cost optimization of free-form grid-shells

Abstract

Two well known constructional problems, related to the geometry of grid shells, are solved by means of the VFDM.
An example of multi-objective optimization is then proposed by coupling geometrical and static performance criteria.
The optimal solution is approached iteratively starting from configurations that can be sub-optimal, random defined or deriving from the early stages of conceptual design.

6.1. Conceptual design of grid-shells: polyhedrons generation processes

On one side information technology allows designers to develop their formal expression, leading to the blob as the extreme reference of their thinking, on the other side the resolution of new problems connected to free forms is approached by creating new instruments of form optimization and research which are developed "ad hoc". Grid shells are strategically included in this scenario. They were initially studied as a building typology merely from the engineering point of view, from the

109

constructive characteristics to the research of a structurally efficient form, in association with thin concrete shells and cable nets structures.

Generally speaking, a grid-shell with plane faces is a polyhedron. We can classify such geometrical shapes on the basis of the shape of their faces, on the number of faces, sizes and vertices, and on the ratio of the faces dimension over the overall size.

Faces can be triangular, quadrilateral or with a larger number of sides (pentagon, hexagon) and usually just one of these polygons is used repeatedly for the whole project. Exceptions to these rules can be found in the edges of the grid shells, where triangular faces are necessary, and in the Fuller's domes, where pentagons are required at each vertex of the underlying icosahedron, as it can be observed in the famous Eden Project designed by Grimshaw and Partners.

Figure 6.1 –Panoramic view of the geodesic dome structures of the Eden Project. The Eden Project is a large-scale environmental complex near St Austell, Cornwall, England, United Kingdom.

The relation between the number *V* of vertices, *F* of faces and *S* of sides is a topological property completely defined by the Euler's theorem:

$$V - F + S = 3 - h \tag{6.1}$$

in which *h* is the connection order of the polyhedron [Hilbert and Cohn-Vossen, 1932]. Many structural projects have been conceived starting from regular or quasi-regular polyhedrons, as the Fuller's domes, while in others the final polyhedral shape is obtained by faceting a reference smooth surface. The underlying surface

110

can be more (as in the case of revolved surface) or less regular (as in free form shapes).

When involved shapes are regular or quasi-regular the generation of desired polyhedrons is possible through analytical rules. In this case the design process consists in the choice of the shape that best fits the design requirements from a kind of catalogue previously defined. Besides regular, quasi-regular and revolved polyhedrons, a large family of such solutions can be obtained by means of translation and scaling of curves (Figure 6.1), as it has been described by Holgate [1997] about the work of Schlaich Bergermann und Partner.
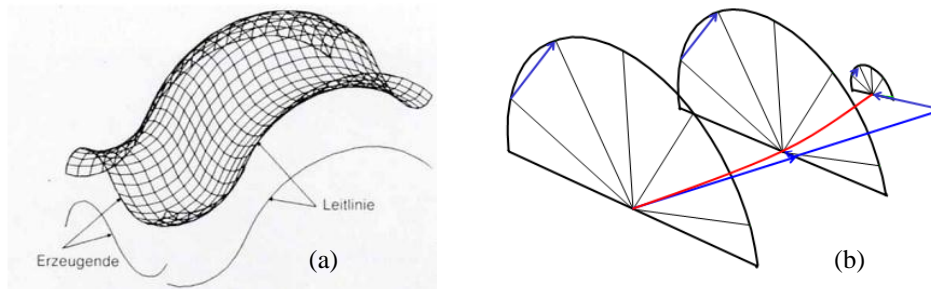
Figure 6.1 – Generation of quasi-regular grid-shells (a) translating and (b) translating and scaling curves.

Following this approach, one generates a continuous smooth surface by translating a spatial curve, called generatrix, parallel to itself, along another spatial curve called directrix. Surfaces obtained in this way intrinsically satisfy planarity and standardization requirement. Considering two sets of equally spaced curves, parallel, respectively to the directrix and to the generatrix, the intersection points of this curves form a network of spatial points. As it is shown by Schlaich and Schober [5] all the faces of the corresponding mesh are plane parallelograms and it is obvious the repetition of frame typology at least at each row. The procedure can be extended by evenly scaling the generatrix, during translation, with respect to a reference point. In this case, net faces are not longer parallelograms but they remain plane. This geometrical construction technique has been applied successfully in many projects. From a general point of view, this approach consists in shrinking the field of feasible shapes to a restricted family, obtained by the generation rule.

111

In projects where a complex shape is defined already at the conceptual stage and the boundaries of the structure have to fit specific geometrical constraints, the problem can be alternatively solved through an optimization process. Following this procedure, generic meshes representing grid-shells are transformed iteratively into grids that fit the previously set requirements by modifying step by step the position of points. The final configuration can be optimal or just sub-optimal if the requirements are satisfied only with a defined level of approximation.

6.2.   Frames standardization

Assuming the shape of a freeform grid-shell is fixed, the possibility to design that shape with a limited number of frame typologies is investigated.

(+) PERFORMANCE

(-) COSTS   (+) CONSTRUCTABILITY

6.2.1. Problem and purpose

In huge free-form glass roofing, such as in the long covering designed by Fuksas and Schlaich for the trade fair in Milan (Figure 6.2), the complexity of the shape leads to a great heterogeneity in the element typologies. If the structural elements might be chosen from a catalogue instead, the risk to deal with a puzzle of numbered pieces on the building site could be avoided. Moreover, the number of different typologies of cladding elements may not be a decisive factor in the case of glass slabs, easily 'mass customized', but quite important, for instance, in the case of solar panels that are themselves a composition of different elements. In this section the purpose is then to make the closest possible approximation of a given free form grid-shell shape made with standardized element typologies.

Figure 6.2 – Trade Fair in Milan by Fuksas and Schlaich (2005).

112

6.2.2. Objective function

The improving process of the starting mesh can be analyzed as a comparison between the frames lengths at each step of the optimization process and a set of referential measures, chosen "a priori" as a database for the final tessellation of the initial shape.

The fitness function that allows to monitor the effectiveness of the developed algorithms is:

$$f = \sum_{i=1}^{n}(l_i - l_{dat}^*) \rightarrow 0 \qquad\qquad (6.2)$$

where n is the number of frames, l_i is the length of the ith frame and l_{dat}^* is the nearest database measure to l_i.

The database is the set of measures, decided 'a priori' by the designer, as the only allowable for frames of the structure.
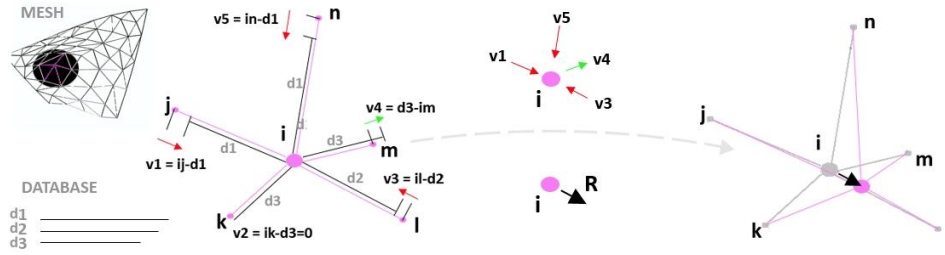
Figure 6.3 – Graphical representation of the vectors generation rule for the standardization problem.

The convergence of the fitness function f to zero is the optimal searched solution.

6.2.3. Optimum database

A particularly effective step, in order to improve previously shown procedures, has been the development of an auxiliary algorithm, the function of which is to optimize the database by choosing a set of "smart" measures.

Starting from the original mesh it is possible to know exactly the measure of each frame and is also possible to define a mean value from all these measures. In the same way, it is possible to divide the range of measures in smaller intervals and find out the mean value of each one. Consequently it is immediate to understand that the fitness calculation result is improved by assuming these mean values as database measures and moreover this is true if intervals are designed to contain as many frame measures as possible.

To perform this process a standard "divide et impera" algorithm has been implemented. It has to be noticed that avoiding a direct choice of database measures does not mean a loss of control on the final result since the lengths of starting mesh frames are managed by the designer.

6.2.4. Test of the algorithm's consistency

In order to prove the feasibility of the tolerances derived from the application of the algorithm, a first test is performed and a physical model corresponding to the resulting optimized geometry is built (Figure 6.4). Figure 6.5 shows how the database measures are assigned in the Graphical User Interface implemented in the open source modeler Blender[17] and how the visual output of the frame lengths produced by the software already demonstrates the effectiveness of the algorithm.

---

[17] www.blender.org
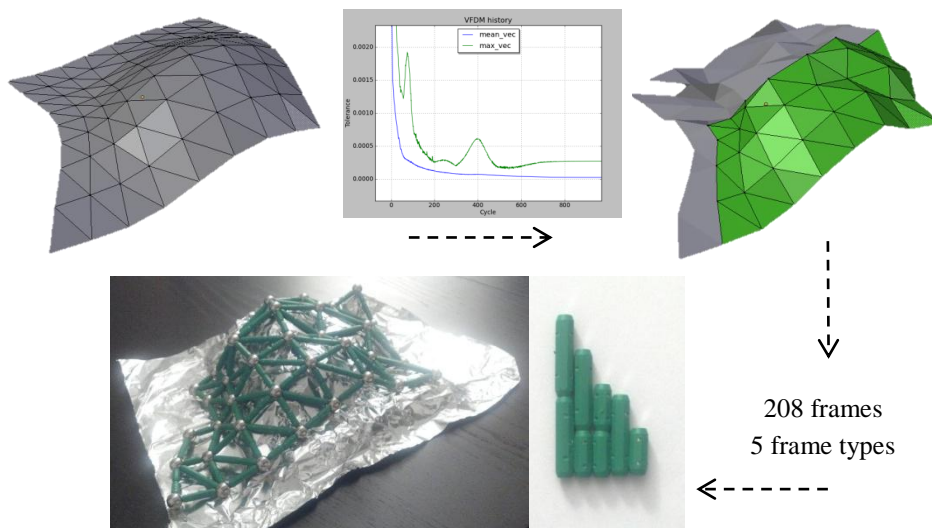
Figure 6.4 – Graphical representation of the vectors generation rule for the standardization problem.
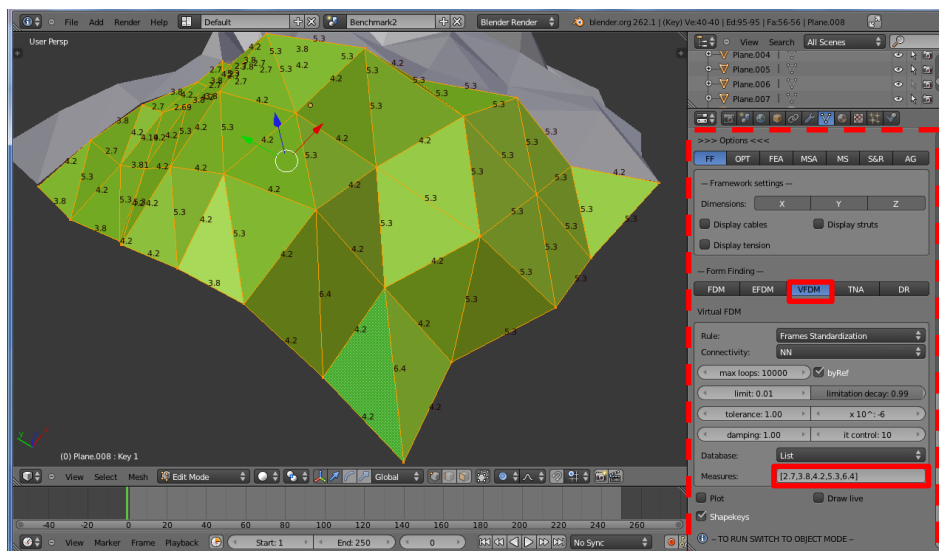
Figure 6.5 – Graphical User Interface of the VFDM implemented in the open source software Blender.

115

6.2.5. Case study A – Benchmark geometry

This first case study shows the consequences of using different databases in the same optimization process. An increasing number of database measures allows a time saving in terms of computation and also a better approximation of the original surface and consequently smoother shapes. Anyway the algorithm seems to work quite well, adapting all the frames lengths to database measures, even if the database is 'small'.

| Original mesh (2474 frames) | Final configuration with 51 database measures | Final configuration with 16 database measures |

Convergency history
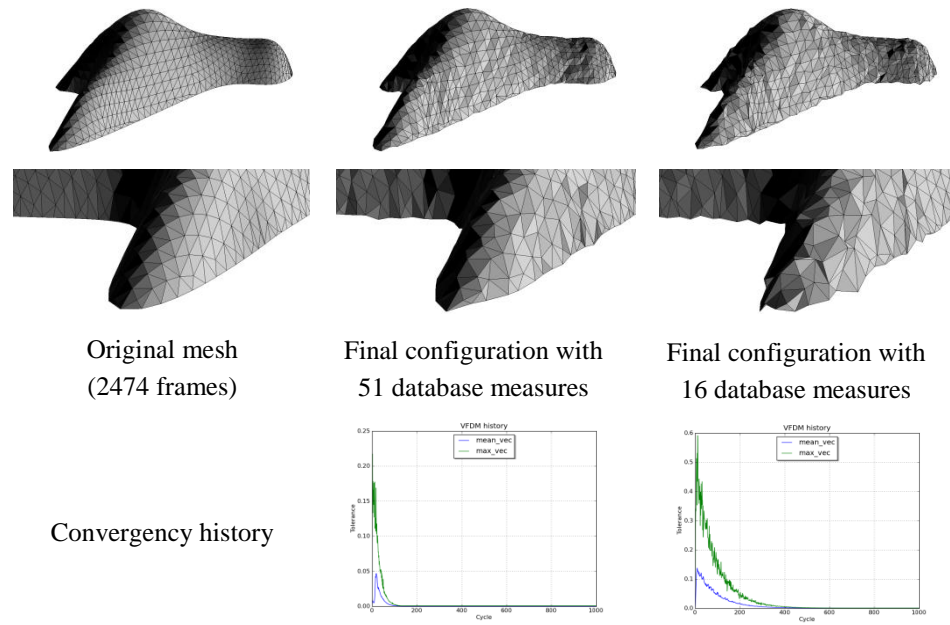
Figure 6.6 – Shape smoothness evaluation.

6.2.6. Case study B – Auditorium of Padua

This second application shows consequences in algorithm efficiency when a significantly high number of constrained joints is set. When the original shape to approximate has a very irregular geometry or there are characteristic lines the maintenance of which is of primary importance, the possibility to fix some joints or to link their movement to curves or surfaces during the optimization process is

116

requested. On the other hand, too rigid boundary conditions could make a total convergence of the algorithm impossible as shown in Figure 6.7.

(a)

(b)

Convergency history

(c)
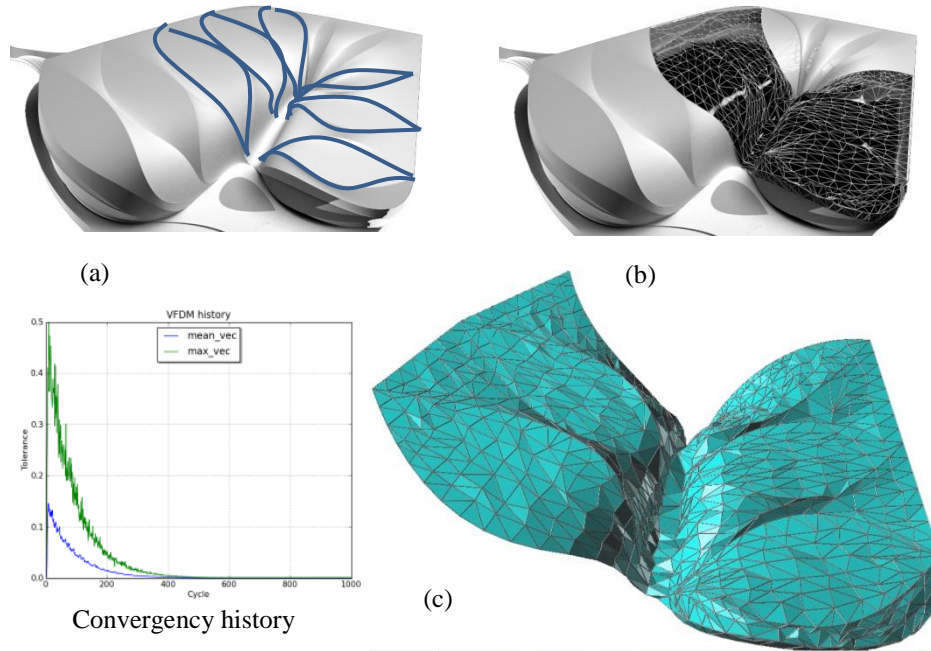
Figure 6.7 – Redesign of part of the Auditorium of Padua roof as a grid-shell and standardization of the frames measures according to the set constraints. The blue lines in (a) show where the nodes of the mesh have been constrained while (b) and (c) are two view representations of the final morphology of the grid-shell.

Table 6.1 – Results of the frames standardization.

Mesh frames	Database measures	Database frames	% of database frames	Constrained joints	% of constrained joints
2743	36	2326	85	392	15

117

6.3.   Multi-objective optimization

The possibility of a combination between the frames standardization process and a static enhancement of the structure has been tested. The optimization process is led by a Memetic Algorithm (MA) (Elbeltagi et al., 2005) which takes advantage of the commercial FEM software Ansys™ to evaluate the statics of the structure.

The MA implements the evolution of a NURBS surface acting on the vertical movement of 16 control points into a square basis parallelepiped volume (Figure 6.8).
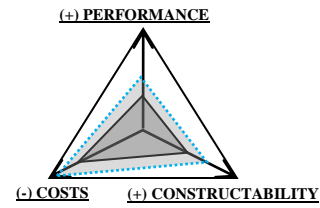
Boundary conditions	
Domain	Square Basis Parallelepiped Volume (9m x 9m x 6m)
Nr of NURBS control points	16
Constraints	4 fixed joints (the four corners of the square basis of the parallelepiped volume)
Restraints	No relative rotations among frames
Material	Steel (ρ=7850 kg/m^3, E=210000 N/mm^2, v=0.3)
Frame Section	Pipe D101.6 mm x 3.6 mm (A=11,1 cm^2, J=133 cm^4)
Load Pattern	1kN/m^2
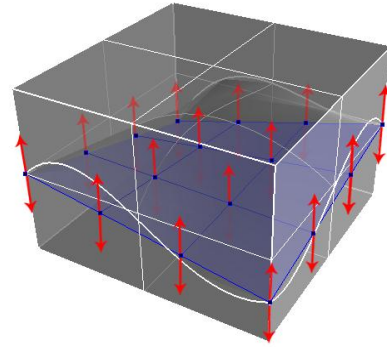
Figure 6.8 – Design space and boundary conditions.

All the NURBS surfaces are then changed into a correspondent mesh, automatically generated by the software, and geometrically optimized through the VFDM before the static performance evaluation. The shell static performance evaluation is based on the strain energy of the structure under a uniform force field (Sasaki, 2005). The VFDM applies after the mutation operator of the GA such that the frames are standardized. The results obtained from the study of a simple benchmark are shown below.

| 4.55e-04 m | 1.43e-03 m | 2.57e-03 m |

Figure 6.9 – Three reference configurations and the respective maximum values of deflections.

9.97e-04 m
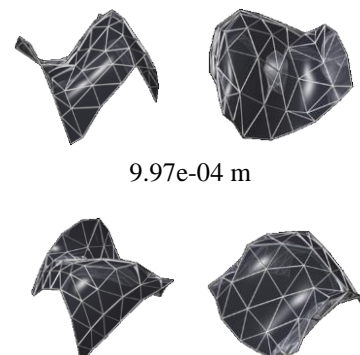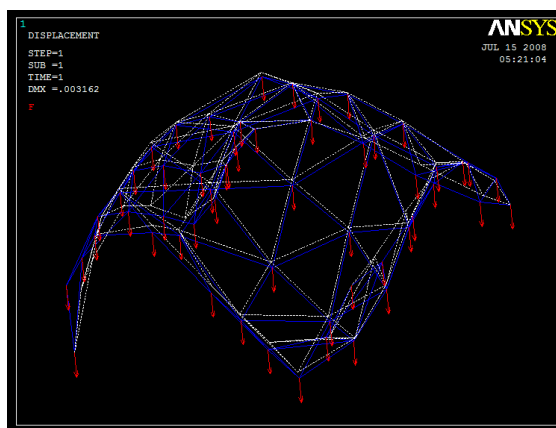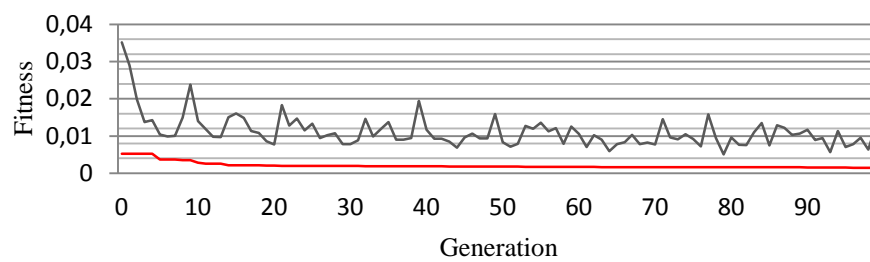
Figure 6.10 – Results of the multi-objective optimization as a combination of geometrical and static performance improvement.

119

The static behavior of the resulting grid-shell (Figure 6.10) is comparable to other traditionally effective configurations (Figure 6.9) and the free-form structure (139 elements) is made only by 8 frame typologies.

6.4. Planar Quadrilateral meshes

6.4.1. Problem and purpose

The aim is to make an effective approximation of a given free form shape by a composition of Planar Quadrilateral (PQ) glass elements. Usually, cladding glass elements are planar because they are directly cut from planar glass plates industrially produced. When a plane rigid panel is used to cover a net face with more than three sides, it is then necessary to make sure that all the corner points lay on the same plane. Only if the cladding material is soft and can be freely curved, as in the case of inflated ETFE pillows this requirement loses its importance.

The focus is specifically on quadrilateral grids since almost all NURBS modeling software can effectively generate quadrilateral meshes starting from a general free-form surface.
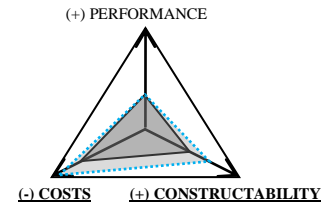
6.4.2. Objective function

A quadrilateral mesh, generated starting from a free-form surface, is in general skewed, and the four vertices lay on different planes. Considering a group of four adjacent points, the 'skeweness' is what is referred to as the 'planarity error'. The simplest way to measure such error is to pick three points out of the four and to measure the distance between the fourth and the plane defined by the first three. Given points *P1*, *P2* and *P3*, *a*, *b*, and *c* coefficients of the corresponding plane are the solution of the following linear system:

$$\begin{cases} ax_{p1} + by_{p1} + cz_{p1} + 1 = 0 \\ ax_{p2} + by_{p2} + cz_{p2} + 1 = 0 \\ ax_{p3} + by_{p3} + cz_{p3} + 1 = 0 \end{cases} \quad (6.3)$$

and the distance *d* between the plane and the fourth point *P4* is given by:

$$d = \frac{|ax_{p4} + by_{p4} + cz_{p4} + 1|}{\sqrt{a^2 + b^2 + c^2}} \quad (6.4)$$
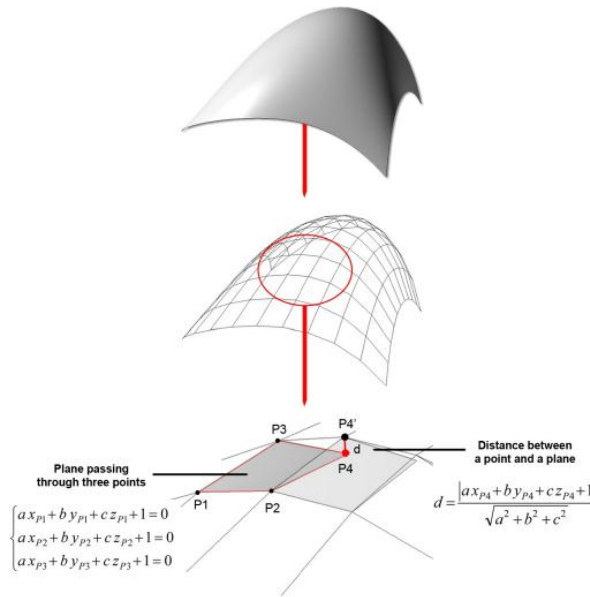
Figure 6.11 – Visual representation of the planarity error.

A measure of the planarity error based only on one face could be misleading, because each point in general belongs to four different faces, except points along boundaries. Hence the measure should take into account the planarity of all the four adjacent faces, that have one common point. A simple way to do that is to sum the error values of the adjacent four faces: it can be shown that this sum is a good

approximation of the local gradient of the planarity error, if only the coordinates of one point are considered as variables.

When a suitable error measure for each face or for each point of the polyhedral configuration is defined, an overall measure of the configuration error is to be evaluated. Both the whole local errors vector and its Euclidean norm can be used in the optimization process, depending on the computational procedure. Consequently the objective function reads:

$$f = \sum_{i=0}^{n} \sqrt{\sum_{j=0}^{m} d_j^2} \to 0 \qquad (6.5)$$

where n is the number of vertices, m is the number of faces touching the ith vertex, d_j is the planarity error between the ith vertex and the plane defined by the points of the jth face.

The convergence of the fitness function f to zero is the optimal searched solution.

6.4.3. Case study A – Benchmark geometries

The VFDM is applied on a group of reference geometries with different boundary conditions which depend on the number of geometrical constraints applied on the edge of the open polyhedron. A genetic algorithm (GA) is applied on the same problems to make a comparison.

Only the vertical coordinate of each point is assumed as a design variable, so that the plan projection of the points is constant. Different results can be obtained if all the three coordinates can change, or even if the points are forced to move on an assigned surface. In this case the optimal pattern, when it exists, is generally smooth as the underlying surface, but a scattering appears in the horizontal position, making the grid shell look very irregular.

In the first benchmark (Figure 6.12a), the boundaries of the polyhedron are the side of a plane square, so that just one optimal solution exists and it corresponds to the plane shape. The second benchmark (Figure 6.12b) is the hypar, i.e. a boundary constrained surface with four skewed sides. Given such boundary condition, no

polyhedrons with plane faces exist, so that no optimal solutions can be found by the algorithms. The global minimum (or local minima) of the fitness function are sub-optimal solutions and the algorithm is expected to converge to them. Benchmarks 3-4 (Figure 6.13) is a variation of the first one: a barrel vault with two parallel straight sides and two curved generatrices. In this case two different constraint conditions are considered: a) only the curved sides are fixed; b) only the straight sides are fixed.

This group of applications has been developed as a reference for tuning the algorithm: the number of design variables describing the geometric configurations is relatively small and the behaviour of the algorithm under three different conditions, uniqueness of the optimal solution, absence of any optimal solution and existence of an infinite number of solutions, is considered.

In the upper parts, figures show the intermediate results obtained during the iterative optimisation process, comparing the GA with the VFDM. Intermediate solutions are compared when they reach the same value of the fitness function. The numbers accompanying pictures indicate the number of iterations necessary to reach the same fitness value. In the lower part of each figure the convergence of the fitness function is depicted, comparing again VFDM (red line) and genetic algorithm (black line best fitness, grey line average fitness).

As expected, in the first benchmark both algorithms converge, with different speed, to the optimal plane solution. In the second benchmark, where no optimal solutions exist, both the algorithms converge to the configuration of minimal surface, that is not optimal, because quadrilateral are not plane, but is a minimum of the fitness function.

In both barrel vault benchmarks the problem is largely indeterminate. Starting from only two of the four sides, indeed, all the curves connecting one point of the first side with the corresponding point on the second side can be used as a path curve in the curves translation generation, so that an infinite number of solution can be found. This situation is an example of under-constrained problem, in which the optimization algorithm can converge on many different optimal solutions.

The comparison between solutions reached at intermediate stages of the procedure, but with the same fitness value, explicates that the VFDM converge dramatically quickly and always outperforms the GA. Of course the optimization path depends much on the choice of the algorithms parameters, and in particular on

123

the way the search domain is adapted through the optimization process in order to improve the convergence speed.
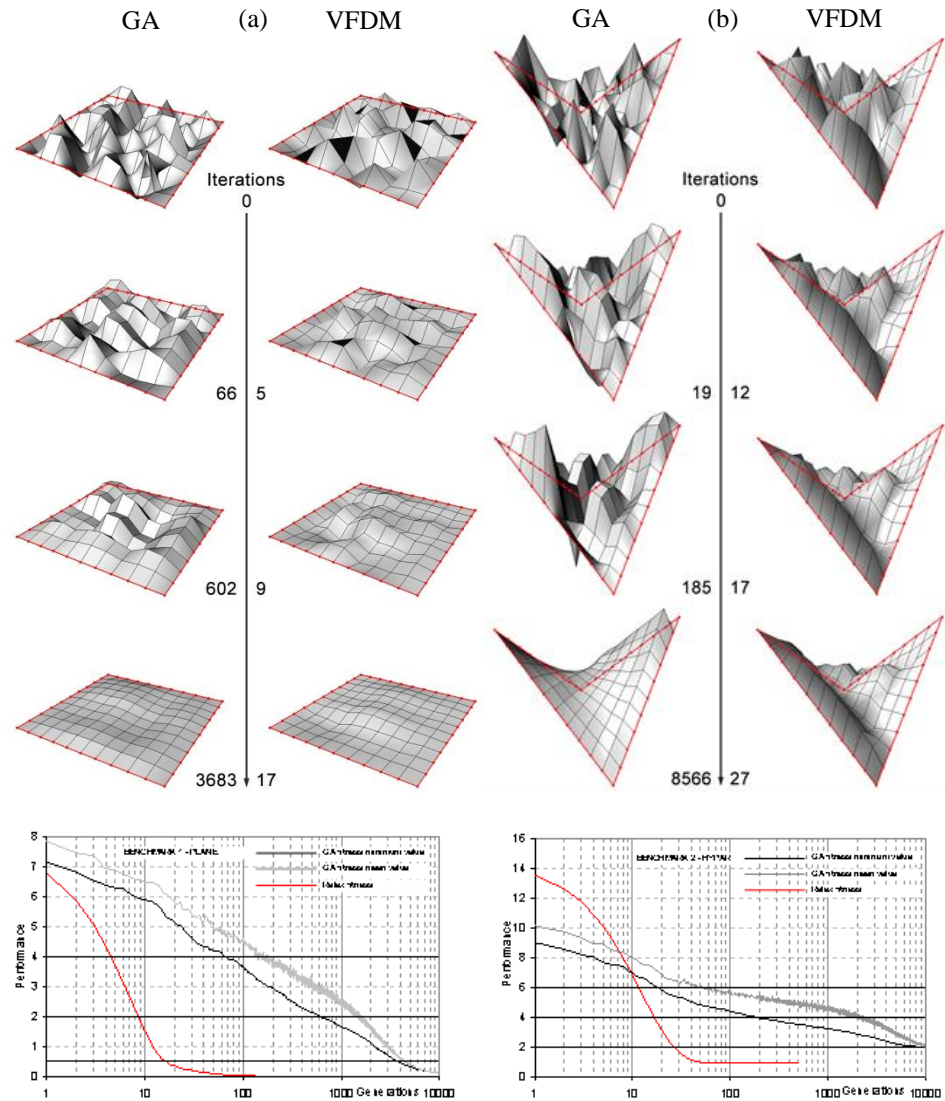
Figure 6.12 – (a) Benchmark 1 (Plane) and (b) Benchmark 2 (Hypar).

124
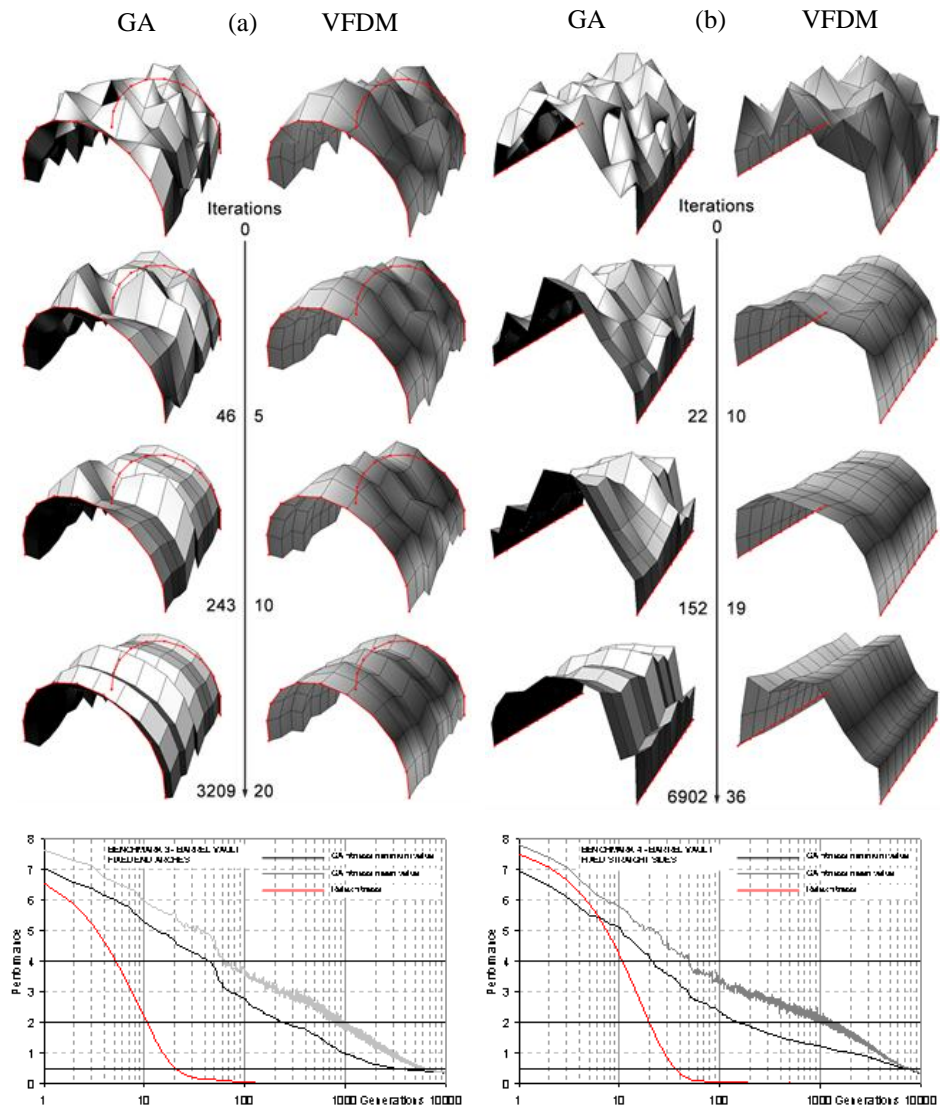
Figure 6.13 – (a) Benchmark 3 (Barrel vault - fixed end arches) and (b) Benchmark 4 (Barrel vault - fixed straight sides).

6.4.4. Case study B – Tergesteo Gallery in Trieste

This real case study consists in the glass canopy of a cross shaped commercial space, inside a historical building in Trieste (Italy). Erected in 1842 with a traditional glass covering for the inner gallery Figure 6.14 (a) it was renovated after the second post-war with a new roof realized in reinforced concrete and glass blocks vaults. Due to the excessive loading on existing walls, generated by this heavy structure, at present it is necessary another renovation process that can be seen as an opportunity to design a lighter and transparent roof, of higher quality also from the architectural point of view.

Figure 6.14 – From left to right: picture of the first Tergesteo Gallery, 1842; b) New roof of the Fifties.

The general shape of the project for the new glass grid shell is depicted in Figure 6.14 (b). The quadrilateral structural mesh is drawn following the symmetry axes of the gallery. Only the dark portion of the roof has been optimized. The architect has defined the initial shape at the conceptual design stage with the aim to emphasize the central space and to reach the maximum transparency effect. The optimization process is then required to improve the grid geometry without radically altering the architectural shape.

At the end of the iterative process, the obtained optimized shapes are very similar to the initial ones, but their fitness is considerably higher. That means that significant improvements of the shape, from the point of view of the planarity requirement, can be reached with slight modifications of the initial shape, preserving the original concept (Figure 6.15).
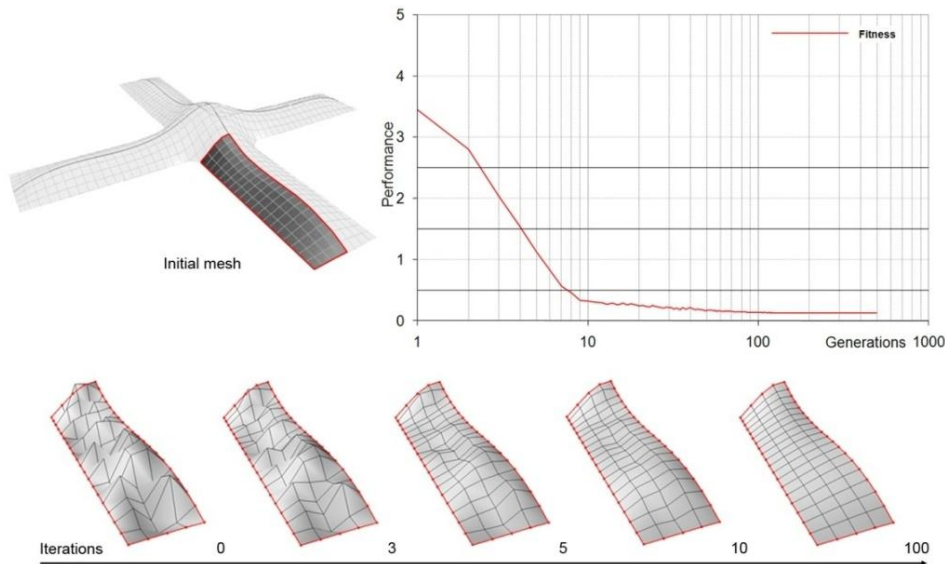
Figure 6.15 – Results of the VFDM application to the Tergesteo gallery project.

6.4.5. Case study C – Ponte Parodi project in Genoa

Ponte Parodi is a project by UNStudio Amsterdam for a commercial building in Genova, Italy, which takes its name from the pier where the building will be located (Figure 6.16). The most complex element of the project, from a geometrical point of view, is represented by the roof which has the function of a "green" public plaza.

127

Figure 6.16 – Ponte Parodi – renders by UNStudio.

The unconventional shape of this covering and the involved dead load ($1700 kg/m^2$) imposed a particular study for the supporting structure. In order to take care of several analyses, such as seismic behavior of the whole structure, suitable approximation of the architectural design and costs optimization, the proposed solution was a composition of planar steel grids which allowed a rigid behavior of the whole structure and a standardization of steel elements. The solution was performed with the aid of the VFDM algorithm and the optimization process took care of several parameters as the position of the columns and the minimum and maximum height allowable for the structure all along the building. Consequently, the algorithm allowed only a vertical movement of planes corners between two values of z coordinate where constraints were represented by columns. Other boundary conditions were necessary to ensure the respect of characteristic lines of the architectural design. The result of the generation process is showed in Figure 6.17.
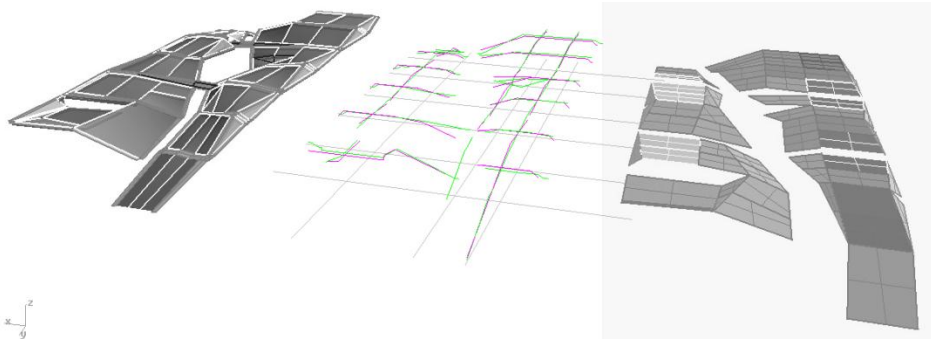
Figure 6.17 – On the left the architectural envelope, on the right a scheme of the structural planes and in the middle a representation of the distances between the optimized mesh and the target surface corresponding to some transversal and longitudinal sections.
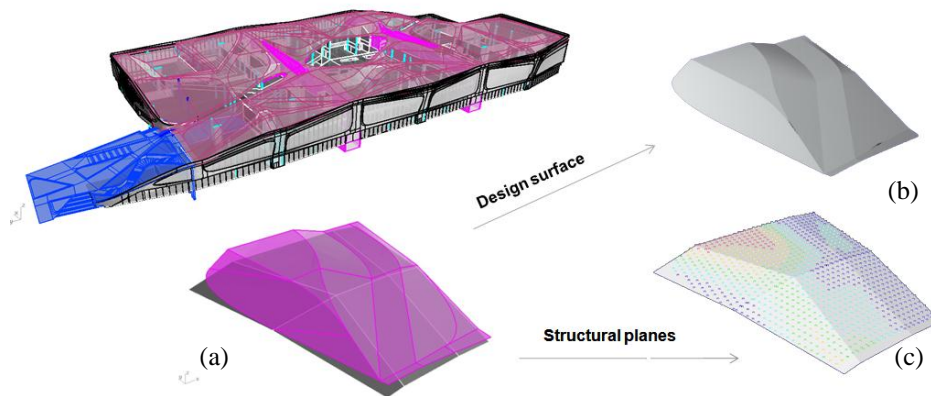
Figure 6.18 – (a) Superposition of target surface and optimized mesh; (b) Target (design) surface; and (c) Optimized mesh (dots represent the deviation from the surface – the darker the closer).

A non-perfect approximation of architectural landscape was allowed considering the possibility to model shapes in a second time with the ground. However the deviation of the solution from the referential envelope was controlled through a point deviation study (Figure 6.18c) and a similar study was necessary to respect internal heights which represent together the solution domain. As a consequence of

grid planarity it was largely possible to standardize elements and joints (maintaining angles of 90° among elements - Figure 6.19).
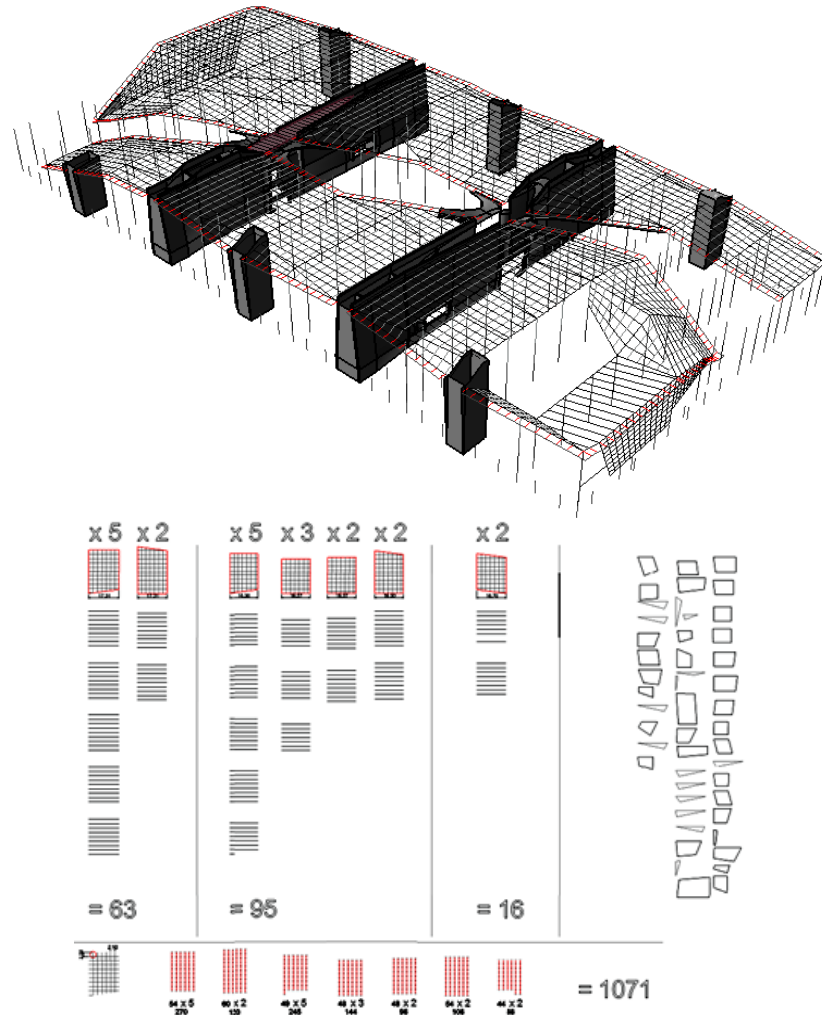
Figure 6.19 – Assembly of the Ponte Parodi roof structure.

Chapter 7

Acoustic enhancement of a concert hall by means of an adaptive ceiling

Abstract

The FSCS is applied to find compatible optimal configuration of an adaptive ceiling in order to enhance a concert hall acoustics depending on the location of the listeners inside the room. The application illustrates how the FSCS can deal with different type of VGSs such as a rigid-foldable origami and a set of MSE. For the origami-case the topology optimization process is also applied allowing a reduction of the actuators needed but without affecting too much the optimal level of performance.

7.1. Problem statement

In this section two of the previously discussed VGSs (Chapter 2) are proposed for the acoustic performance enhancement of a generic architectural space. In particular, the study involves the application of a rigid-foldable origami and of a MSE system as adaptive
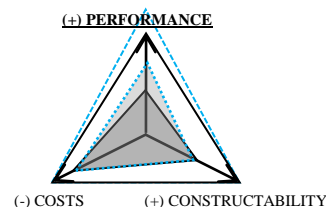
ceilings and starts from the assumption that the optimal acoustics of a room depends on the level of crowd and on the location of listeners inside it.

The two applications have not to be considered in a comparative way but are meant to be a first numerical validation of the proposed optimization algorithm.

Assuming that we know through a sensing system where people are placed inside the room, the aim is then to change the configuration of the responsive ceiling to make it possible that the sound inside the room results concentrated over the areas where listeners are effectively placed with a homogeneous distribution. This task leads to the challenge of finding a unique envelope which is able to switch among different optimal configurations. Since in the presented case study the focus is more on the effectiveness of the optimization method than on the evaluation of all the possible combinations of listener locations inside the room, only two possible conditions will be considered: a fully crowded room and a room which is only crowded in its first half (Figure 7.1). The FSCS is used to manage the whole design process.

The geometry has been handled inside the commercial NURBS software Rhinoceros™ while the MA, the VFDM and an acoustic propagation model have been implemented in Python, starting from the results of a previous research [Mendez et al, 2008].
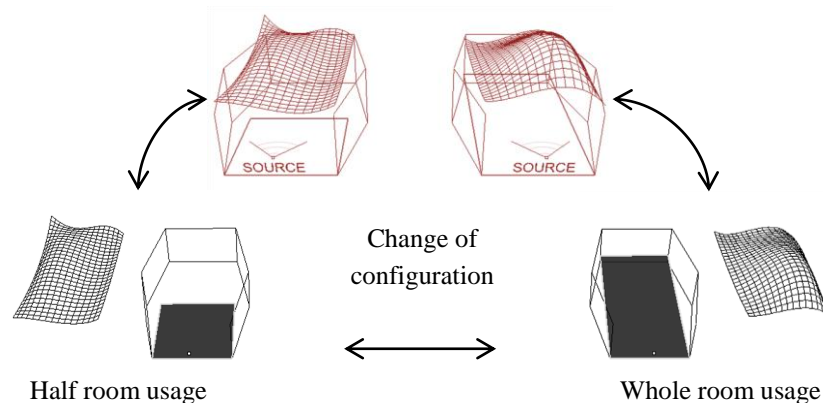
Figure 7.1 – Concept: skin adapts to changes in room usage.

132

7.1.1. Optimization domain, objective function and boundary conditions

Since the skin is supposed to be hanged to the room's roof, the domain inside which the skins are generated is represented in Figure 7.2 by the grey volume between the top and the minimum internal height of the room.
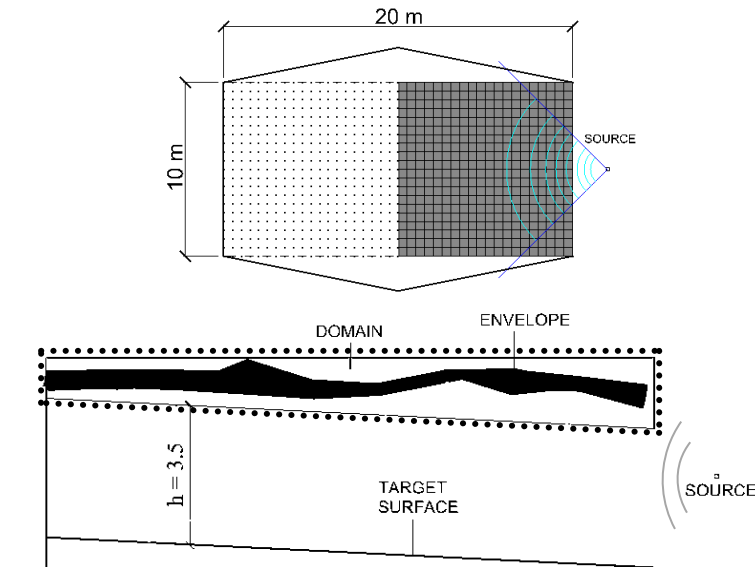
Figure 7.2 – The dotted line represents the domain for the MA mutation.

The objective function that drives the MA is based on the acoustic performance of the room so, to analyze it, an acoustic simulator has been implemented inside Rhinoceros™ using the method of Raytracing (Figure 7.3). In this method sonic energy is simulated by the uniform casting of rays, from a sonic source, towards the object, following the principles of geometric acoustics. The acoustic properties of materials have been also considered in the model. Each ray represents a part of the acoustic energy. This energy becomes weaker every time the ray hits a surface, and all of the energy is added up when it reaches the desired receiving area. This reflected ray will ultimately arrive at the public's or listener's area, at which point

its energetic value is determined. By casting many rays and mapping the locations in which their reflections end up it is possible to evaluate the uniformity of the sound reflection of a given surface. Specifically for this case study each ray's acoustic energy at start is set to 100% and each reflection on the boundary walls or on the adaptive ceiling is assumed to adsorb respectively the 15% and the 30% of the energy of the ray. The rays, emitted by the source from the height of 2.70 m, propagate within an initial horizontal and vertical angle of 90° (45° each side); the ray-tracer generates a ray every 2° inside this domain, as to say a total of 2025 rays.
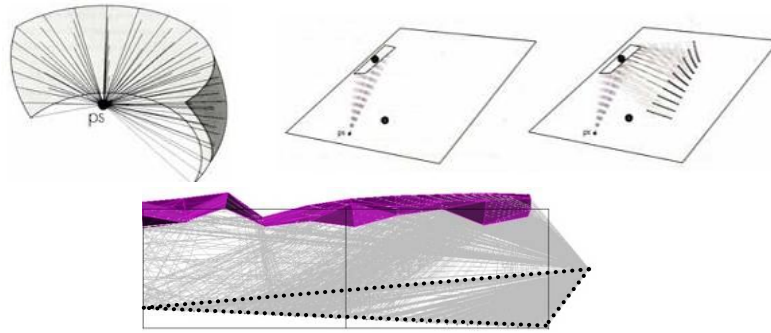
Figure 7.3 – Representation of rays from an omni-directional source and scheme of rays (vectors) reflection with the roof and boundary walls. Rays inside the dotted line triangle directly hit the target surface.

The listeners' area is divided into sections. Usually in acoustic simulation software this spaces represent each single listener, therefore their dimension should be of about 50x50 centimeters (the average dimension of an audience seat). We then establish the level of uniformity of the sound distribution in the listeners' area and compare the amount of energy that reaches each single listener with the situation of a perfect uniform sound distribution. Standard deviation, calculated between the each surface's acoustic response and an ideal one, reads:

$$\delta = \sqrt{\frac{1}{n} \sum_{i=1}^{n} [e_i - \mu_e]^2} \qquad (7.1)$$

where:

n = number of sections composing the listener's area;

e_i = level of energy that reaches listener i;

μ_e = mean level of energy over the whole area.

Finally the fitness of individuals in the MA is calculated as:

$$fitness = {}^{1}\!/\!\mu_e + \delta^2 \ \to 0 \tag{7.2}$$

In a real acoustic performance evaluation also other important parameters should be considered, first of all the reverberation time, but for the current purpose the convergence of (2) to zero can be accepted as the optimal searched solution.

7.1.2. Algorithm settings

For the illustrated purpose, the finite state control strategy introduced in Chapter 5 is used.

Since the main structure of the algorithm follows the idea of a traditional MA while the VFDM (placed as an additional operator inside the MA) controls the maintenance of the VGS kinematics during the optimization, a double advantage is obtained. On the one side, only the VFDM settings need to be modified when the problem moves from the case of the rigid-foldable origami to the one of the MSE; on the other side the structure of the MA remains the same as in the case of a "static" optimization. In both the origami and the MSE cases, in fact, the MA just generates a population of meshes, which practically represent the responsive skins, and, after a fitness evaluation, decides to kill the process or to combine and mutate the meshes on the basis of a pseudo-random selection. Mutation acts on the z coordinate of the mesh nodes, randomly moving them vertically inside the domain.

The VFDM, which is called before every new fitness evaluation over all the meshes which have been recombined and/or mutated, practically acts as a constraint over the kinematics of the transformation. The VFDM specific settings are reported together with the related applications in the next sections.

The used MA parameters are reported in Table 7.1.

Table 7.1 – MA parameters.

Parameter	Value
No. of generations	500
Population size	15
No. of élite individuals	1
No. of individuals for the local search	2
No. of individuals to be discarded	1
% of population mutation	30
% of individual mutation	20

7.2. Rigid-foldable origami approach

A rigid-foldable origami can be simply represented by a triangular mesh. In order to ensure the "foldability" of the mesh it is possible to perform a matrix analysis of the corresponding framework, as explained in 0 and the analysis should result in enough independent inextensional mechanisms without self-stiffness. For the case study presented here, the mesh has the crease pattern represented in Figure 7.4 (a) and is composed by 50 nodes (n) and 121 frames (f).

The number of internal independent inextensional mechanisms (m) can be derived as follows as a function of k and s:

$$m = 3n - f - k - s \qquad (7.3)$$

$$m = 50 \cdot 3 - 121 - k - s = 29 - k - s$$

where:
k = number of kinematic constraints to a rigid foundation;
s = number of independent states of self-stress.

Consequently, the possibilities in constraining mesh nodes to match the target surface depend on equation (4) or, in other words, the choice of the k value and the location of the constraints affect the range of achievable configurations. For the presented case study, it is assumed that the skin is hanged at the roof structure with no fixed nodes and the only constraint is that the solution must be enclosed in the defined domain. This assumption ensures the maximum flexibility in the search for the optimal configurations.

In the case in which the procedure is applied to a multiplicity of states, once the set of optimal configurations has been defined, it could make sense to perform a further analysis to look for the minimum number of degrees of freedom (i.e. for the minimum number of actuators) which allows the necessary transformations.

As the faces of the mesh representing the rigid-foldable origami are triangular it is possible to ensure the kinematic compatibility of two different configurations of a mesh simply by maintaining the lengths of the frames constant during the optimization process. This consideration results in a specific setting of the VFDM connectivity matrix C and of the vector generation rule r.

$$C = \begin{pmatrix} 0 & 1 & \cdots & 0 & \cdots & 0 \\ 1 & \ddots & \ddots & \vdots & \ddots & \vdots \\ \vdots & \ddots & \ddots & 0 & \ddots & 1 \\ 0 & \ddots & 0 & \ddots & \ddots & 0 \\ \vdots & \ddots & \ddots & \ddots & \ddots & \vdots \\ 0 & \cdots & 1 & 0 & \cdots & 0 \end{pmatrix}$$
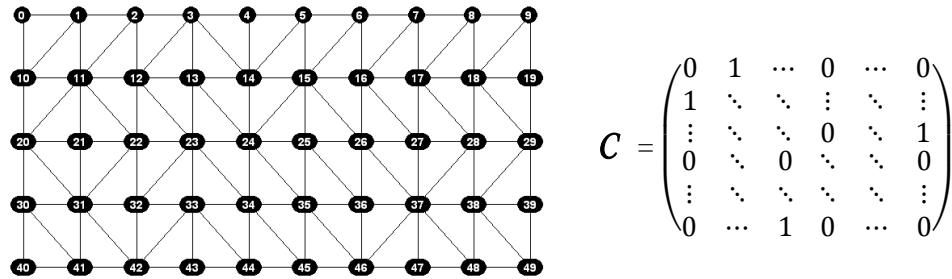
Figure 7.4 – From left to right: (a) representation of the rigid-foldable origami mesh and (b) the related connectivity matrix C.

The connectivity matrix C for this problem is reported in Figure 7.4(b) and is a m x m symmetric matrix where m is the number of mesh nodes. The ones in the matrix represent a connection between two nodes; the sum of the values at row i corresponds to the number of frames sharing node i.

The vector generation rule for the generic i node reads:

137

$$r_i = \sum_{j=1}^{n} \left[\vec{v}_{ij} \cdot \frac{|v_{ij0}|}{|v_{ij}|} \right] \tag{7.4}$$

where:

n = number of nodes connected to node *i* by a frame;

$\vec{v}_{ij0}$ = vector from node *i* to node *j* at start;

$\vec{v}_{ij}$ = vector from node *i* to node *j*.

Table 7.2 – Results of the MA for the rigid-foldable origami.

Generation	Acoustic Energy - Whole room		Acoustic Energy - Half room	
	$\mu = f(t)$	$\delta = f(t)$	$\mu = f(t)$	$\delta = f(t)$
1	0.0657 t	0.0852 t	0.0938 t	0.1066 t
5	0.0657 t	0.0852 t	0.0957 t	0.1067 t
20	0.0681 t	0.0854 t	0.0946 t	0.1066 t
50	0.0682 t	0.0854 t	0.0988 t	0.1069 t
100	0.0671 t	0.0848 t	0.0987 t	0.1062 t
300	0.0692 t	0.0848 t	0.1055 t	0.1060 t
500	0.0718 t	0.0846 t	0.1063 t	0.1059 t

Results of the improving process are presented in Table 7.2 as a function of the total energy *t* emitted by the source. The μ and δ values of the first generation correspond to the planar mesh case. Figure 7.5 shows the difference in the room acoustics between the starting planar mesh and the optimized skin for both the case of the whole room usage and the case of the half room usage. A 50x50 cm grid, which represents the target surface, is colored using a blue scale (grey in the printed version); dark blue represents the lowest acoustic energy level and light blue the highest. White dots on the grid represent instead the locations where the acoustic rays hit the target surface. Fitness improvement and the contemporary maintenance of frames lengths (with a tolerance of 1mm) prove the effectiveness of the proposed algorithm.

INITIAL PLANAR CONFIGURATION

| WHOLE ROOM USAGE | HALF ROOM USAGE |

MIN ENERGY ████████████████ MAX ENERGY
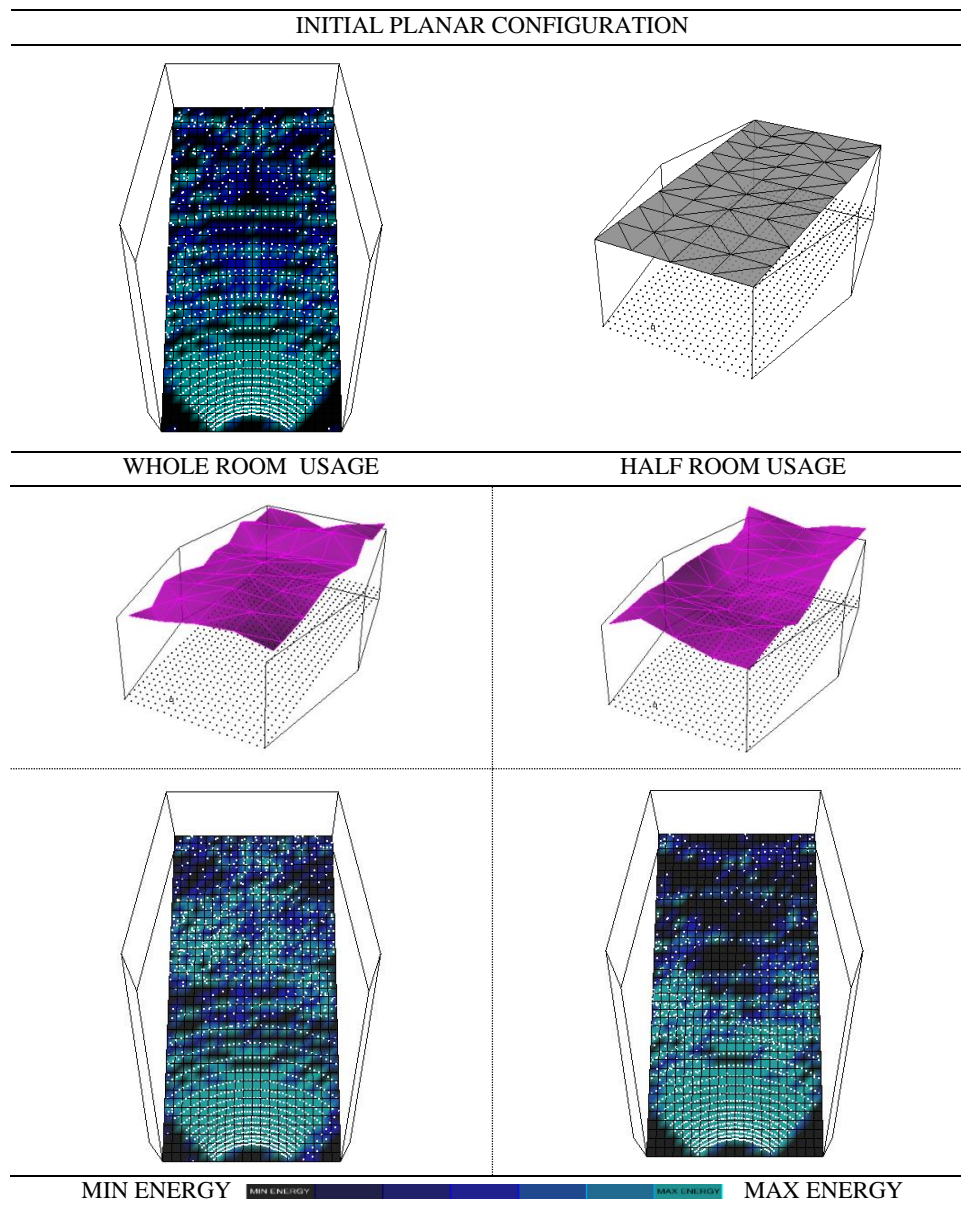
Figure 7.5 – Origami-Skin optimized configuration for the whole room usage (left) and for the half room usage (right).

139

Acoustic performance could be enhanced by a higher number of MA generations.

The optimal configurations are then further analyzed as explained in section 5.5 in order to proceed to the optimization of the framework topology. Table 7.3 illustrates how the reduction of DOFs from 23 to 14 partially affects the possibility of the envelope to find its best configuration in the case of the half room usage while has practically no impact in the case of the whole room usage. This result is also visually confirmed by Figure 7.6.

It can be expected that increasing the number of nodes in the pattern would further take advantage of the proposed topology optimization procedure.

Table 7.3 – Comparison of the results of the MA for the rigid-foldable origami before and after topological optimization..
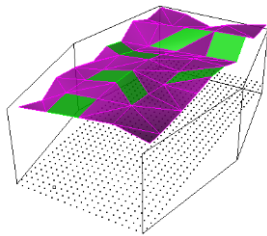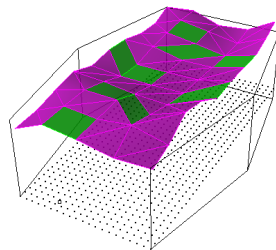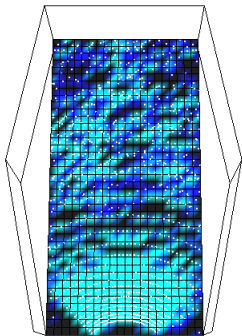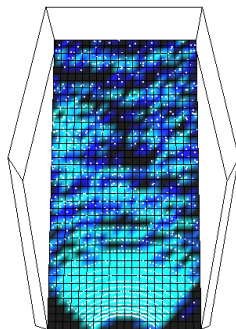
Generation	Acoustic Energy - Whole		Acoustic Energy - Half		DOFs
	$\mu = f(t)$	$\delta = f(t)$	$\mu = f(t)$	$\delta = f(t)$	
1	0.0657 t	0.0852 t	0.0938 t	0.1066 t	23
…	…	…	…	…	…
500	0.0718 t	0.0846 t	0.1063 t	0.1059 t	23
Topology opt.	0.0719 t	0.0846 t	0.1016 t	0.1062 t	14

WHOLE ROOM USAGE   HALF ROOM USAGE

MIN ENERGY   MAX ENERGY

Figure 7.6 – The 9 light gray quadrilateral faces take the place of 18 triangles as the result of the topology optimization process.

141

7.3.   Mutually supported elements approach

Assuming that the module for the MSE is the square one in Figure 7.1, then it is possible to represent a set of such modules by a quadrilateral mesh with nodes ordered in the **p** vector as in Figure 7.1(b). In order to allow the skin to change its configuration it is sufficient to identify the internal independent inextensional mechanisms 0 and then to set a reasonable number of constraints leaving one or more DOFs.

As in the case of the origami mesh, no MSE nodes have been constrained and only the inclusion inside the domain is requested. The purpose is still to force the mesh towards optimal configurations for the two different states of room usage previously explained.
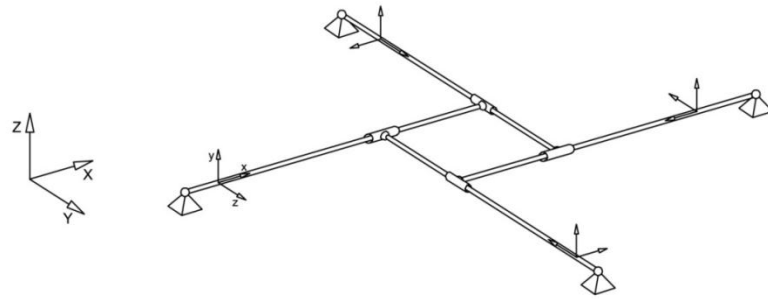
Figura 7.1 – Reference MSE module.

$$C = \begin{pmatrix} 0 & 1 & \cdots & 0 & \cdots & 0 \\ 1 & \ddots & \ddots & \vdots & \ddots & \vdots \\ \vdots & \ddots & \ddots & 0 & \ddots & 1 \\ 0 & \ddots & 0 & \ddots & \ddots & 0 \\ \vdots & \ddots & \ddots & \ddots & \ddots & \vdots \\ 0 & \cdots & 1 & 0 & \cdots & 0 \end{pmatrix} \qquad C = \begin{pmatrix} 0 & 1 & \cdots & 0 & \cdots & 0 \\ 1 & \ddots & \ddots & \vdots & \ddots & \vdots \\ \vdots & \ddots & \ddots & 0 & \ddots & 1 \\ 0 & \ddots & 0 & \ddots & \ddots & 0 \\ \vdots & \ddots & \ddots & \ddots & \ddots & \vdots \\ 0 & \cdots & 1 & 0 & \cdots & 0 \end{pmatrix}$$
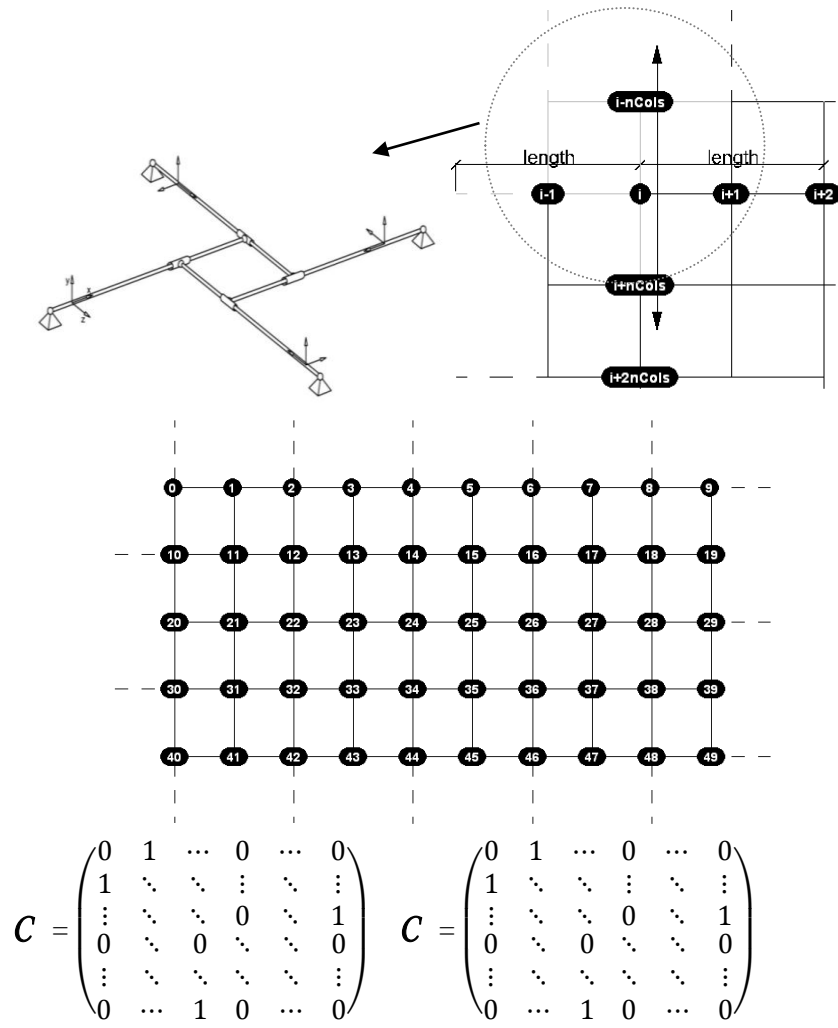
Figure 7.7 – From top left to bottom right: (a) relations among mesh nodes, (b) representation of the MSE mesh, (c) connectivity matrix C for maintenance of the MSE system, (d) connectivity matrix C for maintenance of frame lengths.

Compared to the case of the rigid-foldable origami, the MSE mesh must be associated with some more information in order to ensure both the VGS mechanics and the maintenance of the frame lengths. In particular the first objective is achieved by forcing the position of each node *i* to lie along the line defined by the vertices *i-nCols* and *i+nCols* (or by vertices *i-1* and *i+1* depending on the position of *i* in the mesh), where *nCols* is the number of nodes in each row of the mesh. Consequently, virtual force vectors are created from each node to its projection on the defined line, being the magnitude of the vector the distance between the node and its projection.

Keeping constant the initial frame lengths requires that each node *i* refers to node *i-2* and *i+2* (or *i-2nCols* and *i+2nCols* depending on the position of *i* in the mesh).

These considerations, graphically represented in Figure 7.1(a), lead to the construction of two different connectivity matrices – Figure 7.1(c),(d) – to manage the geometry changes .

The vector generation rule for the generic *i* node reads:

$$r_i = \vec{u}_i + \sum_{j=1}^{n} \left[\vec{v}_{ij} \cdot \frac{|v_{ij0}|}{|v_{ij}|} \right] \tag{6}$$

where:

n = number of nodes connected to node *i* by a frame

    (only frames which share node *i* as the start or the end point are considered);

$\vec{v}_{ij0}$= vector from node *i* to node *j*. at start;

$\vec{v}_{ij}$= vector from node *i* to node *j*;

$\vec{u}_i$ = vector from *i* node to the closest point on line $\overline{u_{i-1} u_{i+1}}$

    (or $\overline{u_{i\text{-nCols}} u_{i+\text{nCols}}}$ depending on the position of *i*).

<div align="center">**Table 7.4** – Results of the MA for the MSE system.</div>

Generation	Acoustic Energy - Whole room		Acoustic Energy - Half room	
	$\mu = f(t)$	$\delta = f(t)$	$\mu = f(t)$	$\delta = f(t)$
1	0.0657 t	0.0852 t	0.0938 t	0.1066 t
5	0.0663 t	0.0852 t	0.0956 t	0.1065 t
20	0.0675 t	0.0852 t	0.0981 t	0.1060 t
50	0.0686 t	0.0852 t	0.1086 t	0.1059 t
100	0.0683 t	0.0849 t	0.1085 t	0.1056 t
300	0.0691 t	0.0843 t	0.1099 t	0.1055 t
500	0.0698 t	0.0841 t	0.1105 t	0.1051 t

Results of the improving process are presented in Table 7.4 as a function of the total energy *t* emitted by the source. The μ and δ values of the first generation correspond to the planar mesh case. Figure 7.8 shows the difference in the room acoustics between the starting planar mesh and the optimized skin for both the case of the whole room usage and the case of the half room usage. A grid 50x50 cm, which represents the target surface, is colored using a blue scale (grey scale in the printed version); dark blue represents the lowest acoustic energy level and light blue the highest. White dots on the grid represent instead the locations where the acoustic rays hit the target surface. Considerations about the fitness improvement and the system geometry maintenance are analogous to the previous case study. Compared to the case of the rigid-foldable origami the MSE system seems to result in a better acoustic performance improvement. However, it is not possible to make a true comparison between the two VGSs because different assumptions of the starting configurations could have been produced different results. Moreover, the optimization processes through the MA are not repeatable so there are no certainties about the two fitness trends unless a more complete statistics is made by running the algorithm several times.

INITIAL PLANAR CONFIGURATION

WHOLE ROOM USAGE	HALF ROOM USAGE

MIN ENERGY   `MIN ENERGY`   `MAX ENERGY` MAX ENERGY
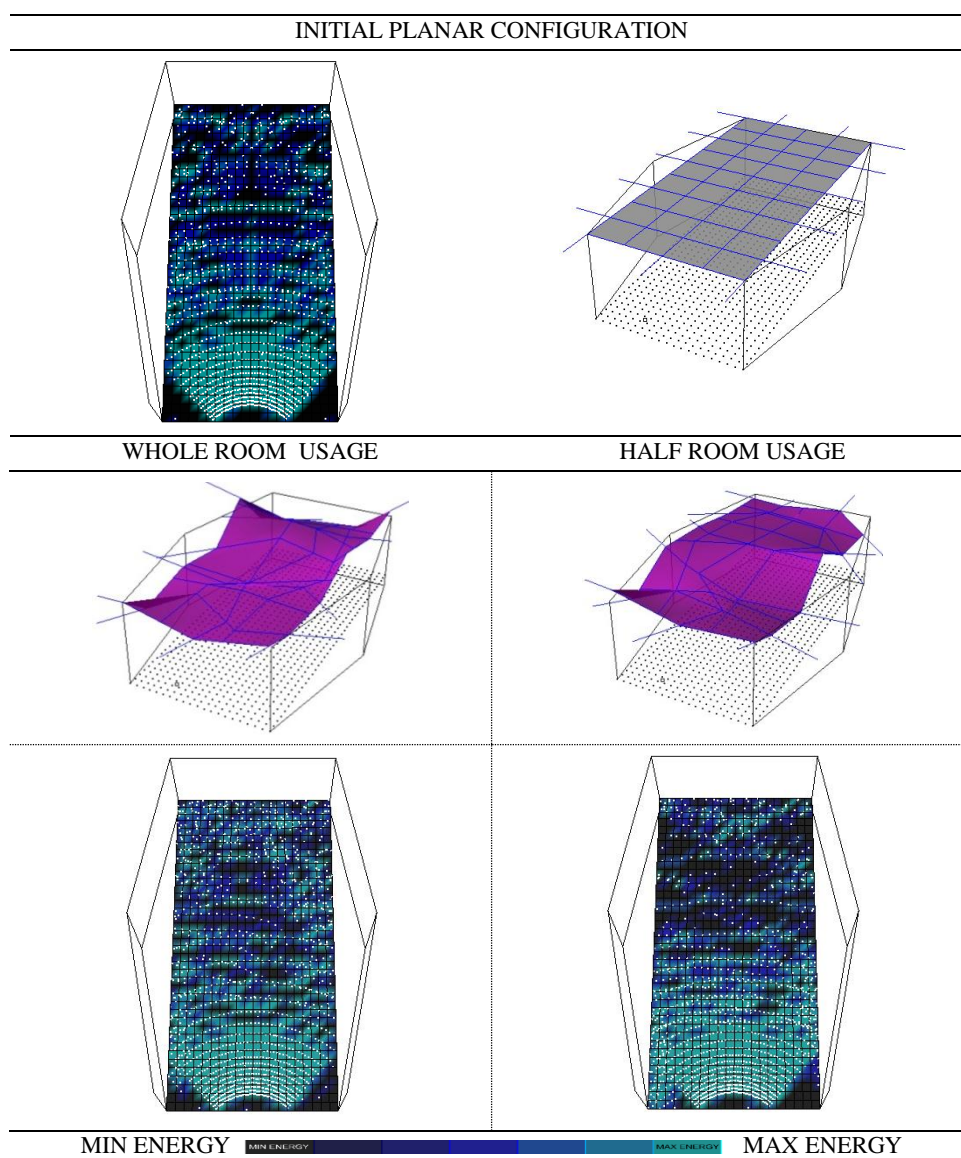
Figure 7.8 – MSE-skin optimized configuration for the whole room usage (left) and for the half room usage (right). Lines which extend outside the room boundaries have to be considered only representative for a better visualization of the MSE system module since they are not part of the optimization process.

146

Chapter 8

High-rise buildings responsive skin

Abstract

Firstly the *vortex shedding* phenomenon is presented and its relevance in the context of high-rise buildings design is explained. The case study of a skyscraper possessing an adaptive envelope is then analyzed and the potential effects of the shape variation of the building are evaluated by means of CFD simulation. The study is finally included in the FSCS framework.

8.1. Problem statement

Assuming a high-rise building to possess an adaptive envelope, the beneficial effects of the geometrical variation of this envelope against the von Karman instability, induced by the wind excitation, are investigated.
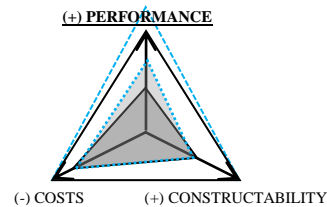
8.1.1. Vortex shedding phenomenon

A body immersed in a fluid stream produces, in general, a trail of vortices formed by trains (von Karman street) that detach alternately from the body itself, with a frequency provided by the Strouhal relationship:

$$n_s = \frac{St \cdot v_m}{b} \tag{8.1}$$

where:

- St is a dimensionless parameter, called the Strouhal number, which depends mainly by the shape of the body section;
- v_m is the average wind speed;
- b is the reference dimension of the cross section.

The detachment of alternating vortices generates instantaneous fluctuating pressure on the body surface, the integration of which gives rise to forces and moments. These actions may be especially important for slender structures. In these cases it is possible to outline the physical phenomenon as two-dimensional even if, strictly speaking, it has a three-dimensional nature.

The main actions acting on the body are manifested in the transverse direction to the flow, L, with frequency equal to the dominant vortex shedding frequency n_s. These actions are also longitudinal, D, (generally minor, with a dominant frequency of *2n_s*) and torsion actions, M, (dominant frequency of about n_s). In the following only the case of fluctuating forces transverse to the main flow direction (i.e. perpendicular to the axis of mean flow and the structure) will be considered.

Figure 8.1 – Von Karman street.

If the body has a natural frequency $n_{L,i}$, associated with a transverse mode of vibration, which is next to the n_s frequency of vortex shedding, then the lateral force L becomes resonant with the detachment of the vortices.

The critical velocity of separation of the vortices for the *i-th* transverse mode of the structure is defined as the average wind speed that determines the resonance condition $n_s = n_{L,i}$. Using Eq. (8.1), this is defined by the expression:

$$v_{cr,i} = \frac{n_{L,i} \cdot b}{St}$$

(8.2)

Since the average wind speed varies with height, a structure with a main vertical development may show the critical values of average wind speed at different locations along its axis. In order to carry out precautionary assessments, the critical vortex shedding should be evaluated for each mode of vibration considered, at the positions where the mode shows the maximum amplitude. For example, considering structures with a shelf-like static scheme, the excitement of the first mode is maximum when the vortex shedding is in resonance at the top while the excitement of the second mode can be maximum if the vortex shedding happens at the top or at the relative maximum of the second mode (Figure 8.2).
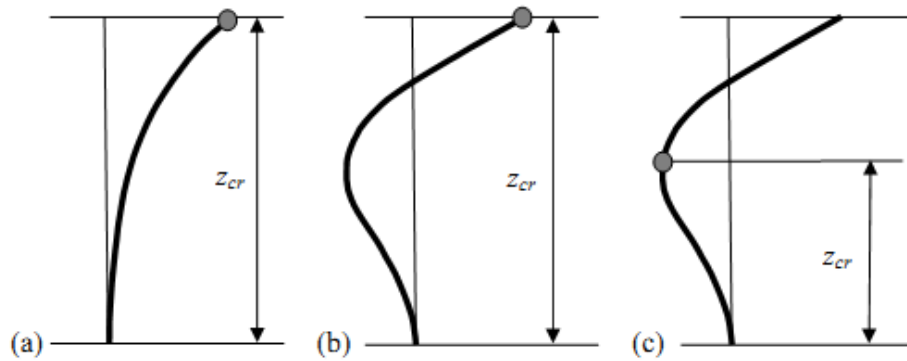
Figure 8.2 – Point of evaluation of the vortex shedding frequency according to the first mode (a) and the second mode (b and c) of a shelf-like static scheme.

149

Vortex shedding tends to occur with steady continuous winds at a critical velocity. The periodic frequency of the vortex shedding can lock in on the natural frequency of the pole, resulting in very large alternating forces acting transverse to the wind flow direction.

Occasionally, the vibration is so severe that fatigue cracks will appear.

Although vortex shedding can "lock in" and continue as the velocity increases or decreases slightly, if the velocity changes by more than 20 percent, the vortex shedding will stop. Gusty variable winds, such as might occur in a severe storm typically will not cause vortex shedding.

In summary, the winds that are dangerous for vortex shedding are steady winds.

Recent studies have verified that vortex shedding can occur in tapered as well as prismatic circular poles with almost any diameter. Although nearly periodic in a smooth air stream, vortex shedding in turbulent boundary layer flow conditions, which is characteristic of natural wind, tends to become less regular, with energy distributed over a band of frequencies around ωe (frequency at which vortex shedding occurs at a specific location [Hz]).

These considerations provide additional reasons to the use of the FSCS as explained later in Section 8.3.

8.1.2. Skin structure morphology design and management

For the building skin the choice has been to use a MDOF pin-jointed single-layer framework (i.e. rigid foldable origami structure) with a triangular pattern as the one shown in Figure 8.3. Such a particular structural system has a great potential for applications as an adaptive building envelope since:

- the pattern of the structure can be filled with rigid panels to achieve a watertight and rigid surface;
- mechanisms are purely geometric, i.e. they do not rely on the elasticity of materials and robust kinetic structure in a larger scale under gravity can be realized;
- the transformation from one configuration to another can be controlled by a limited number of degrees of freedom enabling a semi-automatic actuation of the structure.

150

A building section of 30 m on the average is assumed. Since the core of the building is supposed to be rigid, its volume imposes a restriction of the possible configurations achievable by the skin as. Moreover a maximum distance between the core and the skin has been imposed. These conditions and the resulting design space are represented in Figure 8.4.

High rise building adaptive skin as a MDOF single-layer framework
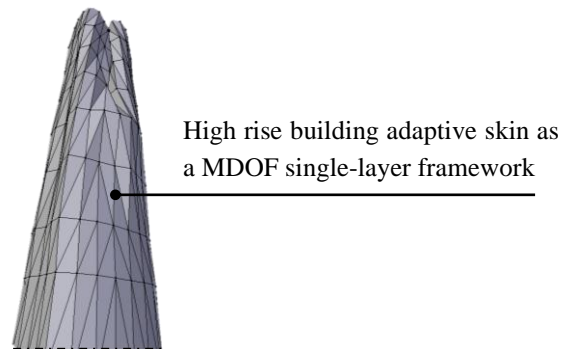
Figure 8.3 – MDOF pin-jointed single-layer framework.
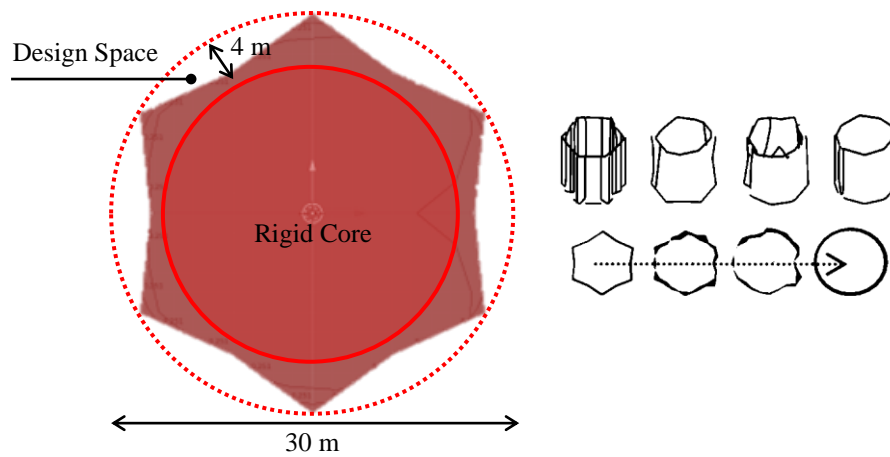
Figure 8.4 – The design space and different possible compatible sections.

8.2. Feasibility study

In order to prove the effectiveness of the proposed approach, the incidence of a feasible variation of the building skin section on the vortex shedding frequency has been investigated using CFD simulations in the two dimensional space. Specifically, sections of the skin have been extracted at different levels of the building from one of the three-dimensional compatible configurations (Figure 8.5).

Compatible 3D configurations of the building skin

Feasible 2D section
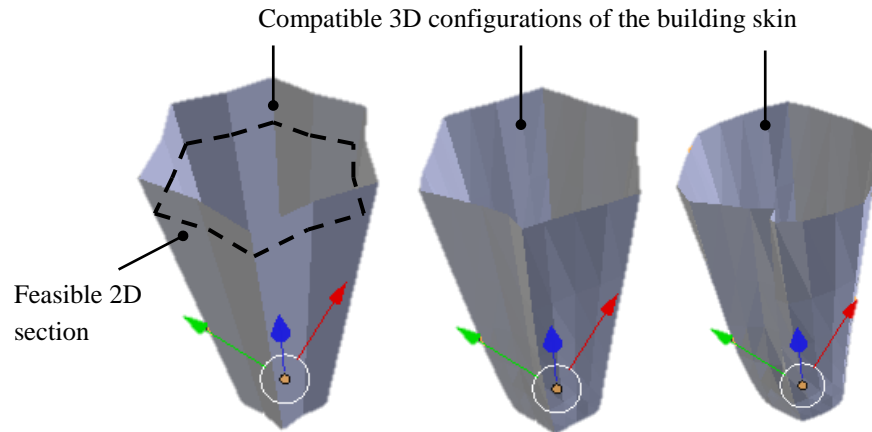
Figure 8.5 – Simulation of the building skin transformation.

The next two sub-sections illustrate the adopted CFD simulation settings and the results of the simulations respectively.

8.2.1. CFD simulation settings

The CFD simulations were carried out in 2-dimensional cartesian coordinates using the FlowSolve solver of the Elmer multiphysics software[18], mainly developed by CSC - IT Center for Science (CSC). 2nd order bdf time-stepping method was selected. Several tests were run to define a suitable simulation time in order to keep it as low as possible but, at the same time, allowing the vertex shedding

---

[18] http://www.csc.fi/english/pages/elmer

phenomenon to totally develop. It was found that 2000 steps for a total simulation time of 80 seconds were a good compromise for almost all cases. However, it was necessary to extend the simulation to 120 seconds for one case. The defaults solver specific settings were used except for a little relaxation of the convergence tolerances to get speedier simulation (Nonlinear system: Convergence tol. = 1.0e-4; Linear System: Convergence tol. = 1.0e-6). Navier-Stokes equation was used. The following fluid properties were set: density = 1.205 kg/m^3, viscosity = 1.983e-5 Pa·s.

The FE mesh was designed according to Figure 8.6. Three different kinds of boundaries were set: inlet, no-slip walls, and outlet. The inlet has a fully developed laminar profile with a velocity of 20 or 25 m/s in the X direction depending of the test to be run. Additionally, for the inlet the velocity component in the Y direction is assumed zero. The building section and the two walls along the X direction are given the no-slip treatment. For the outlet, only the vertical component was set to zero since the default discretization weakly imposes a zero pressure condition if the normal velocity component is not defined.
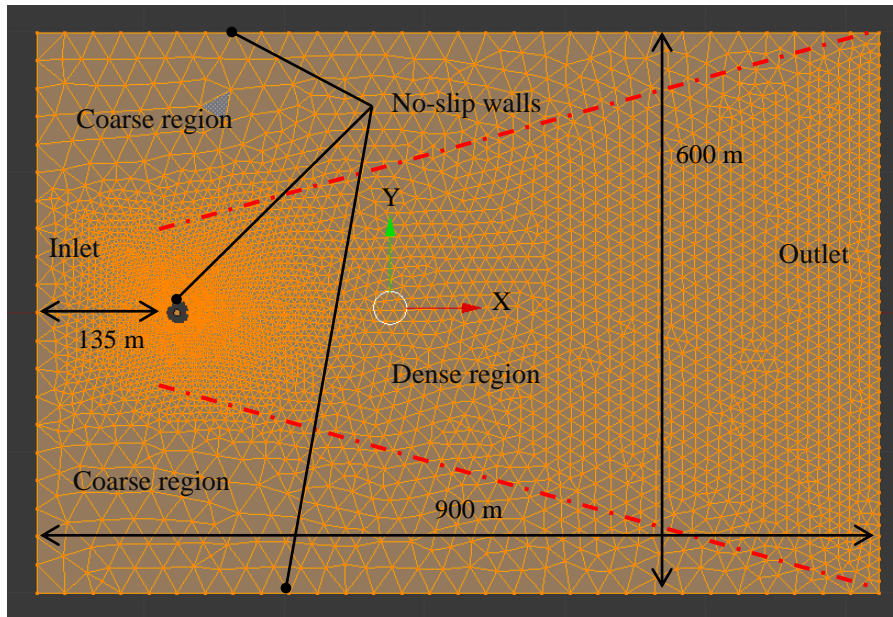
Figure 8.6 – Design of the mesh for the CFD simulation.

153

8.2.2. Results

Simulations have been carried out for the four compatible sections represented in Figure 8.7. The results are reported first in terms of absolute velocity fields at discrete time intervals (Figure 8.9 to Figure 8.16) and then in terms of pressure over time at two opposite locations of the transversal axis (Y-axis) of the analyzed building section (Figure 8.8 to Figure 8.18). Figure 8.8 summarizes the relationship among the results.
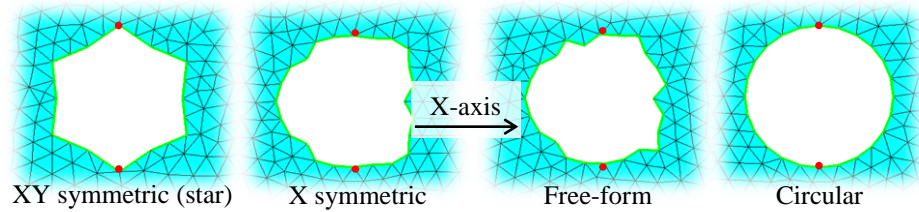
Figure 8.7 – Sections for the CFD analysis. Red dots represent the monitored locations for the reported pressures.
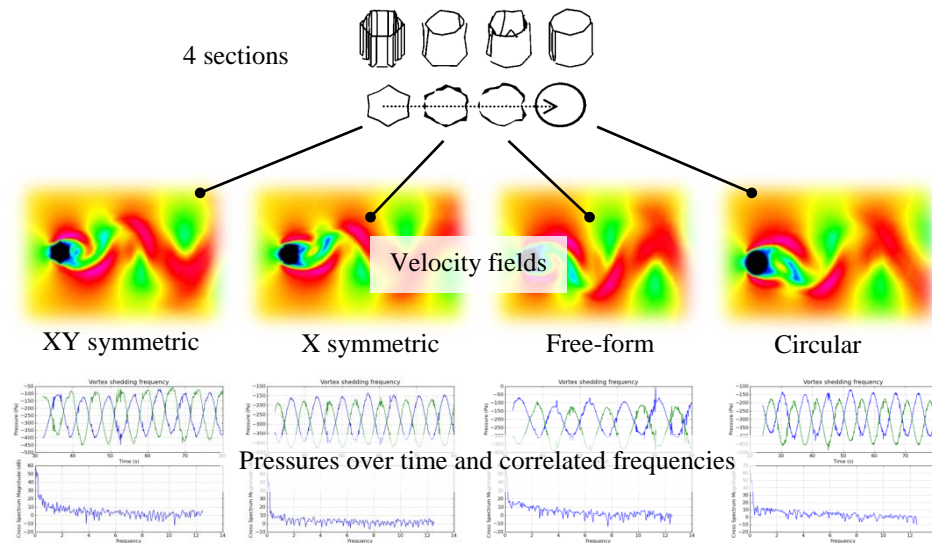
Figure 8.8 – Summary of the results relationship.

154
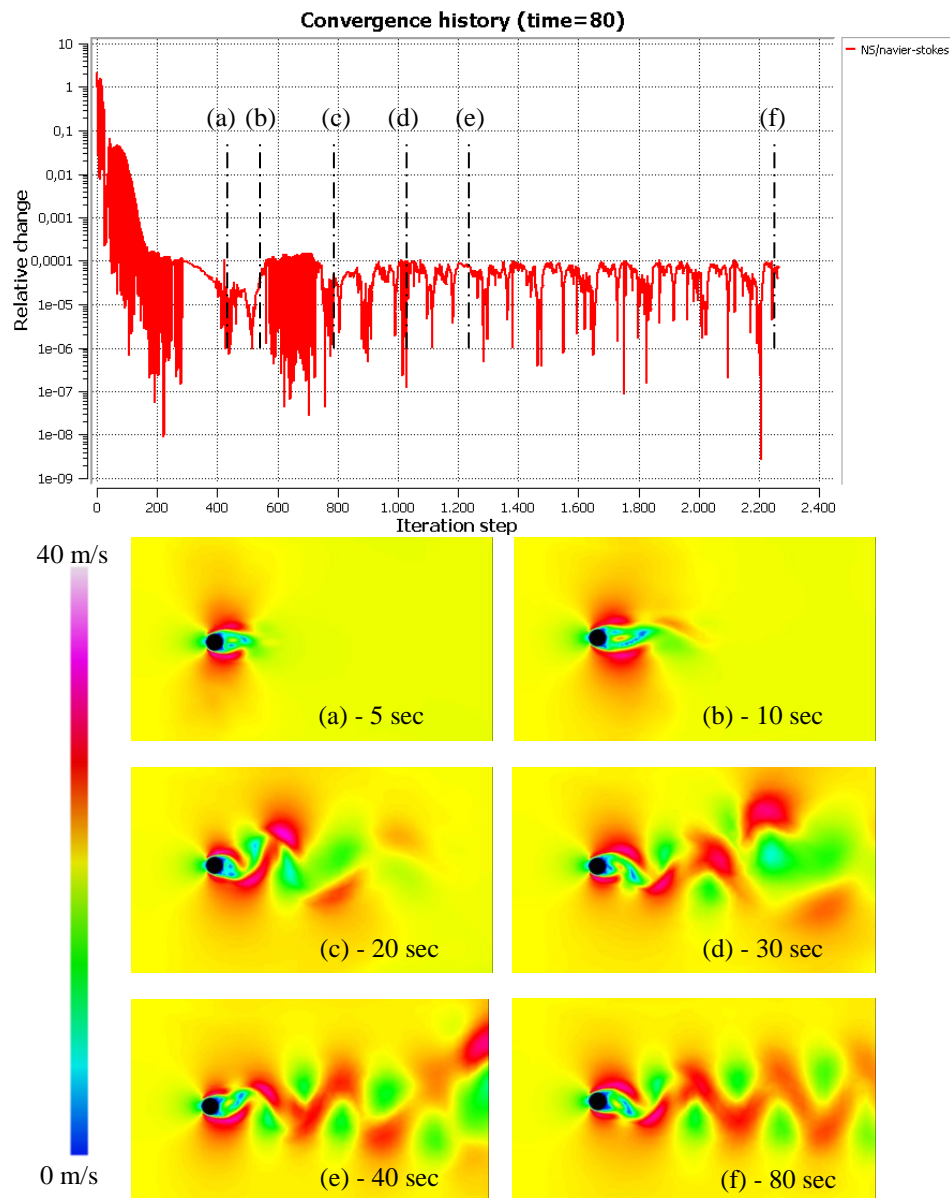
Figure 8.9 – Simulation of the vortex shedding for the circular section case and for a wind inlet velocity of 20 m/s.
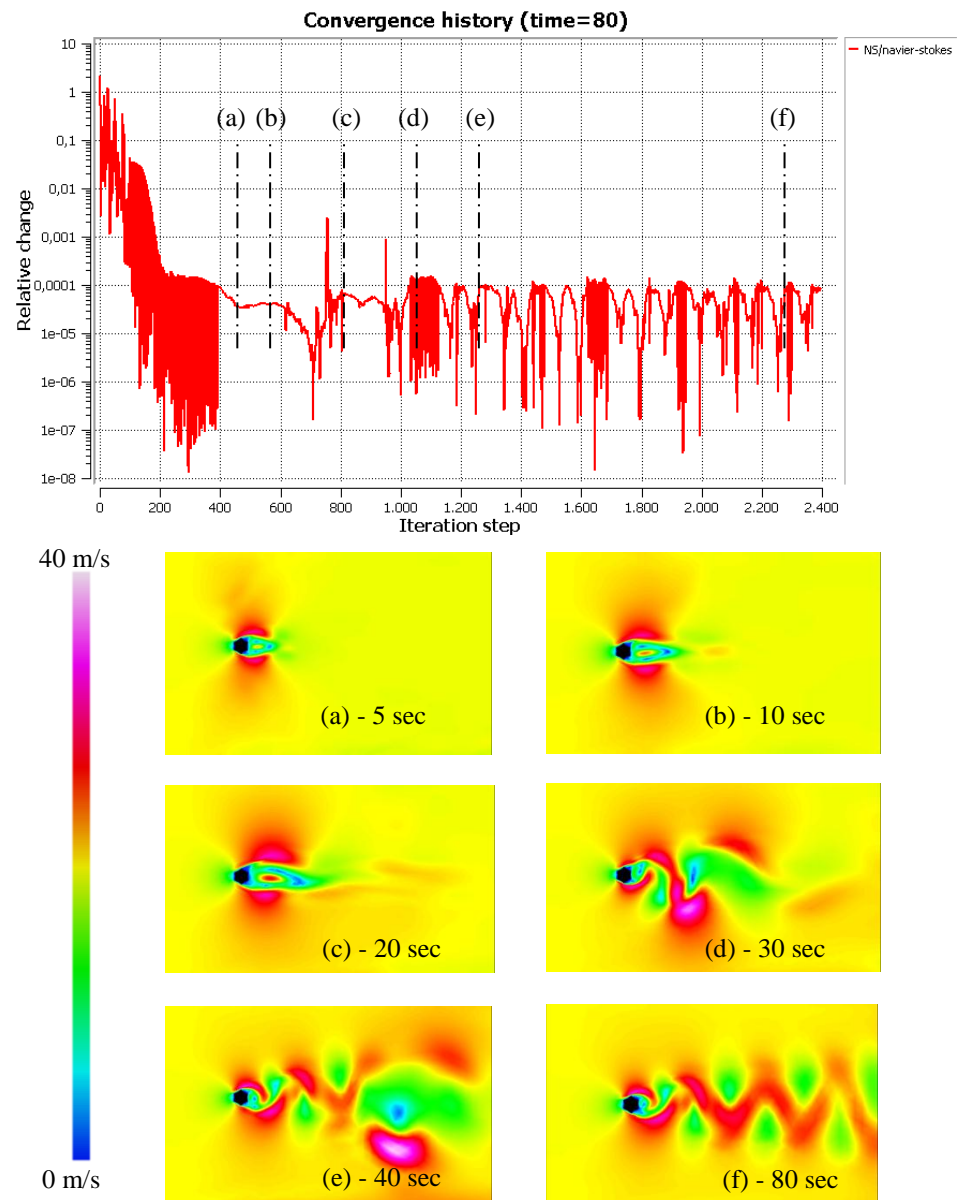
Figure 8.10 – Simulation of the vortex shedding for the xy-symmetric (star) section case and for a wind inlet velocity of 20 m/s.
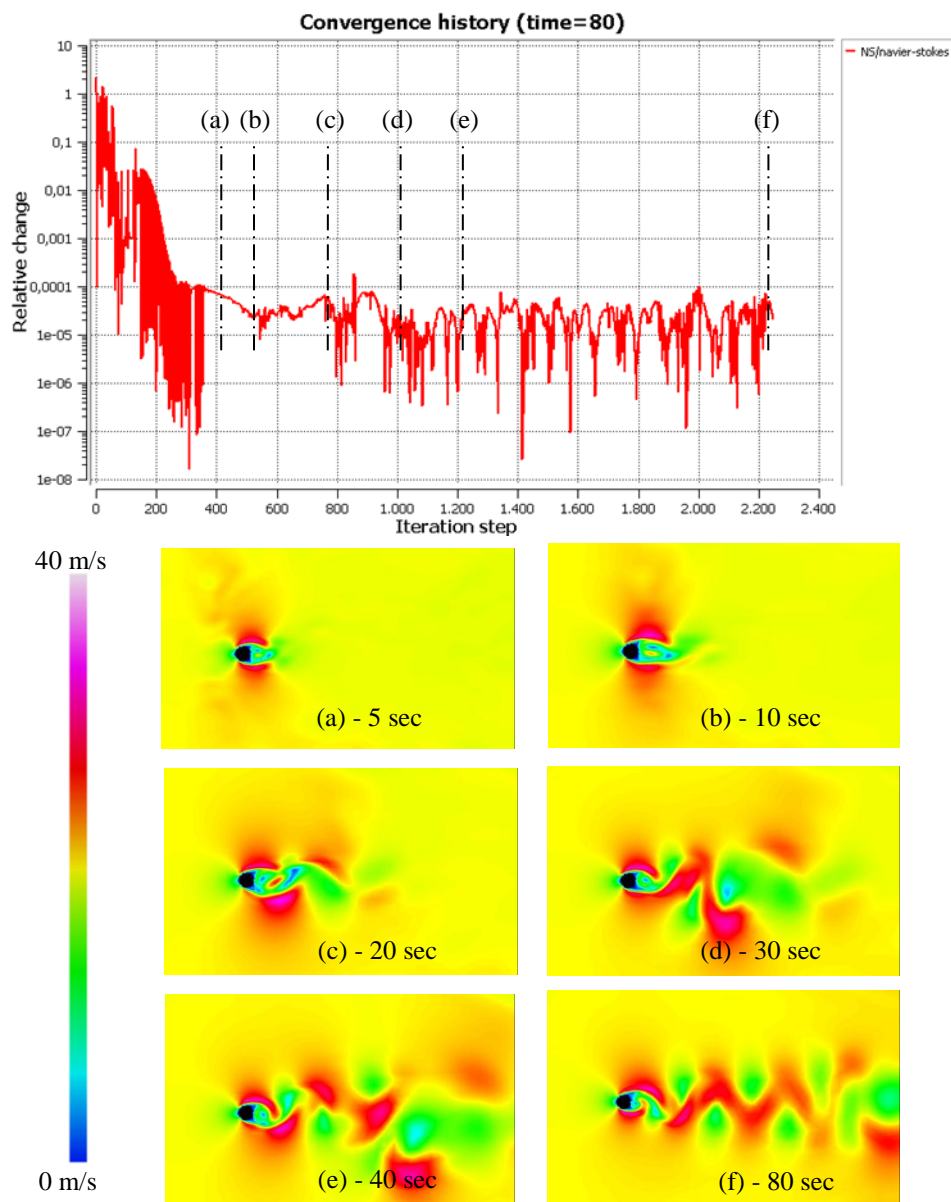
Figure 8.11 – Simulation of the vortex shedding for the freeform section case and for a wind inlet velocity of 20 m/s.
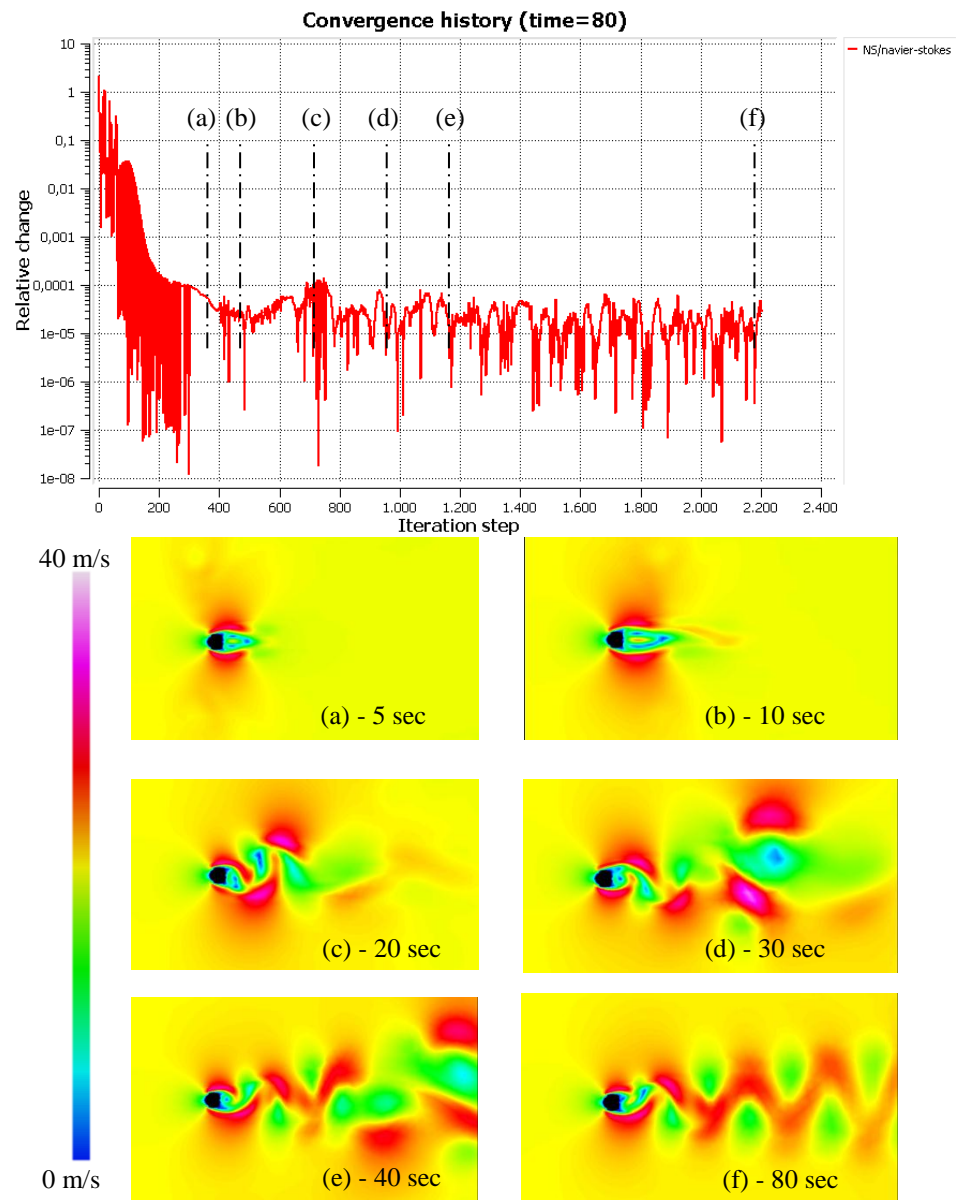
Figure 8.12 – Simulation of the vortex shedding for the x-symmetric section case and for a wind inlet velocity of 20 m/s.
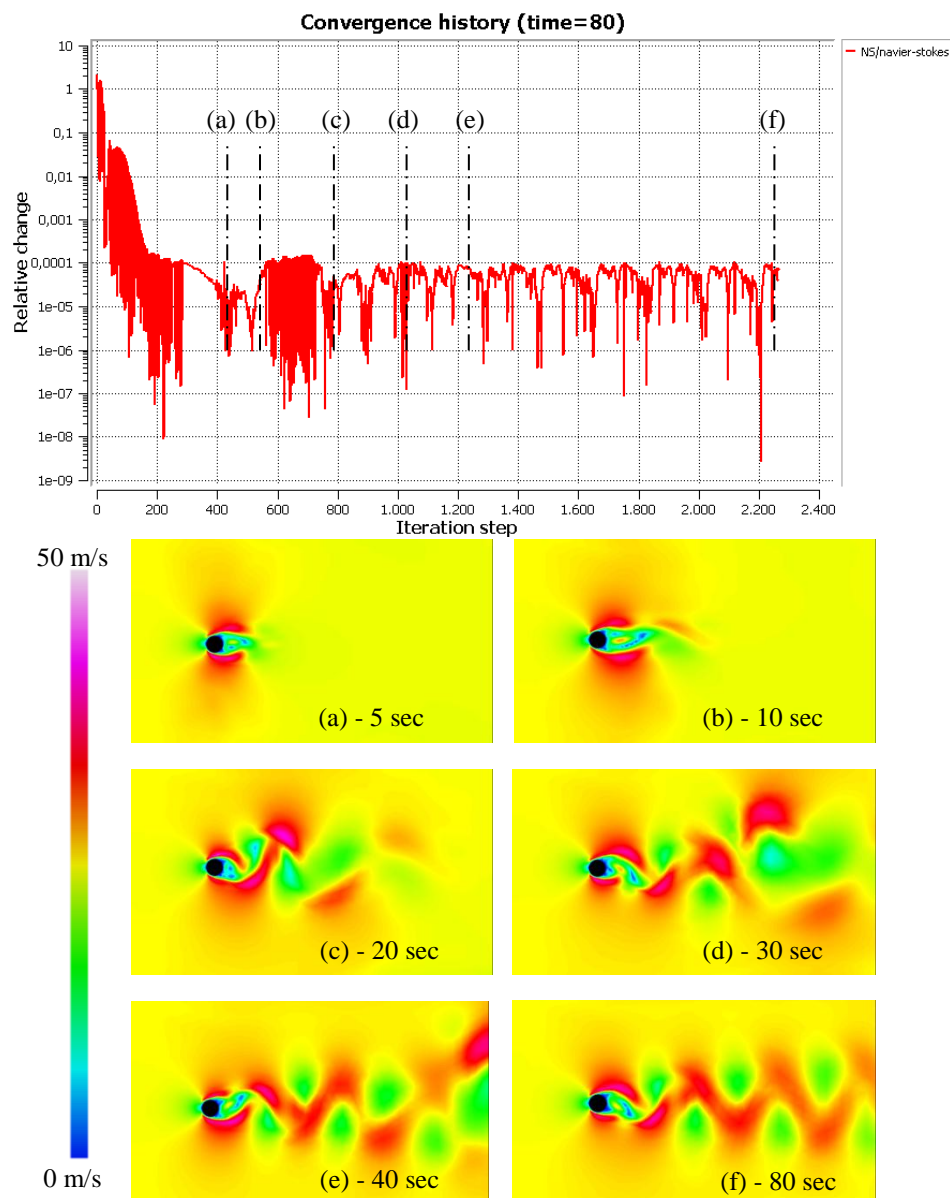
Figure 8.13 – Simulation of the vortex shedding for the circular section case and for a wind inlet velocity of 25 m/s.
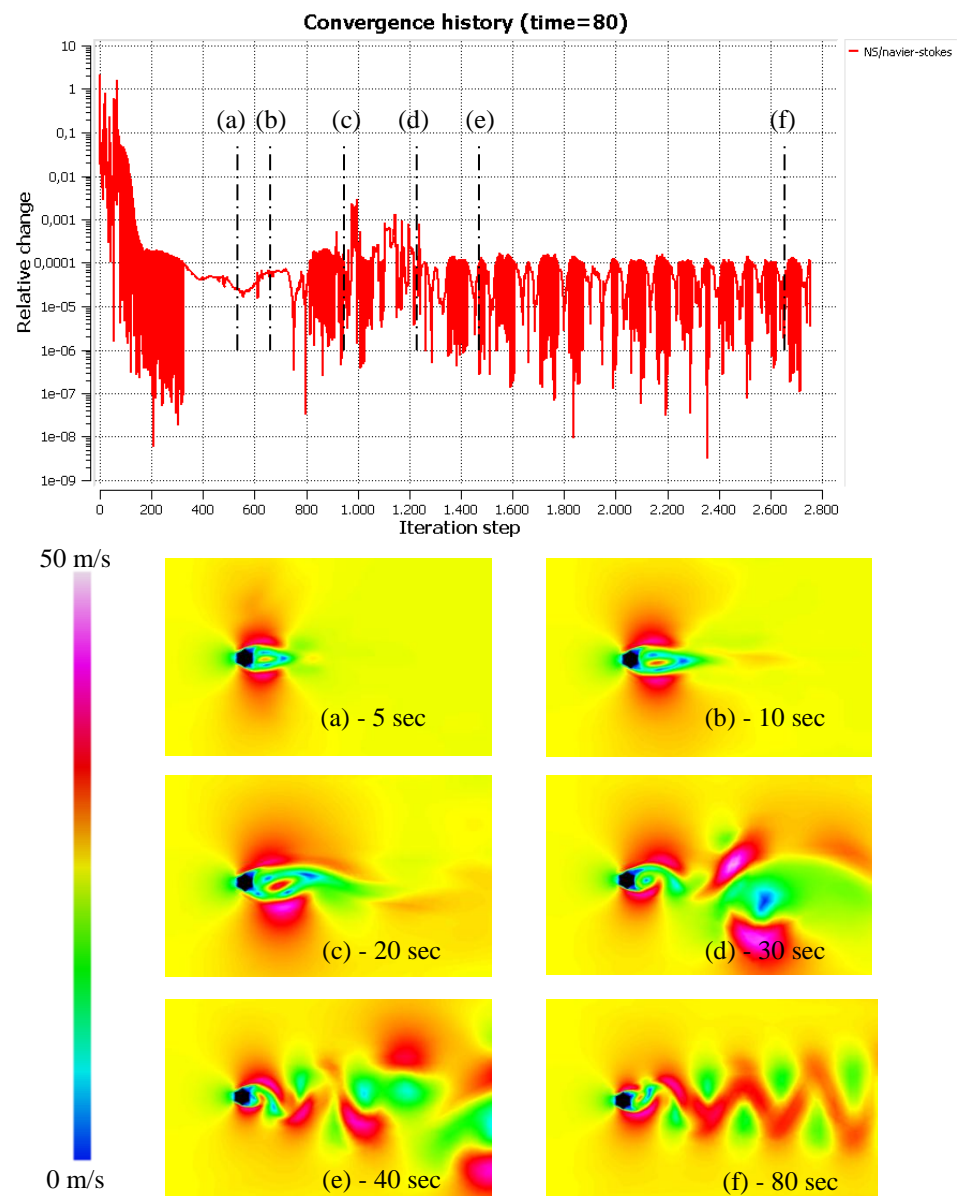
Figure 8.14 – Simulation of the vortex shedding for the xy-symmetric (star) section case and for a wind inlet velocity of 25 m/s.
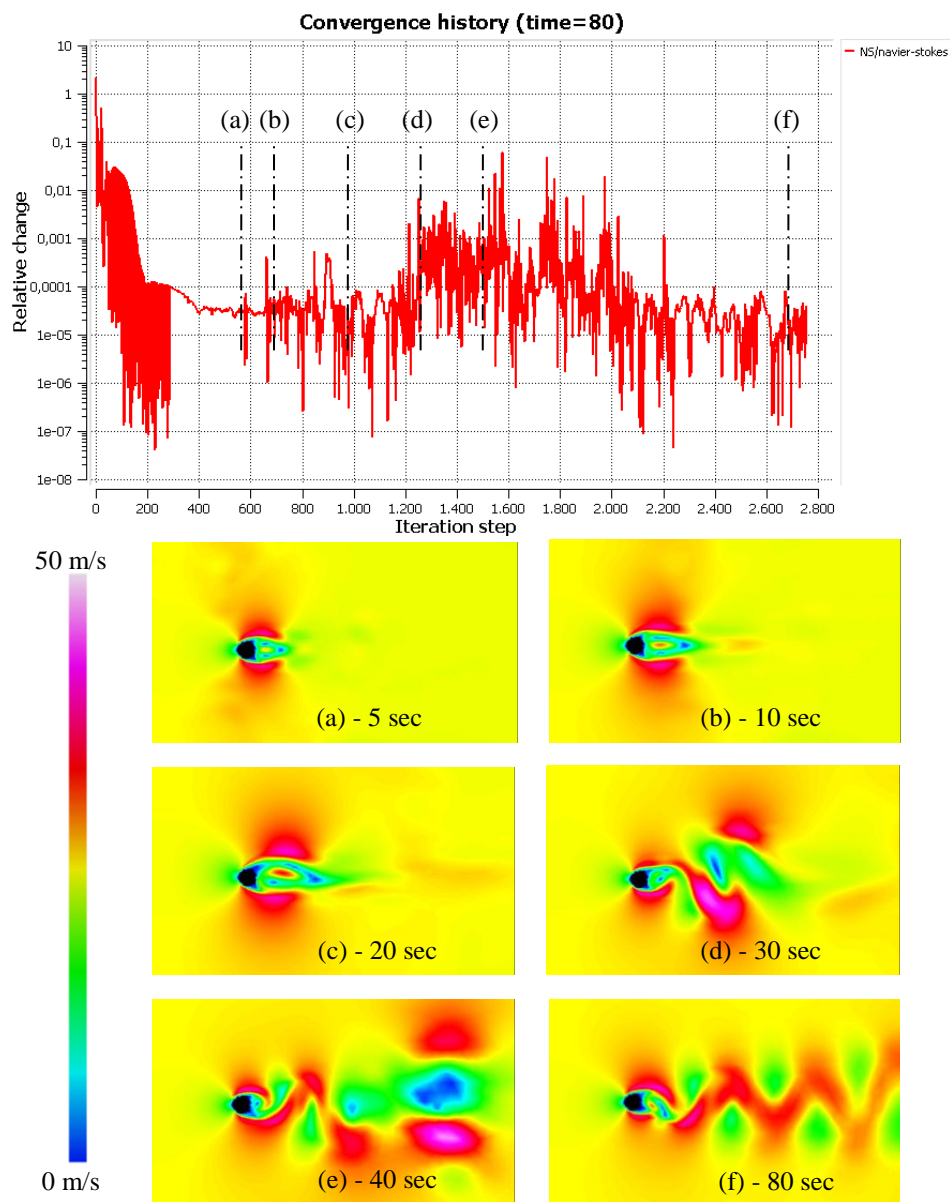
Figure 8.15 – Simulation of the vortex shedding for the freeform section case and for a wind inlet velocity of 25 m/s.
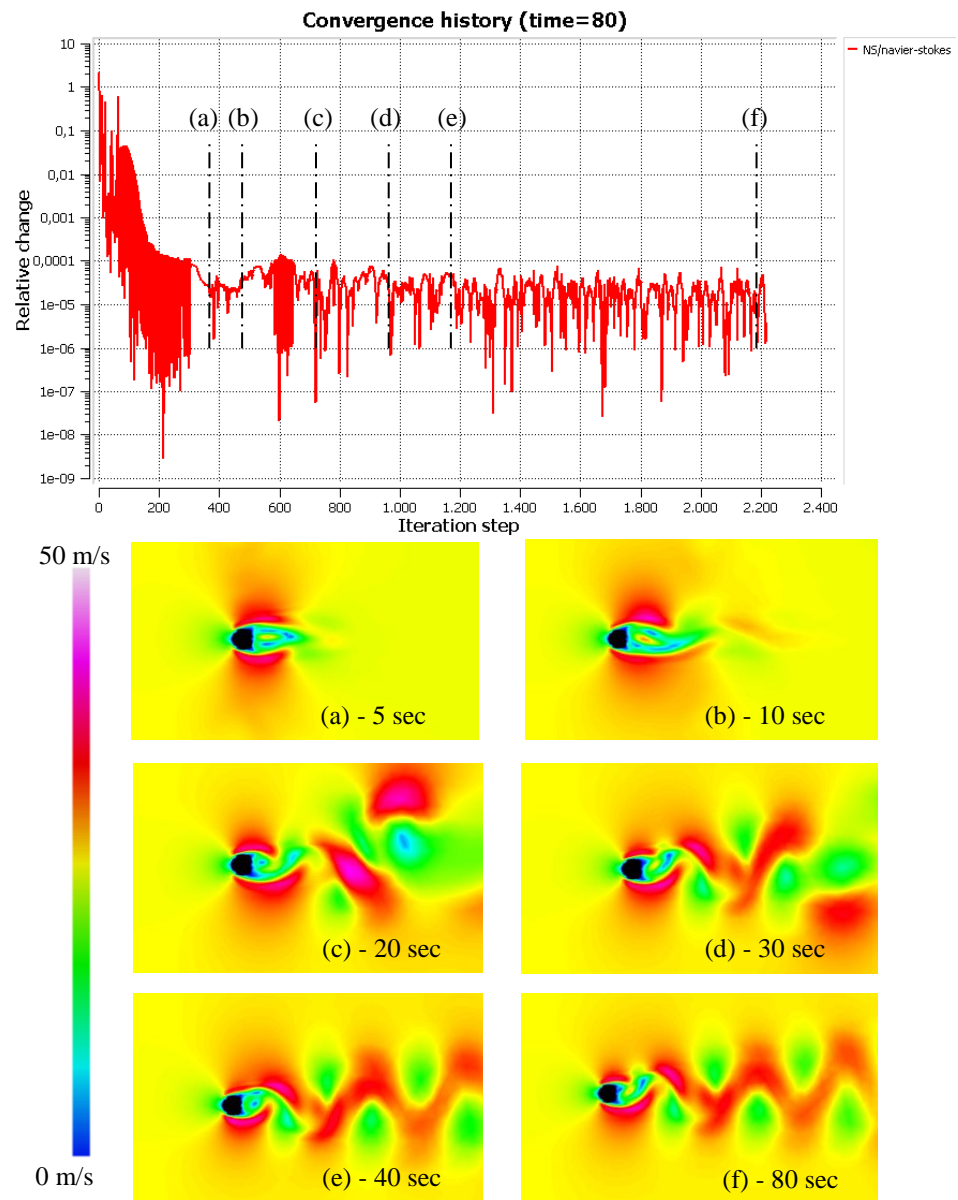
Figure 8.16 – Simulation of the vortex shedding for the x-symmetric section case and for a wind inlet velocity of 25 m/s.

XY symmetric (star)

X symmetric

Free-form

Circular
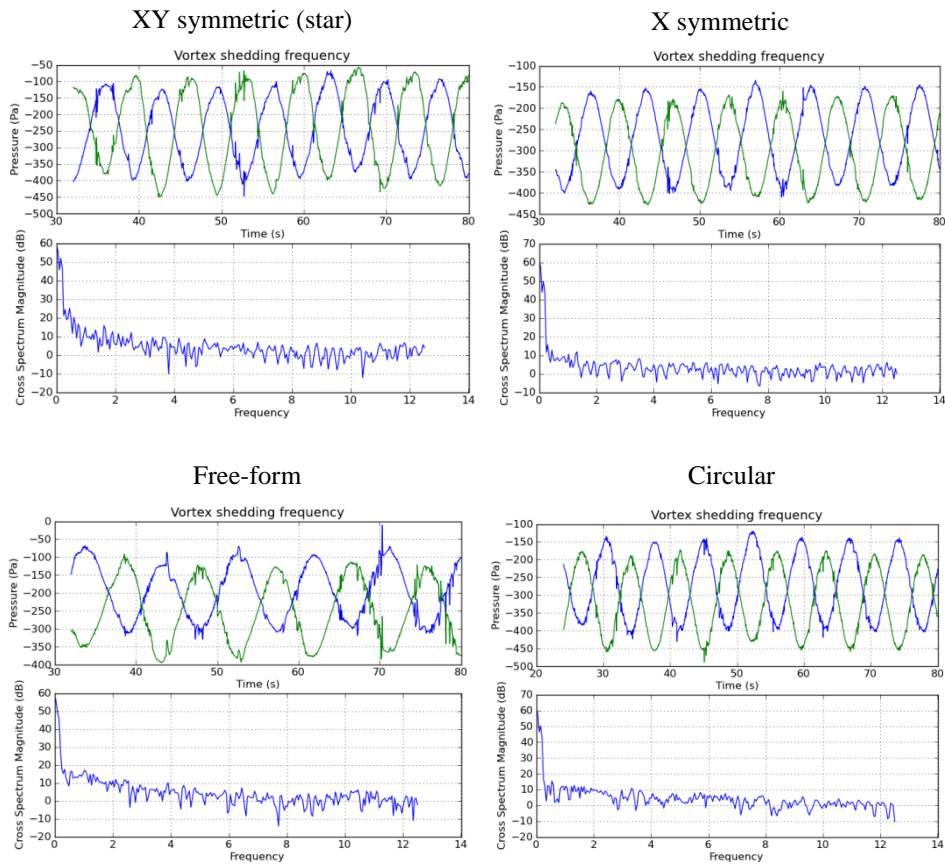
Figure 8.17 – Comparison of the vortex shedding frequencies for the different analyzed sections with a wind inlet velocity of 20 m/s.

XY symmetric (star)   X symmetric

Free-form   Circular
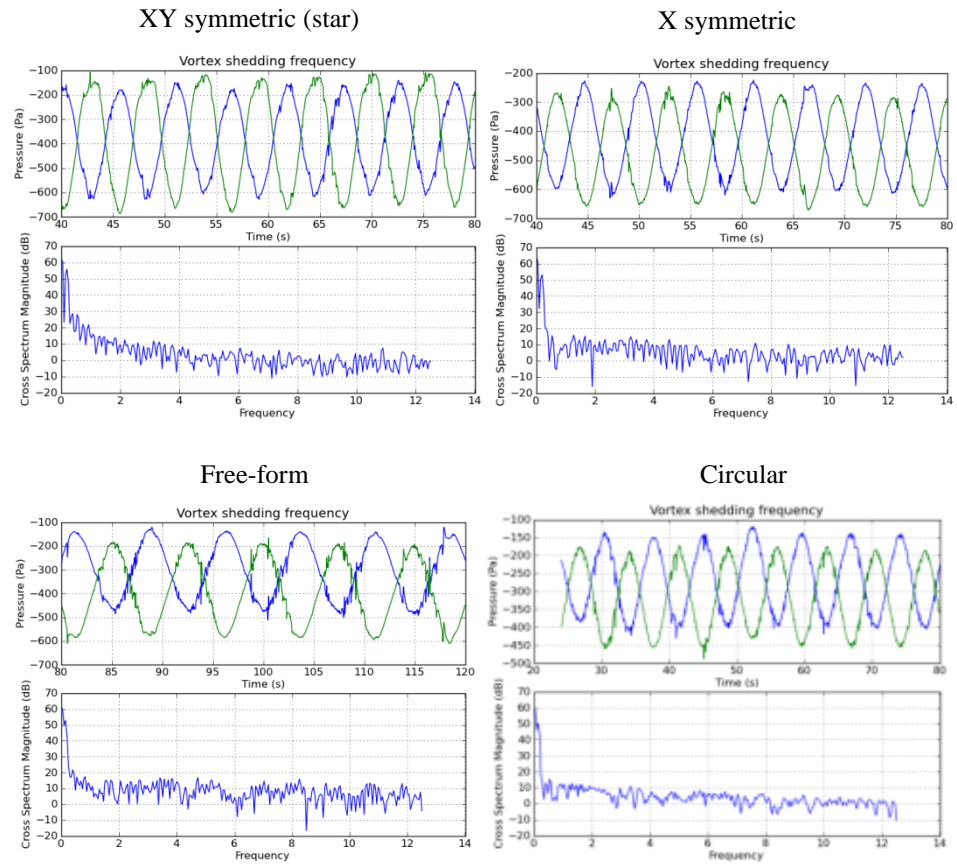
Figure 8.18 – Comparison of the vortex shedding frequencies for the different analyzed sections with a wind inlet velocity of 25 m/s.

The results of the simulations have shown that feasible changes of the building section are effective in determining variations of the vortex shedding frequencies. The vortex shedding periods vary, in fact, from around 7 to 10 seconds for the 20 m/s scenario and from around 5 to 8 seconds for the 25 m/s scenario. Particularly, slight changes are noted when the building section maintains its symmetry with respect to the X-axis (along wind direction) whereas the freeform section case allows a relevant variation (increment) of the vortex shedding period.

8.3. Consideration for the application of the FSCS

The results obtained from the simulation are promising since they show that slight variations of the section shape may sensibly influence the vortex shedding frequency. In view of fully developing the idea of an adaptive skin able to control this frequency, the FSCS may be easily set up to find optimal configurations of the skin relative to a range of inlet velocities. This would however imply a very large number of simulations to be performed. Moreover the simulations should preferably be set in the three dimensional space and, even if it would be proved that a discrete number of 2D simulations at different sections of the building were enough to evaluate the obtained effect of a 3D shape variation, the whole process would still result in a computational cost which is not affordable by a notebook. Because of all these reasons the application of the FSCS to this problem was not possible for the time of this book. Some considerations are however worth to be exposed, highlighting the potential of the FSCS on this specific case.

The discussed problem is in fact a perfect example to compare the FSCS with real-time control and to show the main advantages of the proposed approach.

Let's suppose for instance that the real-time control is based on simulation like the FSCS. Due to the high computational cost of the CFD simulations it is hardly believable that they may be performed real-time, at least for several years from now. Even it was the case, it is unfeasible (nor necessary in the case of vortex shedding since it tends to occur with steady continuous winds at a critical velocity) to adapt the real scale structure to instantaneous changes of the wind velocity, neither is convenient to use actuation energy to perform unnecessary transformations. Consequently the dimensions and masses of the civil structure still suggest a discrete number of possible skin configurations instead of a continuous movement, thus making real-time data useless the most of the times.

Thinking instead of using physical data to manage the transformation process real-time, this would imply a great number of sensors distributed all over the skin, much more than the ones expected by applying the FSCS, with consequent repercussions on costs. Moreover it may be hard to predict the effects of a change of configuration without simulating it in advance.

Finally, a real-time control system arguably requires even more care in the maintenance process because it may include more components (e.g. sensors) and because of the likely greater number of data to be managed.
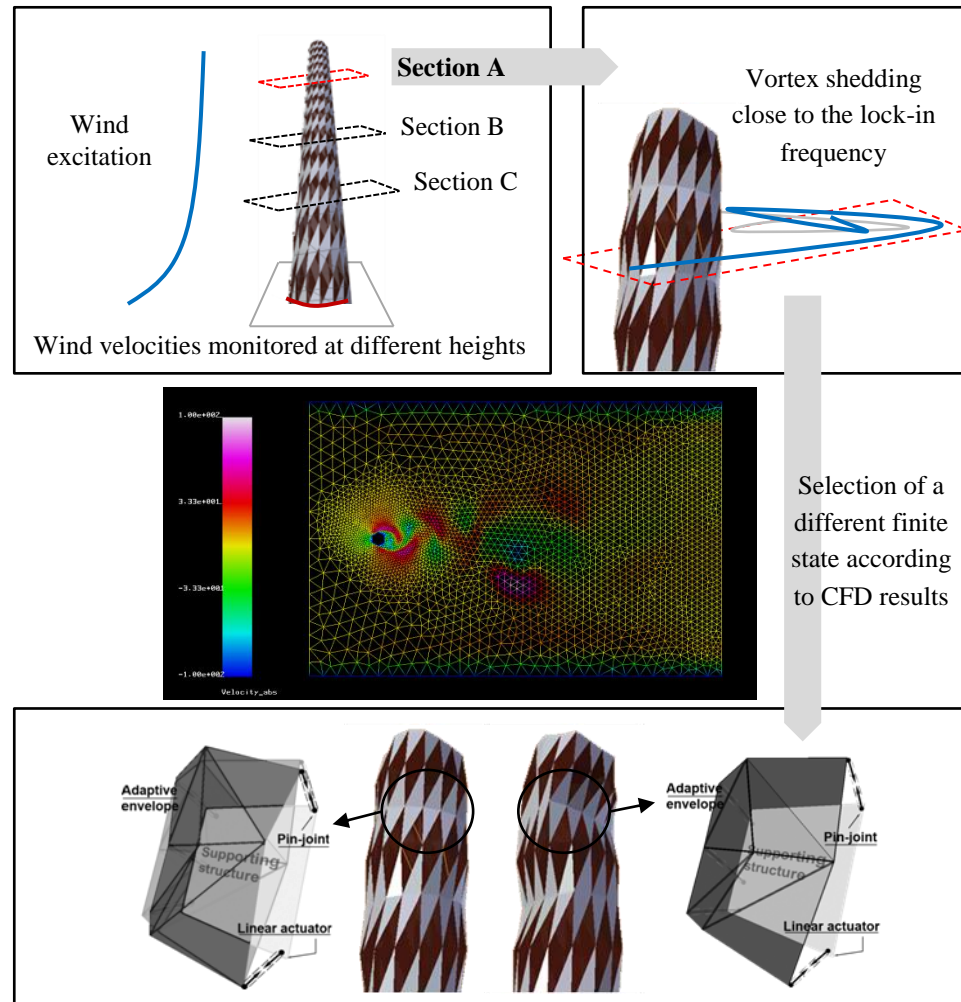
Figure 8.19 – Conceptual visualization of the skin morphing process as a consequence of the wind action and according to the FSCS framework.

Part IV
Conclusions

Chapter 9

Conclusions

Abstract

Conclusions underline both the *flexibility* and the *effectiveness* of the proposed methods in order to face current and future form-finding problems in structural design. A particular important role is also assigned to the *clarity* of the formulation which makes it not only possible but even simple to be adapted to different purposes.

The position of the author concerning possible future developments and trends in the research field is finally exposed.

9.1. Summary of results

The results of this dissertation are discussed in three parts: 1) the general development of the methodology; 2) its applications and contributions in the form-finding field; and 3) applications for the design exploration of complex and variable geometry structures.

9.1.1. Methodology

A new method, the VFDM, has been proposed for the multi-purpose optimization of framed structures. The method extends the functionality of the well

known Force Density Method (FDM), allowing purely geometrical problems to be faced. The method has also been successfully included in a multi-objective optimization process where both the statics and the constructability of the final structure have been involved. Moreover, the formulation of the method allows it to be adapted to different purposes in an easy and clear way.

A new strategy, the FSCS, has then been proposed to apply the developed methodology also to kinematic systems, thus bridging the approaches to the design of static and kinematic structures.

9.1.2. Contributions to the form-finding field

The proposed approach has been developed starting from the existing methods in the form-finding field and graph theory. The abstraction gained from the latter has provided with a new meaning of equilibrium and has made possible to extend the potential of the used form-finding techniques and to exploit their relationship with structural and geometrical optimization.

The research has also emphasized the common aspects of the static and kinematic problem by comparing the change of shape with the change of configuration. The form-finding problem involving a kinematic structure has then been treated using the static approach and geometric constraints.

9.1.3. Applications for the design exploration of complex and variable geometry structures

Several design issues related to static and kinematic spatial framed structures has been faced and solved successfully.

Referring to the field of free-form structures it has been explained how to standardize the element typologies in freeform grid-shells and generic spatial trusses of minimal deformation energy and how to design freeform meshes with planar quadrilateral elements.

Referring to the field of variable geometry structures it has been shown how to optimize the distribution and the intensity of the sound in a room using different

kinds of adaptive systems for the envelope. The potential effectiveness of using a responsive skin to manage the von Karman instability due to the wind-structure interaction in high-rise buildings has also been demonstrated. Finally a way of minimizing the number of actuators of a pin-joint framework has been proposed.

9.2. Final remarks

Various design drivers influence the design process, such as performance requirements, architectural criteria or environmental issues. Many of these conditions can be effectively managed acting on the building morphology by means of form-finding techniques and optimization processes. Many conditions are instead time dependent, which leads to the challenge that the building system should be able to respond to or to interact with these conditions, in order to create high performance systems. This leads to the overall framework of adaptive systems and, since the building skin represents the interface among the user, the environment and the building itself, this is a reasonable element to be considered in the design process. Current research has presented several potential but seldom applied solutions in this direction. Challenges are still many and vary according to the chosen approach.

9.3. Future development

The shape is the foremost design parameter and the most effective to change the static and dynamic structural behaviour. However, assuming that the structural shape is also the architectural shape, it typically forms a major part of the architectural expression that only in exceptional circumstances may be negotiated. Further research therefore could consider the macroscopic geometry as fixed and instead looks at "shape-invariant" geometric parameters on different levels of scale that can be considered to affect the structural behaviour.

Let's consider the equation of motion for a generic structure:

$$\mathbf{M\ddot{w}} + \mathbf{D\dot{w}} + \mathbf{Kw} = \mathbf{f} \qquad (9.1)$$

171

Where **M** is the mass matrix, **D** is the damping matrix, **K** is the stiffness matrix, **w** is the displacement vector (super dots denote time derivatives) and **f** is a time-dependent loading. In order to optimize the dynamic behaviour of a single-layer grid-shell, acting on **M** seems not so promising because it means likely increasing or, at least, redistributing the total weight of a structure which would generally already have been designed to be as lightweight as possible. It is possible to effectively work on **D** by applying passive, active or semi-active dampers [Lago and Sullivan, 2010] but it is not easy to achieve a predictable result using the elements of the structure only without further modifications. In the present study the focus is on the stiffness of the structure **K** which, in turn, can be represented as the sum of two contributions:

$$\mathbf{K} = \mathbf{K}_E + \mathbf{K}_G \qquad\qquad (9.2)$$

where, according to Przemieniecki [1968], $\mathbf{K}_E$ is the element stiffness matrix and $\mathbf{K}_G$ is the geometrical (initial-stress) stiffness matrix. While it does have the potential to affect the structure's dynamic behaviour while leaving the shape intact, prestress is at present not considered in this research. Therefore, when the structure is not in a state of pre-stress and small displacements are assumed then $\mathbf{K} = \mathbf{K}_E$. According to the assumptions made, the following is the list of "shape invariant" parameters which can be used to affect the stiffness, locally as well as globally:

- Material
- Thickness (in case of surface structures) or element sections (in case of reticulated structures)
- Joints restraints, internally between members or as boundary condition
- Pattern geometry in 2D (on the surface, density), or in 3D (out-of-plane, depth)

Further research may address all these parameters extending the proposed holistic approach of this dissertation.

172

References

Publications by the author

JOURNALS

Del Grosso A. E., Basso P., (2010a). Adaptive building skin structures, *Smart Materials and Structures*, Vol. 19 No. 12, December n. 124011, ISSN: 0964-1726. doi: [10.1088/0964-1726/19/12/124011](10.1088/0964-1726/19/12/124011) (Selected papers from the 20th International Conference on Adaptive Structures and Technologies - ICAST 2009 - Hong Kong, 20–22 October 2009)

Basso P., Del Grosso A. E., Pugnale A., Sassone M., (2009a). Computational morphogenesis in architecture: the cost optimization of free-form grid-shells, *IASS Journal*, Vol. 50 No. 3, December n.162, pp. 143-150, ISSN: 1028-365X. (Hangai Prize Awarded)

TECHNICAL REPORTS

Del Grosso A. E., Lanata F., Basso P., (2012), Final Partner Report – University of Genoa, *Integrated Europen Risk Reduction System (IRIS),* Contract n. CP-IP 213968-2, Project n. FP7-NMP-2007-LRGE-1, 01 Oct 2008 – 31 Mar 2012

Basso P. (2011), Elaborazione Dati da Monitoraggi Statici in Ambito Portuale (Analysis of data from the static monitoring of harbor structures - in Italian), DICAT Progress Report in the context of the Integrated Europen Risk Reduction System (IRIS), Contract n. CP-IP 213968-2, Project n. FP7-NMP-2007-LRGE-1.

PROCEEDINGS

Del Grosso A.E., Basso P., (2012), Deployable Structures, 4th International *Conference on Smart Materilas, Structures and Systems (CIMTEC 2012)*, June 10-14, Montecatini, Italy.

Del Grosso A. E., Basso P., 2012. Multi-DOF single-layer truss structures control by means of a Finite State Strategy - *Proceedings of the EACS 2012,* June 18-20 2012, Genoa, Italy.

Basso P., Casciati S., Faravelli L., (2012). Estimating the remaining service life of a historical railway bridge, Bridge maintenance, safety and management - Proceedings of the IABMAS Symposium 2012, July 8-12, Milan, Italy.

Del Grosso A. E., Basso P., (2011). A Finite State Strategy for the Control of Adaptive Structural Envelopes, *ICAST2011 : 22nd International Conference on Adaptive Structures and Technologies,* October 10-12, Corfu, Greece.

Basso P., Del Grosso A. E., (2011a). Form-finding methods for structural frameworks: a review, *Taller, Longer, Lighter - Proceedings of the IABSE–IASS Symposium 2011,* September 20-23, London, UK.

Basso P., Del Grosso A. E., (2011b). Adaptive frameworks topology optimization, *Taller, Longer, Lighter - Proceedings of the IABSE–IASS Symposium 2011,* September 20-23 2011, London, UK.

Lago A., Basso P., Veltkamp M., (2011a). Optimization of Free-Form Grid Shells' Dynamic Performance, *Taller, Longer, Lighter - Proceedings of the IABSE–IASS Symposium 2011,* September 20-23, London, UK.

Lago A., Basso P., Veltkamp M., (2011b). Shape invariant stiffness optimization, *Smart Morphology Group International Seminar 2011,* September, London, UK.

Del Grosso A. E., Basso P., (2010b). Unconventional Structural Forms in Pedestrian Bridge Design, *34th IABSE Symposium*, Venice, Italy, September 22-24, 2010.

Basso P., Del Grosso A. E., (2010). Adaptive Structures Optimization by means of the Virtual Force Density Method, *Spatial Structures – Permanent and Temporary, Proceedings of the International Association for Shell and Spatial Structures (IASS) Symposium 2010,*November 8-12, Shanghai, China.

Del Grosso A. E., Basso P., (2009). Adaptive building skin structures, *20th International Conference on Adaptive Structures and Technologies (ICAST 2009)*, Hong Kong, October 20-22.

Basso P., Del Grosso A. E., Pugnale A., Sassone M., (2009b). Applications of a Virtual Force Density Method. *Evolution and trends in design, analysis and construction of shell and spatial structures – Proceedings of the IASS Symposium 2009*, Valencia, Spain, Sept. 28 – Oct. 2.

Basso P., Del Grosso A. E., Pugnale A., Sassone M., (2009c). Computational morphogenesis in architecture: the cost optimization of free-form grid-shells. *Evolution and trends in design, analysis and construction of shell and spatial structures – Proceedings of the IASS Symposium 2009*, Valencia, Spain, Sept. 28 – Oct. 2.

Basso P., Del Grosso A. E., Pugnale A., Sassone M., (2009d). Computational Morphogenesis Of Free-Form Grid Shells. *Innovative Design & Construction Technologies - Building complex shapes and beyond, ID&CT 2009*, Maggioli Editore (ITA), Milano, Italy, May, 6-7.

Other publications

Adaptive Structures: Engineering Applications, (2007). David Wagg (Editor), Ian Bond (Co-Editor), Paul Weaver (Co-Editor), Michael Friswell (Co-Editor), ISBN: 978-0-470-05697-4

Agarwal, J., Haberland, M., Holicky, M., Sykora, M. and Thelandersson, S. (2012), „Robustness of Structures: Lessons from Failures", *Structural Engineering International* Vol.22, N.1, February 2012, pp. 105-111.

Akgün, Y., Haase, W. and Sobek, W. (2007). Proposal for a New Scissor-Hinge Structure to Create Transformable and Adaptive Roofs. *IASS Symp. - Architectural Engineering -Towards the future looking to the past* (Venezia, Italy, 2007).

Akgün, Y., Charis, J., Gantes, C. J., Kalochairetis, E. K. and Kiper, G. (2010). A novel concept of convertible roofs with high transformability consisting of planar scissor-hinge structures. *Engineering Structures,* vol. 32(9), pp. 2873-2883.

Azadi, M., Behzadipour, S. and Faulkner, G. (2009). Antagonistic variable stiffness elements. *Mechanism and Machine Theory* 44, no. 9 (September), pp. 1746-1758.

Balkcom, D.J., Demaine, E.D., and Demaine, M.L. (2004). Folding Paper Shopping Bags, *14th Annual Fall Workshop on Computational Geometry* (Cambridge, Massachusetts, November 19–20, 2004).

Bar-Cohen Y (ed), (2005). *Biomimetics—Biologically Inspired Technologies* (Boca Raton, FL: CRC Press), pp. 1–552.

Baldassini, N. (2007). 25 years of evolution in structural glass technologies, in: *Proceedings of the IASS Symposium - Shell and Spatial Structures: Structural Architecture – Towards the future looking to the past*, Venice, Italy, December 3-6, 2007.

Barents, R., Schenk, M., Van Dorsser, W.D., Wisse, B.M., & Herder, J.L. (2011), "Spring-to-Spring Balancing as Energy-Free Adjustment Method in Gravity Equilibrators", *ASME Journal of Mechanical Design*, Volume 133, Issue 6, pp 061010.

Barnes, M., (1988). Form-finding and analysis of prestressed nets and membranes. *Computers & Structures*, 30(3), pp.685-695.

Baudriller, H, B Maurin, P Canadas, P Montcourrier, A. Parmeggiani, and N Bettache. (2006). Form-finding of complex tensegrity structures: application to cell cytoskeleton modelling. *Comptes Rendus Mécanique* 334(11), pp. 662-668.

Baverel, O. (2000) *Nexorades: A family of interwoven space structures* (PhD thesis, University of Surrey).

Belcastro, S.M. and Hull, T. (2002). Modelling the folding of paper into three dimensions using affine transformations. *Linear Algebra and its Applications*, Vol. 348, pp. 273-82.

Bellés, P., Ortega, N., Rosales, M. and O. Andrés (2009). Shell form-finding: Physical and numerical design tools. *Engineering Structures*, 31(11), pp.2656-2666.

Bletzinger, K., (2001). Structural optimization and form finding of light weight structures. *Computers & Structures*, 79(22-25), pp.2053-2062.

Bletzinger, K, R Wuchner, F Daoud, and N Camprubi. (2005). Computational methods for form finding and optimization of shells and membranes. *Computer Methods in Applied Mechanics and Engineering* 194, no. 30-33.

Bletzinger, K-U, Firl, M., Linhard, J. and Wüchner. R. (2009). Computational morphogenesis of free form shells : Filter methods to create alternative solutions. In *Evolution and Trends in Design, Analysis and Construction of Shell and Spatial Structures - IASS Symposium 2009*, ed. A Domingo and C Lazaro, 536-547. Valencia.

Bletzinger, K-U, Firl, M., Linhard, J. and Wüchner. R. (2010). Optimal shapes of mechanically motivated surfaces. *Computer Methods in Applied Mechanics and Engineering* 199(5-8), pp. 324-333.

Block, P. (2009). Thrust Network Analysis: exploring three-dimensional equilibrium. *Engineering Sciences*. PhD thesis, Massachusetts institute of Technology.

Block, P., and Ochsendorf, J. (2007). Thrust Network Analysis : a new methodology for three-dimensional equilibrium. *J IASS* 48, no. 3: 167-173.

Böegle, A., Schlaich, M., Hartz, C. (2009). Pneumatic structures in motion. *Evolution and Trends in Design, Analysis and Construction of Shell and Spatial Structures, Proc. of the IASS Symposium* (Valencia, Spain, 28 Sept. – 2 Oct. 2009).

Bonet, J. (2001). Form finding of membrane structures by the updated reference method with minimum mesh distortion. *International Journal of Solids and Structures* 38(32-33), pp. 5469-5480.

Briccoli Bati, S., Rotunno, T., Tapputi, M. (2009). Design criteria for a novel self-locking mechanism for deployable structures. *Building Complex Shapes and Beyond, Proc. of the ID&CT Symposium.* (Milan, Italy, 6-7 May 2009).

Buckminster Fuller R., (1978). *Synergetics explorations in the geometry of thinking*. (London: Collier Macmillan Publishers)

Calatrava, S. (1981) *Zur Faltbarkeit Von Fachwerken* (Phd Thesis, ETH Zurich, Switzerland).

Calladine, C. R., and Pellegrino, S. (1991). First-order infinitesimal mechanisms. *Int. J. Solids Structures* 27, no. 4, pp. 505-515.

Calladine, C. R., and Pellegrino, S. (1991). Author's closure. *Int. J. Solids Structures* 27, no. 4: 521-522.

Calladine, C. R., and Pellegrino, S. (1992). Further remarks on first-order infinitesimal mechanisms. *Int. J. Solids Structures* 29, no. 17: 2119-2122.

Casciati, F., Faravelli, L., and AlSaleh, R., (2009), „Dynamic Architecture vs. StructuralControl". *Proceeding of the IV Eccomas Thematic Conference on Smart Materialsand Structures (SMAR'09)*. Porto- Portugal. pp.203-213.

Chandana, P., Lipson, H. and Valero Cuevas F. J., (2005). Evolutionary form-finding of tensegrity structures. *Proceedings of the 2005 conference on Genetic and evolutionary computation - GECCO '05*: 3.

Chi Tran, H. and Lee. J. (2010). Advanced form-finding for cable-strut structures. *International Journal of Solids and Structures* 47(14-15), pp.1785-1794.

Clark, R. L., Saunders W.R. and Gibbs G. P., (1998), *Adaptive Structures: Dynamics and Control*, Wiley, ISBN: 0471122629.

Connelly, R. (1980). The Rigidity of Certain Cabled Frameworks Rigidity of Arbitrarily Triangulated Convex Surfaces. *Advances in Mathematics* 299.

Connelly, R., (1982) Rigidity and energy, *Inventiones Mathematicae*, 66 (1), pp. 11-33.

Connelly, R., (1999). Tensegrity structures: why are they stable?, in: M.F. Thorpe and P.M. Duxbury, ed., *Rigidity theory and applications*, Plenum Press, New York, pp. 47-54.

Connelly, R. (2009). *Tensegrities and Global Rigidity* 0209595, pp. 1-29.

Deng, H, Q Jiang, and a Kwan. (2005). Shape finding of incomplete cable-strut assemblies containing slack and prestressed elements. *Computers & Structures* 83, no. 21-22 (August): 1767-1779.

Deng, H, and a Kwan. (2005). Unified classification of stability of pin-jointed bar assemblies. *International Journal of Solids and Structures* 42, no. 15 (July): 4393-4413.

Del Grosso, A.E., Barsotti, A. and de Barbieri, F. (1999). Active Control of Self-Deployable Structures. *2nd World Conf. on Structural Control* (T. Kobori et al. Eds., Wiley & Sons) 1957-66.

Del Grosso, A.E., Caviglione, L. and Pedretti, M., (2000). Stabilisation and Control of large Tensegrity Structures. *2nd European Conf. on Structural Control* (Paris, France 2000).

Del Grosso A. E., Caviglione, L. and Valfrè, L., (2002), Active Control Strategies for Harbour Cranes: Application Studies, *3rd World Conference on Structural Control*, 7-12 April 2002, Como, Italy.

Del Grosso, A.E. (2008). Examples of Future Potential Smart Civil Structures. *Advances in Science and Technologies* **56** (Trans Tech Publications, Switzerland) 287-96.

Deng, H, Q Jiang, and a Kwan. (2005). Shape finding of incomplete cable-strut assemblies containing slack and prestressed elements. *Computers & Structures* 83, no. 21-22, pp.1767-1779.

Descamps, B., R. Filomeno Coelho, L. Ney, and Ph. Bouillard. (2011). Multicriteria optimization of lightweight bridge structures with a constrained force density method. *Computers & Structures* 89, no. 3-4 (February), pp. 277-284.

Diestel, R. (2010). *Graph Theory*, Springer-Verlag, Heidelberg.

d'Estree Sterk, T. (2006). *Shape Control in Responsive Architectural Structures. Responsive Architectures-Subtle Technologies* (ed. C. Turner, Riverside Architectural Press)

Elbeltagi, E., Helgazy, T. and Grierson, D. (2005). Comparison among five evolutionary-based optimization algorithms. *Advanced Engineering Informatics* **19** 43-53.

Ellingwood, B. (1987), „Design and construction error effects on structural reliability", *Journal of Structural Engineering* Vol.113, N.2, pp. 409-422.

Estrada, G, H Bungartz, and C Mohrdieck. (2006). Numerical form-finding of tensegrity structures. *International Journal of Solids and Structures* 43, no. 22-23 (November), pp. 6855-6868.

Fu, F. (2005). Structural behavior and design methods of Tensegrity domes. *Journal of Constructional Steel Research* 61, no. 1 (January), pp. 23-35.

Golabchi, M.R. and Guest, S.D. (2009). Morphing multistable textured shells. *Evolution and Trends in Design, Analysis and Construction of Shell and Spatial Structures, Proc. of the IASS Symposium.* (Valencia, Spain, 28 Sept. – 2 Oct. 2009).

Gründig, L., Hangleiter, U. (1975). Computation of prestressed cable-nets with the force densities method, *IASS-Symposium Cable Structures*, Bratislava.

Gründig, L., (1985). The Force-Density - Approach and Numerical Methods for the Calculation of Networks. *Proceedings of 3rd International Symposium - Weitgespannte Flächentragwerke*, Stuttgart.

Grundig, L. (1988). Minimal surfaces for finding forms of structural membranes. *Computers & Structures* 30, no. 3, pp. 679-683.

Guest, S.D., Kebadze, E. and Pellegrino, S. (2011) A zero-stiffness elastic shell structure*, Journal of Mechanics of Materials and Structures*, 6(1-4): 203-212.

Guest, S.D. and Pellegrino, S. (2006). Analytical models for bistable cylindrical shells. *Proc. of the Royal Society A* **462**(3) 839-54.

Guest, S. (2006). The stiffness of prestressed frameworks: A unifying approach. *International Journal of Solids and Structures*, vol. 43, February, pp. 842-854.

Hall, St Edmund. (2002). Analogy between equilibrium of structures and compatibility of mechanisms by.

Hanaor, A. (1988). Prestressed pin-jointed structures—Flexibility analysis and prestress design. *Computers & Structures* 28, no. 6, pp. 757-769.

Hanaor, A. and Levy, R. (2001) Evaluations of Deployable Structures for Space Enclosures, *Int. J. of Space Structures* **16** 211-29.

Heinzelmann, F. (2009). Lightweight origami structures and day lighting modulation. *Evolution and Trends in Design, Analysis and Construction of Shell and Spatial Structures, Proc. of the IASS Symposium* (Valencia, Spain, 28 Sept. – 2 Oct. 2009).

Hilbert, D and Cohn-Vossen, S, (1932), *Anschauliche Geometrie*, Springer, Berlin.

Holgate, A, (1997), *The Art of Structural Engineering: The Work of Jörg Schlaich and his Team*, Edition Axel Menges, Stuttgart, London.

Hoberman, C. (1993). Unfolding Architecture: An Object That is Identically a Structure and a Mechanism. *Architectural Design* **63** 56-59.

Hilbert D. and Cohn-Vossen, S (1932). *Anschauliche Geometrie*, Springer, Berlin.

Holgate, A., (1997). *The Art of Structural Engineering: The Work of Jörg Schlaich and his Team*, Edition Axel Menges, Stuttgart, London.

Holland John H., (1992), *Adaptation in natural and artificial systems: an introductory analysis with application to biology, control, and artificial intelligence*, The MIT Press, Cambridge. First edition: The University of Michigan, 1975.

IASS, (2011), Fifty years of progress for shell and spatial structures, Ihsan Mungan and John F. Abel editors, Madrid.

Inoue, F. (2008). Development of Adaptive Construction Structure by Variable Geometry Truss. *Robotics and Automation in Construction* (Carlos Balaguer and Mohamed Abderrahim, InTech Education and Publishing) 253-272.

Juan, S, and J Miratstur. 2008. Tensegrity frameworks: Static analysis review. *Mechanism and Machine Theory* 43, no. 7 (July): 859-881.

Jurecka, F, M Ganser, and K Bletzinger. 2007. Update scheme for sequential spatial correlation approximations in robust design optimisation. *Computers & Structures* 85, no. 10 (May): 606-614.

Kawaguchi, M. (1999). Optimum shapes of a cable dome structure. *Engineering Structures* 21, no. 8 (August): 719-725.

Koiter, W.T., (1984). On Tarnai's conjecture with reference to both statically and kinematically indeterminate structures. *Report No.788 of Laboratory for Engineering Mechanics*, Delft.

Kota, S., Rodgers, M.S. and Hetrick, J.A. (2001). Compliant Displacement-Multiplying Apparatus for Microelectromechanical Systems. *United States Patent No. 6,175,170*.

Kovacs, F. (2004). A class of expandable polyhedral structures. *International Journal of Solids and Structures* 41, no. 3-4 (February): 1119-1137.

Kovács, F., and T. Tarnai. (2009). Two-dimensional analysis of bar-and-joint assemblies on a sphere: Equilibrium, compatibility and stiffness. *International Journal of Solids and Structures* 46, no. 6 (March 15): 1317-1325.

Koza John R., (1992), *Genetic Programming: On the programming of computers by means of natural selection*, The MIT Press, Cambridge.

Kronenburg, R. (2007). *Flexible: Architecture that responds to change* (London: Laurence King Publishing LTd).

Kuznetsov, E.N., (1979). Statistical-kinematic analysis and limit equilibrium of systems with unilateral constraints. *International Journal of Solids and Structures* 15, no. 10, pp. 761-767.

Kuznetsov, E.N., (1988). Underconstrained structural systems. *International Journal of Solids and Structures* 24, no. 2, pp. 153-163.

Kuznetsov, E.N., (1991a). Systems with infinitesimal mobility. Part I: Matrix analysis and first-order mechanisms. *J. Appl. Mech* 58, pp. 513-519.

Kuznetsov, E.N., (1991b). Systems with infinitesimal mobility. Part II: Compound and higher order mechanisms. *J. Appl. Mech* 58, pp.520-526.

Kuznetsov, E.N., (1991c). *Underconstrained Structural Systems*. Springer, New York.

Kuznetsov, E.N., (1991d). Letter to the editor. *Int. J. Solids Structures* 27, no. 4, pp. 517-519.

Kuznetsov, E.N., (1997). Orthogonal load resolution and statical-kinematic stiffness matrix. *Int. J. Solids Structures* 34, no. 28, pp. 3657-3672.

Kuznetsov, E.N., (1999). Singular configurations of structural systems. *International Journal of Solids and Structures* 36, no. 6 (February 1), pp. 885-897.

Kuznetsov, E. (2000). On the evaluation of statical-kinematic stiffness matrix for underconstrained structural systems. *International Journal of Solids and Structures* 37, no. 15 (April), pp. 2215-2223.

Kuznetsov, E. (2000). On the physical realizability of singular structural systems. *International Journal of Solids and Structures* 37, no. 21 (May 1), pp. 2937-2950.

Kwan, a. (1994). Matrix formulation of macro-elements for deployable structures. *Computers & Structures* 50, no. 2 (January 17): 237-254. doi:10.1016/0045-7949(94)90299-2. http://linkinghub.elsevier.com/retrieve/pii/0045794994902992.

Kwan, a SK. (1998). A new approach to geometric nonlinearity of cable structures. *Computers & Structures* 67, no. 4 (May 15): 243-252. doi:10.1016/S0045-7949(98)00052-2. http://linkinghub.elsevier.com/retrieve/pii/S0045794998000522.

Li, Yue, Xi-Qiao Feng, Yan-Ping Cao, and Huajian Gao. (2010). A Monte Carlo form-finding method for large scale regular and irregular tensegrity structures. *International Journal of Solids and Structures* 47, no. 14-15 (July): 1888-1898.

Linkwitz, K. (1999). About formfinding of double-curved structures. *Engineering Structures* 21, no. 8 (August), pp. 709-718.

Linkwitz, K., and Schek, H.J. (1971). Einige Bemerkungen zur Berechnung vonvorgespannten Seilnetzkonstruktionen. *Ingenieur-Archiv* **40** 145-58.

Lu, K.J. (2004). *Synthesis of Shape Morphing Compliant Mechanisms* (Ph.D. Thesis, The University of Michigan).

Luo, Y, and J Lu. (2006). Geometrically non-linear force method for assemblies with infinitesimal mechanisms. *Computers & Structures* 84, no. 31-32 (December): 2194-2199. doi:10.1016/j.compstruc.2006.08.063. http://linkinghub.elsevier.com/retrieve/pii/S0045794906002549.

Masic, M, R Skelton, and P Gill. (2005). Algebraic tensegrity form-finding. *International Journal of Solids and Structures* 42, no. 16-17 (August), pp. 4833-4858.

Maurin, B. (2001). Investigation of minimal forms with conjugate gradient method. *International Journal of Solids and Structures* 38, no. 14 (April), pp. 2387-2399.

Maurin, B, and Motro. R. (1998). The surface stress density method as a form-finding tool for tensile membranes. *Engineering Structures* 20, no. 8 (August): 712-719.

Maurin, B, M Bagneris, and R Motro. (2008). Mechanisms of prestressed reticulate systems with unilateral stiffened components. *European Journal of Mechanics - A/Solids* 27, no. 1 (January): 61-68. doi:10.1016/j.euromechsol.2007.05.009. http://linkinghub.elsevier.com/retrieve/pii/S0997753807000526.

Mele, Tom VAN, and Block, P., (2010). A Novel Form Finding Method for Fabric Formwork for Concrete Shells. In *Spatial Structures – temporary and permanent – IASS Symposium 2010*. Shanghai.

Mendez Echenagucia, T.I., Astolfi, A., Jansen, M., Sassone, M. (2008) Architectural Acoustic and Structural Form. *J. IASS* **49**(3) 181-86.

Michalski, a., P.d. Kermel, E. Haug, R. Löhner, R. Wüchner, and K.-U. Bletzinger. (2011). Validation of the computational fluid–structure interaction simulation at real-scale tests of a flexible 29m umbrella in natural wind flow. *Journal of Wind Engineering and Industrial Aerodynamics* (January).

Micheletti, A, and Williams W. (2007). A marching procedure for form-finding of tensegrity structures. *Journal of Mechanics of Materials and Structures* 2, no. 5 (July), pp. 857-882.

Micheletti, A. (2008) On Generalized Reciprocal Diagrams for Self-Stressed Frameworks. *International Journal of Space Structures*, vol. 23, September, pp. 153-166.

Michell A. G. M., (1904). The Limits of Economy of Material in Frame-structures, *Phil. Mag.,* Series 6, Vol. 8.

Migayrou, F and Mennan, Z (2003) *Non standard architectures*, Editions du Centre Pompidou, Paris.

Miki, M., and Kawaguchi. K. (2010a). Extended Force Density Method for Form-Finding of Tension Structures. *J IASS* 51, no. 4, pp. 291-303.

Miki, M., and Kawaguchi. K. (2010b). Comparison of Foregoing Methods on Form-Finding of Tension Structures. In *6th China-Japan-Korea Joint Symposium on Optimization of Structural and Mechanical Systems*. Kyoto.

183

Mitchell, M., (1998), *An introduction to Genetic Algorithms*, The MIT Press.

Miura, K. (1970). Proposition of pseudo-cylindrical concave polyhedral shells, *Proc. of IASS Symp. on Folded Plates and Prismatic Structures 1970*.

Miura, K. (2009). Triangles and Quadrangles in Space. *Evolution and Trends in Design, Analysis and Construction of Shell and Spatial Structures, Proc. of the IASS Symposium* (Valencia, Spain, 28 Sept. – 2 Oct. 2009).

Moretti L., (1951). Struttura come forma, in *Spazio* n°6, December.

Moretti L., (1951). *Spazio*, a. III, n. 6, December.

Moretti L., (1971). *Moebius*, a. IV, n. 1, 1971.

Müller, Andreas. (2009). Generic mobility of rigid body mechanisms. *Mechanism and Machine Theory* 44, no. 6 (June): 1240-1255. doi:10.1016/j.mechmachtheory.2008.08.002. http://linkinghub.elsevier.com/retrieve/pii/S0094114X08001602.

Musmeci S., (1979). Le tensioni non sono incognite, in *Parametro* n°80, October. Reprint in: *Parametro* n°237, Janauary-February 2002.

Musmeci S., (1977). Ponte sul Basento, *L'industria Italiana del Cemento*, n. 2

Musmeci S., (1979). Architettura e pensiero scientifico, in *Parametro* n°80, October.

Musmeci S., (1979). La genesi della forma nelle strutture spaziali, in *Parametro* n°80, October.

Nagaraj, B.P., R. Pandiyan, and Ashitava Ghosal. (2009). Kinematics of pantograph masts. *Mechanism and Machine Theory* 44, no. 4 (April): 822-834. doi:10.1016/j.mechmachtheory.2008.04.004. http://linkinghub.elsevier.com/retrieve/pii/S0094114X08000876.

O'Dwyer, D. W. (1999). Funicular analysis of masonry vaults. *Computers and Structures* 73(1-5), pp.187–197.

Ohsaki, M, and J Zhang. (2006). Stability conditions of prestressed pin-jointed structures. *International Journal of Non-Linear Mechanics* 41, no. 10 (December): 1109-1117.

Otto F., Rasch B., (1996) *Finding Form: Towards an Architecture of the Minimal*, Axel Menges, Feelbach.

Pagitz, M., and Mirats Tur. J.M. (2009). Finite element based form-finding algorithm for tensegrity structures. *International Journal of Solids and Structures* 46, no. 17 (August), pp. 3235-3240.

Parigi, D., Sassone, M., Napoli, P. (2009). Kinematic and static analysis of plane reciprocal frames. *Evolution and Trends in Design, Analysis and Construction of Shell and Spatial Structures, Proc. of the IASS Symposium* (Valencia, Spain, 28 Sept. – 2 Oct. 2009).

Pauletti, R, and P Pimenta. (2008). The natural force density method for the shape finding of taut structures. *Computer Methods in Applied Mechanics and Engineering* 197, no. 49-50 (September), pp. 4419-4428.

Pedretti M., (1998). Smart Tensegrity Structures for the Swiss EXPO. *SPIE Proceedings* **30** 3330-48.

Pellegrino, S., (1986) *Mechanics of kinematically indeterminate structures*, Ph.D. dissertation,University of Cambridge, U.K.

Pellegrino, S., Calladine, C.R. (1986). Matrix analysis of statically and kinematically indeterminate frameworks, *Int. J. Solids Structures* **22** (4) 409-28.

Pellegrino, S. and You, Z. (1997). Cable-Stiffened Pantographic Deployable Structures, *AIAA Journal* **35** 1348-55.

Pellegrino, S. (1990). Analysis of prestressed mechanisms. *International Journal of Solids and Structures* 26, no. 12, pp. 1329-1350.

Pellegrino, S. (1993). Structural computations with the singular value decomposition of the equilibrium matrix. *International Journal of Solids and Structures* 30, no. 21, pp. 3025-3035.

Pellegrino, S., and Van Heerden. T. (1990). Solution of equilibrium equations in the Force Method: a compact band scheme for undetermined linear systems. *Computers & Structures* 37, no. 5, pp. 743-751.

Piegl, L. and Tiller, W. (1995). *The NURBS Book*, 2nd ed., Berlin: Springer.

Piñero, E.P. (1962). Expendable Space Framing. *Progressive Architecture* **12** 154-5.

Popovic, O. (1996). *The architectural potential of the reciprocal frame* (PhD thesis, University of Nottingham).

Przemieniecki, J.S., (1968). *Theory of Matrix Structural Analysis.* McGraw-Hill, New York.

185

Pugnale, A. and Sassone, M., (2007) M, Morphogenesis And Structural Optimization of Shell Structures with the aid of a Genetic Algorithm, *IASS Journal*, 48(155); 161-166.

Reitinger, Reiner, Kai-Uwe Bletzinger, and Ekkehard Ramm. 1994. Shape Optimization of Buckling Sensitive Structures. *Science* 5, no. 1: 65-75.

Resch R.D. and Christiansen, H. (1970) The design and analysis of kinematic folded plate systems. In *Proceedings of IASS Symposium on Folded Plates and Prismatic Structures*.

Rizzuto, J.P. (2006). Notched Mutually Supported Element (MSE) Circuits in Space Structures. *Proc. of IASS-APCS Symp.* (Beijing, China, 2006).

Rogers, D.F. (2001). *An introduction to NURBS: with historical perspective*, 1st ed., San Francisco: Morgan Kaufmann, pp. 17-36.

Salerno, G., (1992). How to recognise the order of infinitesimal mechanisms: a numerical approach. *Int. J. Number. Methods Eng* 35, pp. 1351-1395.

Sanchez, J, M Serna, and P Morer. (2007). A multi-step force–density method and surface-fitting approach for the preliminary shape design of tensile structures. *Engineering Structures* 29, no. 8 (August), pp. 1966-1976.

Sasaki M., *Flux Structure*, TOTO, Tokyo, (2005).

Sassone, M., and Pugnale, A., (2008) Optimal design of glass grid shells with quadrilateral elements by means of a genetic algorithm, *Proceedings of the 6th International Conference on Computation of Shell & Spatial Structures "Spanning Nano to Mega"*, Ithaca NY, USA, May 28-31, 2008, 204.

Schek, H J. (1974). The Force Density Method for form-finding and computation of general networks. *Computer Methods in Applied Mechanics and Engineering* 3, pp. 115-134.

Schioler, T, and Pellegrino, S. (2004). Multi-Configuration Space Frames. In *Structures, Structural Dynamics, and Materials Conference*. Palm Springs.

Schittich, C. (2001). *In Detail: Building Skins – Concepts, Layers, Materials* (Basel: Birkhauser).

Schlaich, J and Schober, H, (1994), Glass-covered Lightweight Spatial Structures, in: Abel, J F and Leonard, J W and Penalba C U, eds, *Spatial, lattice and tension structures: proceedings of the IASS-ASCE Symposium*, Atlanta, 1994, American Society of Civil Engineers, N.Y.

186

Seffen, K.A. (2007). Hierarchical multi-stable shapes in mechanical memory metals. *Scripta Materilia*, **56**(5) 417-20.

Shepherd, P. and Richens, P., (2011) , Subdivision Surfaces for Integrated Design, Analysis and Optimisation, *Taller, Longer, Lighter - Proceedings of the IABSE– IASS Symposium 2011,* September 20-23, London, UK.

Skelton, R.E. and deOliveira, M.C. (2009). *Tensegrity Systems* (Springer Science + Business Media).

Sofla, A.Y.N., Elzey, D.M. and Wadley, H.N.G. (2008). Two way antagonistic shape actuation on the one-way shape memory effect. *J. of Intelligent Material Systems and Structures* **19** 1017-27.

Sofla, A.Y.N., Elzey, D.M. and Wadley H.N.G. (2007). A rotational joint for shape morphing space truss structures. *Smart Materials and Structures* **16** 1277-84.

Sofla, A Y N, Elzey D M and Wadley H N G (2009). Shape morphing hinged truss structures. *Smart Materials and Structures* **18**.

Stachel, Hellmuth. (2007). A proposal for a proper definition of higher-order rigidity.

Tachi, T. (2009a). Generalization of Rigid Foldable Quadrilateral Mesh Origami. *Evolution and Trends in Design, Analysis and Construction of Shell and Spatial Structures, Proc. of the IASS Symposium* (Valencia, Spain, 28 Sept. – 2 Oct. 2009).

Tachi, T. (2009b). Simulation of Rigid Origami. In *Origami4: The Fourth International Conference on Origami in Science, Mathematics, and Education* (OSME), ed. A. K. Peters, pp. 175–187.

Tachi, T. (2010a). Geometric Considerations for the Design of Rigid Origami Structures. In *IASS Symposium 2010*. Shanghai.

Tachi, T. (2010b). Freeform rigid-foldable structure using bidirectionally flat-foldable planar quadrilateral mesh. *Proceedings of Advanced in Architectural Geometry* (AAG) 2010, Wien.

Tang, X., Thomas, S., Coleman, P. and Amato N.M., (2010). Reachable distance space: efficient sampling-based planning for spatially constrained systems. *The International Journal oof Robotics research* 29(7), pp. 916-34.

Tarnai, T. (1980). Simultaneous static and kinematic indeterminacy of space trusses with cyclic symmetry. *Int. J. Solids Structures* 16, pp. 347-359.

187

Tarnai, T., (1984). Comments on Koiter's Classification of Infinitesimal Mechanisms. *Hung. Inst. Build. Sci*, Budapest.

Tarnai, T, (1989). Higher order infinitesimal mechanisms. *Acta Tech. Acad. Sci. Hung* 102, pp. 363-378.

Tarnai, T. (2000). On the exact equation of inextensional, kinematically indeterminate assemblies. *Computers & Structures* 75, no. 2 (March 1), pp. 145-155.

Tarnai, T. (2003). Zero stiffness elastic structures. *International Journal of Mechanical Sciences* 45, no. 3 (March), pp. 425-431.

Tibert, A.G., and Pellegrino, S. (2003). Review of Form-Finding Methods for Tensegrity Structures. *International Journal of Space Structures* 18, no. 4 (December), pp. 209-223.

Torroja, E. (1960). *Razón y Ser de los tipos estructurales, Instituto de la Construcción y del Cemento*, Madrid.

Tran, Hoang Chi, and Jaehong Lee. (2010). Advanced form-finding of tensegrity structures. *Computers & Structures* 88, no. 3-4 (February), pp. 237-246.

Trease, B. P. and Kota, S., (2006) Synthesis of Adaptive and Controllable Compliant Systems with Embedded Actuators and Sensors, *Proceedings of IDETC/CIE 2006 ASME 2006 Int. Design Engng. Technical Conf. & Computers and Information in Engng. Conf.*, September 10-13, 2006, Philadelphia, Pennsylvania, USA.

Vassart, N, Laporte, R. and Motro, R. (2000). Determination of mechanism's order for kinematically and statically indetermined systems. *International Journal of Solids and Structures* 37, no. 28 (July), pp. 3807-3839.

Veenendaal, D. and Block, P., (2011), A Framework for Comparing Form Finding Methods, *Taller, Longer, Lighter - Proceedings of the IABSE–IASS Symposium 2011,* September 20-23, London, UK.

Veldkamp, G. (1976). On conditions for finite movability of the most simple overconstrained planar and spatial mechanisms. *Mechanism and Machine Theory* 11, no. 3: 241-245.

Vitruvius, M., *The Ten books of Architecture*, (transl. Morris Hicky Morgan, 1960), Courier Dover Publications. ISBN 0486206459.

188

Vizotto, I. (2010). Computational generation of free-form shells in architectural design and civil engineering. *Automation in Construction* 19, no. 8 (December), pp. 1087-1105.

Vrouwenvelder, T., Leira, B., J. and Sykora, M.,. (2012), „Modelling of Hazards", *Structural Engineering International* Vol.22, N.1, February 2012, pp. 73-78.

Wang, J.T. and Johnson, A.R. (2003). *Deployment Simulation Methods for Ultra-Lightweight Inflatable Structures.* NASA/TM-2003-212410 ARL-TR-2973.

Wayburn, T. (1987). Homotopy continuation methods for computer-aided process design. *Computers & Chemical Engineering* 11, no. 1: 7-25.

Werff, K van der. (1977). *Kinematic and dynamic analysis of mechanisms , a finite element approach.* Delft University Press.

Whittier, William Brooks. (2002). Kinematic Analysis of Tensegrity Structures By.

Wood, R. (2002). A simple technique for controlling element distortion in dynamic relaxation form-finding of tension membranes. *Computers & Structures* 80, no. 27-30 (November): 2115-2120.

Wüchner, R., M. Firl, J. Linhard, and K.-U. Bletzinger. (2008). Plateau regularization method for structural shape optimization and geometric mesh control. *Pamm* 8, no. 1 (December): 10359-10360.

Xu, Xian, and Yaozhi Luo. (2010). Form-finding of nonregular tensegrities using a genetic algorithm. *Mechanics Research Communications* 37, no. 1 (January): 85-91.

Yuan, X. (2002). Nonlinear analysis and optimum design of cable domes. *Engineering Structures* 24, no. 7 (July): 965-977.

Yuan, X, L Chen, and S Dong. (2007). Prestress design of cable domes with new forms. *International Journal of Solids and Structures* 44, no. 9 (May): 2773-2782.

Zhang, J, and Ohsaki. M (2006). Adaptive force density method for form-finding problem of tensegrity structures. *International Journal of Solids and Structures* 43, no. 18-19 (September), pp. 5658-5673.

Zils, J., (2006) *Skidmore, Owings & Merrill: SOM from 1936*, Electa, Milano.